METAL ION COMPLEXATION STUDIES OF A SULFUR-OXYGEN MIXED DONOR MACROCYCLIC LIGAND BY SOLVENT EXTRACTION AND NUCLEAR MAGNETIC RESONANCE

By

Leslie Ann Greenbauer

A THESIS

Submitted to
Michigan State University
in partial fulfillment of the requirements
for the degree of

MASTER OF SCIENCE

Department of Chemistry

1978

ABSTRACT

METAL ION COMPLEXATION STUDIES OF A SULFUR-OXYGEN MIXED DONOR MACROCYCLIC LIGAND BY SOLVENT EXTRACTION AND NUCLEAR MAGNETIC RESONANCE

By

Leslie Ann Greenbauer

Measurements of metal ion complexing strengths with three macrocyclic ligands are reported. Two techniques, solvent extraction and nuclear magnetic resonance, were employed to assess the cation-ligand binding strengths.

The extraction equilibrium constants (log K_e) for potassium with dibenzo-18C6 were determined to be 4.79 ± 0.22 and 6.38 ± 0.06 with 18C6. Constants were also obtained for cesium and thallium (I), where log K_e for the $(Cs\cdot18C6)^+$ complex was determined to be 5.56 ± 0.41 and for complexes of thallium (I), with 18C6 and 1,10-dithia-18C6, were found to be 5.81 ± 0.05 and 3.80 ± 0.01, respectively.

Cesium-133 and thallium-205 NMR chemical shift measurements provided a second method for determining complex formation constants. Cesium-1,10-dithia-18C6 complex formation constants (log K_f) were determined in four solvents: nitromethane (0.65 ± 1.09), dimethylformamide (0.56 ± 0.29), acetonitrile (0.90 ± 0.27), and pyridine (0.84 ± 0.15). The thallium ion binding with 1,10-dithia-18C6, in pyridine, produced a stronger complex where log K_f = 1.39 ± 0.19.

A Raman-IR study of the complex formed between the solvent, acetonitrile, and the 18C6 ligand, was performed to identify bands arising due to this interaction.

To my family

Mom Dad

Julie Janet Dan Cindy

and Barney

and my family to be

Gary

ACKNOWLEDGMENTS

Although a thesis is an account of an individual's research accomplishments, the final product is actually a summation of the efforts of several people. I would like to thank Dr. Alexander Popov for serving as my research preceptor and for his recommendations toward completing my masters project. I extend my thanks to Dr. Harvey Nikkel, from Grand Valley State Colleges, for introducing me to research and encouraging me to continue my studies in graduate school.

A very special thanks to my coworkers Fred Smetana, whose professional help and friendship made the time spent a little more worthwhile, and John Hoogerheide, for his help in writing the computer program used in the extraction studies. I would like to thank Davette Whitaker for making 405 more fun to do work in.

My deep thanks to Gary, who provided me with his invaluable gifts of love, support, and understanding which he unselfishly provided when he was trying to complete his own work. Forever my gratitude and love to my parents and family for instilling in me the awareness of

a sound education and the desire to obtain it and to the youngest member, Barney, who quietly listened and helped in his own special way.

To all of you, thank you.

TABLE OF CONTENTS

APPENDICES

LIST OF TABLES

Table Page

LIST OF FIGURES

Figure Page

CHAPTER I

INTRODUCTION

Since the middle 1960s the synthetic macrocyclic ligands and their complexes have received much attention. Extensive investigation of these polydentate ligands have supplied valuable information concerning these molecules and their interaction with a variety of metal cations.

Several subdivisions of the general class of synthetic macrocyclic ligands may be recognized. The divisions may be based upon the number of rings that make up the molecule, the size of the ring, the type of donor atoms which make up the internal surface of the ring (which act as the binding sites for complexation), or by the presence of substituent groups. Another important variation is the possibility of mixed donor atoms.

The broadest classification and commonly used in literature includes:

(a) Macrocyclic polyethers. This group includes the monocyclic polyethers, as well as their nitrogen and sulfur derivatives, first reported in 1967 by Pedersen (1).

(b) Macrobicyclic ligands. These molecules, referred to as cryptands and first synthesized by Lehn and co-workers (2, 3), consist of a tridimensional intramolecular cavity. The central cavity is formed by the three bridges meeting at common nitrogen atoms on each end of the molecule.

Figure 1 contains examples of some of the many types of macrocyclic ligands which have been synthesized and studied. Also shown in Figure 1 are the IUPAC names given to these ligands as well as the more abbreviated "crown nomenclature." Although the IUPAC provides a very descriptive and unique name for each ligand, it is too complicated for convenience. It was for this reason that trivial names were proposed by Pedersen (1). The assignment of the trivial names to the single cycle ligand may be represented by the general expression x-crown-y, where x is the total number of atoms in the macrocyclic ring, crown is the class name, and y is the number of oxygen atoms (or other donor atoms) in the ring (Figure 1-A). Variation in the type of donor atoms within the ring and their positions (Figure 1-B, 1-C, and 1-D) or any substituents attached to the ring (Figure 1-E) are noted initially. Figure 1-F is an example of a bicyclic ligand. The bicyclic ligands are called "cryptands." Since the bicyclic ligands may have a variable number of ether oxygens in each strand,

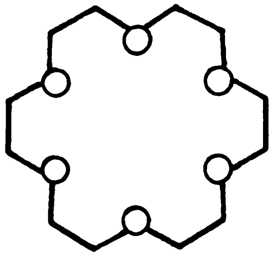

TRIVIAL NAME: 18-Crown-6

IUPAC: 1,4,7,10,13,16-hexaoxacyclooctadecane

Figure 1-A

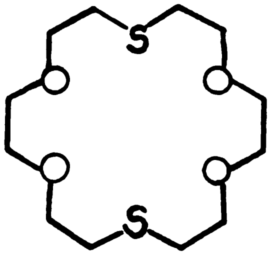

1,10-dithia-18-Crown-6

4,7,13,16-tetraoxa-1,10-dithiacyclooctadecane

Figure 1-B

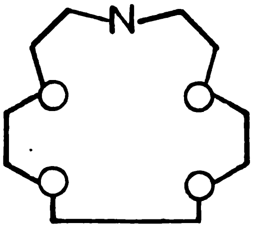

aza-15-Crown-5

4,7,10,13-tetraoxa-1-azacyclopentadecane

Figure 1-C

Fig. 1.--Representative synthetic macrocyclic ligands

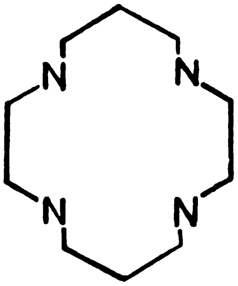

1,4,8,11-tetraaza-14-Crown-4

1,4,8,11-tetraazacyclotetradecane

Figure 1-D

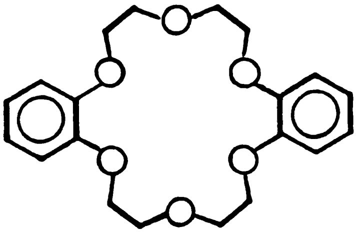

dibenzo-18-Crown-6

2,3,11,12-dibenzo-1,4,7,10,13,16-hexaoxacyclooctadeca-2,
11-diene

Figure 1-E

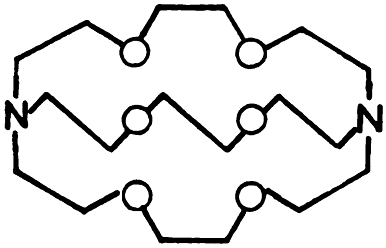

Cryptand-222 (C222)

4,7,13,16,21,24-hexaoxa-1,10-diazabicyclic (8,8,8) hexacosane

Figure 1-F

Fig. 1.--Continued

it is convenient to use the number and the distribution of ether oxygens for coding the cryptand. Thus, cryptand F of Figure 1 is designated by C222.

The attraction of a great number of researchers to the study of the crown and crown-related compounds was a result of Pedersen's findings concerning the binding ability and selectivity the ligands possess for alkali and alkaline earth metals. The ligand-metal complexes formed were stable both in solutions and in the crystalline form. Before Pedersen's work, investigators found alkali salt solutions to be relatively inert toward complexation. Thus began the tremendous and lengthy studies of the complexation properties of the macrocyclic ligands, not only with alkali and alkaline earth cations but also with several transition metal ions.

Although a critical survey of the literature would yield a multitude of articles concerning crown and cryptand complexation, a continuation of these studies is certainly not futile or repetitious. Stability constants of metal complexes are important. These constants are not only important from the point of view of chemical interest but are valuable in many areas of science. For example, in theoretical chemistry they help establish relationships between the stability and certain properties of the ligand or metal ion; in analytical chemistry they allow evaluation of new methods of measurement by a thorough understanding of the extent of interference from system components and in physical chemistry the constants are of interest in studying solution thermodynamics and reaction kinetics involving metal complexes, etc. These values are also of great importance in the various fields of biology when considering the effects of metal ions. Therefore, complete and careful studies of complexation by a variety of techniques are necessary.

The crowns and cryptands do promise applications in different areas of chemistry and biology. The ability of these ligands to selectively bind cations makes possible their use in areas where this selectivity property is important, such as sensing elements in cation selective electrodes (4), in enhancing the solubility of salts in low polarity solvents (5), and in separation processes where they may separate not only different metals (6, 7), but also different isotopes of the same metal (8, 9). They are also excellent models for the naturally occurring antibiotic macrocycles. The cyclic polyethers have not only been shown to be structurally similar to some of the antibiotics but also capable of increasing the transport of alkali metal ions across reconstituted biological membranes (10, 11).

A variety of methods are available for use in studying the formation of the complexes between macrocyclic ligands and metal salts. These include such techniques as calorimetric titration (12, 13), potentiometry with a cation selective electrode (4, 14), electrical conductance (15, 16), optical spectroscopy (17, 18), proton and alkali metal nuclear magnetic resonance (NMR) (19, 20), infrared spectroscopy (21), and distribution equilibria (22).

The work presented here deals with complexation studies of several monocyclic crown compounds utilizing two of the above techniques. Complexation of dibenzo-18C6 (DB18C6) with potassium and, 18C6 and 1,10-dithia-18C6 (DT18C6) with potassium, cesium, and thallium were studied by an extraction technique. The two phase systems were analyzed by the distribution equilibria between the organic and aqueous phases. The intent of this particular study was to compare and contrast the calculated equilibrium extraction constants, due to the cation-crown complexes, of the different metals and ligands employed.

Nuclear magnetic resonance studies were also performed for the mixed donor macrocyclic compound DT18C6 in various nonaqueous solvents. Specifically, Cs-133 and Tl-205 NMR information was collected to deduce the complexing abilities of the sulfur containing crown for the alkali metal, cesium as compared to the toxic, heavy metal thallium.

CHAPTER II

HISTORICAL REVIEW

The ever-growing number of existing synthetic macrocyclic molecules has provided for an exciting area of coordination chemistry research. As mentioned they have already provided many interesting and chemically important applications in the field of metal complexation in solution.

Influences upon Macrocyclic Polyether-Alkali Metal Ion Complexing Stability

Probably the most captivating characteristic of these compounds is their ability to bind cations selectively. This selectivity is a function of not only the various characteristics of the ligand but also of the cation and the solution composition, that is the solvent. Several excellent reviews concerning these parameters, for both the monocyclic and bicyclic ligands, have appeared in literature and, therefore, only a brief description of the effects will be presented and only in reference to the monocyclic crown compounds (23-26).

The metal-ligand complexes are a result of ion-dipole interaction between the cation and the electronegative donor atoms which are symmetrically arranged in the ligand ring. The factors affecting the formation and thermodynamic stabilities of the complexes include:

(a) The relative sizes of the ion and ligand cavity;

(b) The positioning of the donor atoms in the ring;

(c) The type and charge of cation involved in complexation;

(d) The type of donor atom which is present in the ligand;

(e) The number of binding sites in the macrocyclic ring;

(f) Substitution on the crown ring;

(g) The solvent and extent of solvation of the ion and of the donor atoms.

The cyclic polyethers (all donor atoms are oxygens) have been found to exist in predominantly one to one (1:1) metal:ligand complexes. However, depending on the ratio of the diameter of the cavity and metal ion diameters, higher ratio complexes are also formed (27). In the case of the 1:1 complex, Pedersen suggested that the metal was centrally located within the ligand cavity with the oxygen atoms coplanar. This idea was substantiated by x-ray crystal structure analysis performed by Bright and Truter (28). Bush and Truter (29) found that for the potassium complex of DB30C10 and other large ring macrocyclic ligands, the structure of the complex was one in which all the oxygen atoms are wrapped around the potassium ion and are equidistant from it; however, they are not in the same plane.

In reference to the polyethers of 18C6, it appears that the maximum stability, for alkali and alkaline earth cations, occurs in situations where the cation and cavity diameters match. This has also been found for transition metal ions Ag^+, Tl^+, Hg^{2+}, and Pb^{2+} by Izatt and coworkers (12). In the case of smaller and larger ringed crown compounds, not as great a selectivity is observed. In these cases, complexation reactions are complicated by formation of additional species, of stochiometries other than 1:1. Larger crown complexes may exist in which the metal ion is quite small in comparison to the ligand cavity. Hence, cavity size in relation to complex strength loses importance.

The macrocyclic ligands possess a reasonable amount of flexibility and, therefore, conformational changes can often occur during complexation. This idea of nonrigidity appears chemically logical if one considers the basic donor groups, which are directed into the cavity, should possess a repulsive force against each other. In terms of complex formation, Pedersen (30) found that the strongest oxygen donor atom was in a link of $-OCH_2CH_2O-$, followed by $-O(CH_2)_3O-$ and became ineffective beyond $-O(CH_2)_4O-$.

With respect to the alkali and alkaline earth metals, the metal ion appears to the ligand as a positively charged sphere. The binding of the macrocyclic ligand, being electrostatic in nature, requires only that the ligand furnishes an electronically basic environment and that it can successfully compete with the solvation of the cation (15). The smaller ions are more strongly solvated than the larger ions and; therefore, more energy must be gained through ligand-metal complexation to overcome the solvation energy. However, with a small charge density, the localized charge increases the affinity for the ligand. The larger cations possess a comparatively lower charge density, which reduces their affinity for water, and also for the ligand. Therefore, cations of intermediate size yield an optimum change in enthalpy and generally greatest ligand selectivity lies with these ions. In terms of cation charge, the divalent ions generally have larger stability constants than the univalent ions of the same size. Also for large ions the divalent ions are more selectively complexed than the univalent ions. The opposite is true for small ions (24).

Substitution of either nitrogen or sulfur for an ether oxygen in the macrocyclic ring decreases the complexing ability of the ligand for the alkali and alkaline earth metal ions. Frensdorff (4) studied the effect of substitution and reported that for the 18C6 and DB18C6 ligands the potassium ion complexation is weakened by nitrogen and sulfur substitution and that the stability constants decrease in the same order as the electronegativity of the donor atoms, O>NR>NH>S. This is not a surprising trend, since as the negative charge on the heteroatom decreases, the electrostatic attraction between it and the cation lessens. At the same time, however, there is an increase in the affinity toward transition metal ions of proper sizes.

It would seem logical that the larger the number of binding sites, the stronger would be the complex. In the case of the polyether ligands, Pedersen (1) found that those containing five to ten oxygen atoms form the most stable complexes with the alkali and alkaline earth ions, with several transition metal ions, and with several quaternary ammonium organic cations. Cram and coworkers (31) reported that 18C5 complexed t-butylammonium to a much lesser degree than 18C6. Progressive replacement of oxygen atoms by sulfur atoms in the ring increases the stability of silver (I) and mercury (II) complexes (4).

Izatt et al. (12) studied the complexation selectivity of 18C6 and substituted 18C6 ligands. For the two isomers of dicyclohexyl-18C6 (DCH18C6), with cis-syn-cis and cis-anti-cis conformation, quite different stability constants were obtained, with alkali and alkaline earth metal ions, transition metal ions, and quaternary ammonium organic cations. In comparison to the unsubstituted 18C6, complexation of bivalent cations with DCH18C6 (except for Ba^{2+}) yielded enhanced stability constants, for the cis-syn-cis isomer, but no effect was observed on the selectivity for univalent cations. Substitution in the cis-anti-cis conformation lowered the stability of complexes with univalent cations (except in the case of Na^+ and Ag^+) but showed little change with the bivalent cations. Izatt interprets the results as an indication of the cis-syn-cis isomer's cavity being better defined and less sensitive to conformational changes due to the ring rigidity attributable to the cyclohexyl groups.

A comparison of the stability constants of DB18C6 complexes to those of 18C6 complexes shows a more dramatic effect. In methanol solutions the complexation of 18C6 with Ba^{2+} is an order of magnitude greater than with K^+. However, if DB18C6 is used as the ligand, the K^+ binds more strongly than the Ba^{2+}. Lamb et al. (23) have discussed the above results and concluded that the bulkiness of the ligand isolates the cation from the solvent by the hydrophobic groups, which prevents the regain of energy lost in desolvating the cation. The desolvation energy required for a dipositive ion is greater than for a unipositive ion resulting in a destabilization of the complexes of the former species.

In solution studies of ligand-cation complexation, a competition for the cation exists between the ligand and the solvent. Because of this competition and because of the varying properties of different solvents, it is not surprising that the stability constant of a given cation-ligand complex depends upon the environment created by the solvent medium. This dependence may also cause a change in the selectivity of a particular ligand. Arnett and Moriarity (32) observed such change in selectivity in their calorimetric study. Heats of complexing were obtained by measurement of the partial molar heat of solution ($\Delta\bar{H}_s$). Two methods were employed: first, the salt in pure solvent and in a crown ether-solvent solution were measured; and, secondly, by measuring $\Delta\bar{H}_s$ of the crown in pure solvent and then in a salt-solvent solution. It was explained that if there is no ion pair interactions (between the uncomplexed cation and the associated anion), it may be assumed that the formation constant, as well as the enthalpy of formation, for the complex is determined solely by the competition between the ligand and solvent. They explained that the single ion enthalpies of transfer vary in different solvents being greatest for small ions of high charge density. The greatest apparent selectivity of DCH18C6 was found in dimethyl sulfoxide (DMSO) and water, which strongly solvate small cations. With less polar solvents, the fit of the cation in the ligand cavity is more important, with less affinity for the solvent the selectivity factor is reduced. Although the dielectric constant of the solvent has been shown to influence complex stability, it is not the only parameter which affects the stability. Matsuura and coworkers (33) have reported formation constants for alkali metals with DB18C6 in DMSO, dimethylformamide (DMF), and propylene carbonate (PC) and found that the values obtained were in the order of DMSO<DMF<PC. The dielectric constants increase in a different order, DMF<DMSO<PC. Upon consideration of their data they concluded that the donor ability of the solvent also has an important influence on the complexation reaction.

Polythiaethers and Sulfur-Oxygen Mixed Donor Ligands

Structural and complexation studies conducted on many known macrocyclic ligands have been extended to crowns containing donor atoms other than oxygen. These include macrocycles containing either nitrogen or sulfur as the only donor atom, as well as those containing mixed donor atoms, such as oxygen and nitrogen, oxygen and sulfur, nitrogen and sulfur, or all three donor atoms in one ligand.

The interest in this work has been on the mixed donor system containing oxygen and sulfur. However, in order to obtain a better understanding of the affects of an increasing number of sulfur donors, a discussion of cyclic polythiaethers is in order.

Synthesis of these ligands has been performed by several groups (33, 34). The total replacement of the oxygen donor sites in a macrocycle with sulfur causes the ligand to completely lose its complexing ability for the alkali and alkaline earth metals (35).

Black and McLean (36) report that while the macrocycle polyether, 18C6, most often maintains a planar configuration in its metal complexes, the corresponding polythiaether hexathia-18C6 (HT18C6), behaves as a sexadentate ligand, and forms octahedral complexes. Complexes of the HT18C6 ligand with nickel and cobalt were discussed. Rosen and Busch (37, 38) have also prepared and studied octahedral complexes of some smaller ring polythiaethers, 1,4,7,10-tetrathia-13C4, 1,4,7,10-tetrathia-12C4, and 1,5,9-trithia-12C3. These complexes, with nickel (II) tetrafluoroborate were shown to possess a ligand:metal ratio of 3:2 for the first two ligands and 2:1 for the last. Glick and coworkers (39) have also studied the copper-1,5,8,12-tetrathia-14C4 complex and determined its structure as a tetragonal Cu (II) complex, 1:1 stoichiometry, with the associated anion filling the other two coordination sites.

The configuration of the cation-ligand complex is dependent on the ring size and number of sulfur groups (40), which has been demonstrated for the Ni (II) cation (36-38). A tridentate macrocycle gave a complex with a 2:1 ligand to metal ratio, which was interpreted as the formation of a sandwich structure with the metal ion located between the two ligands. In the case of the tetradentate ligands, for ring size of over 14 atoms, the metal ion was found to be within the ligand ring, and in the same plane. With rings of less than 14 atoms, complexes were formed with a 3:2 stoichiometry.

Alkali and alkaline earth metal ions show no evidence of complexation with polythiaether crown ligands. However, complexation is expected with the mixed ligands. Of interest here are those ligands containing sulfur and oxygen as metal binding sites. The synthesis of the oxygen and sulfur containing crown ligands has been performed by several researchers. As early as 1933, Meadow, Tucker, and Reid (41, 42) prepared several sulfur-containing crowns as well as the mixed donor system ligand 1,4,10,13-tetrathia-18C6. The ring compounds were obtained by the reaction of a polymethylene halide with a polymethylene mercaptan. In 1961, Dann, Chiesa, and Gates (33) reported the synthesis of 1,10-dithia-18C6, 1-thia-12C4, 1,7-dithia-12C4, and 1,13-dithia-24C8. They found that by using increased dilution of the reaction mixture, higher yields of the product of interest could be obtained. Pedersen (43) described the preparation of several macrocyclic polyethers (15C5 and 18C6) in which two to four -O- linkages were replaced by -S- linkages.

Probably the most thorough study of synthesis and product yield optimization was conducted by Bradshaw and coworkers (44-47). The macrocyclic polyether sulfides they synthesized were prepared by reacting an oligoethylene glycol dichloride with a dithiol or sodium sulfide in ethanol. Thia-crown-3 through -8 have been prepared. Bradshaw was able to increase the reaction yield by maintaining high dilutions. The oligoethylene glycol dichloride/ethanol solution was added dropwise to the reaction flask containing dithiol (or sodium sulfide) in ethanol, with rapid stirring.

Crystal structure determinations of three cyclic sulfur-containing polyethers, thia-crown-4, -5, and -6, have been performed by Dalley et al. (48). In all three cases the sulfur atoms were directed away from the ring cavity. In the case of the 1,10-dithia-18C6 (DT18C6), the donor atoms were nearly coplanar and formed an elliptical cavity, with the shortest distance across the ring of 4.6A (since the sulfurs are directed away from the ring interior, this is the distance between the symmetry-related oxygen atoms).

In terms of metal ion complexation, Pedersen (43) predicted differences between the polyether and sulfur substituted crown ligands. Oxygen is smaller than sulfur and the bond angle C-O-C is greater than the C-S-C bond angle; therefore, in the sulfur substituted ligand, the symmetrical distribution of negative charge around the cavity is disturbed by the larger atom's presence. Results of his preliminary complexation studies with potassium and sodium ions agreed with his expectations.

Frensdorff (4) prepared the crown DT18C6 and potentiometrically studied its complexating abilities with potassium and silver ions in methanol. In the case of K^+ ion a much stronger complex was formed by 18C6 ($\log K_f = 6.10$) then by DT18C6 ($\log K_f = 1.15$). The opposite results were observed with the silver ion, where the stability constants are $\log K_f = 1.60$ and $\log K_f = 4.34$, respectively. Frensdorff attributed these findings to the bond formation not being purely electrostatic for complexation with DT18C6. The silver ion has the ability to form ionic bonds with oxygen atoms and covalent bonds with the sulfur atoms, while the potassium ion may only form ionic bonds.

Izatt et al. (23) have determined stability constants for 1,7-dithia-15C5 with silver (I) and mercury (II) metal ions, in aqueous solutions. Although both 1:1 and 2:1 (ligand:metal) complexes were reported to exist, only the stability constants for the reaction $ML^+ + L \longrightarrow ML_2^+$ were given. They obtained log K = 2.71 for the Ag^+ complex and 2.91 for the Hg^{2+} complex.

Metz et al. (49) reported that in the crystal structure of the complex of $PdCl_2$ and DT18C6, only the sulfur atoms of the ligand were involved in the metal binding, forming a cis-square planar configuration with the Pd atom lying outside the cavity. Dalley (23) also found, by x-ray crystal structure determination, that the mercury atom in the $HgCl_2$ complex with 1,4-dithia-18C6 binds only the two sulfur atoms and lies outside the ring. These results may explain why no macrocyclic effect* is seen in these thia-substituted ligands (23). No macrocyclic effect would be expected if only outwardly turned sulfur donors are the actual complexation sites.

---

*The macrocyclic effect refers to the increased stability of a metal complex coordinated to a macrocycle ligand over that of its openchain analogue.

Metal Ion-Crown Complexation Studies by the Extraction Technique

The procedure of solvent extraction for the determination of the extent of metal-crown ligand complexation was first used by Pedersen (5). The studies performed were qualitative and used only for comparing the relative complexing powers of the cyclic polyethers for different cations. Although his work did not provide for a mathematical analysis of the data, it did supply a foundation for development of a technique to measure formation constants.

The technique involves the extraction of ion pairs (M^+ Picrate$^-$) from an aqueous to an organic phase. Ion pair extractions have not been used much with the alkali ions until the crown-type compounds were prepared. It was assumed that these ions were not capable of forming stable cationic complexes.

The extraction takes place between an immiscible system of an aqueous and an organic phase. The aqueous solution contains the metal of interest, either in the hydroxide form or as a salt, and a low concentration of picric acid. The organic phase contains the crown ligand whose complexing abilities are to be measured. The presence of the hydroxide ion in the aqueous phase is necessary to maintain the picrate in the anionic form. When an equal volume of each phase is shaken and allowed to reach equilibrium, a certain amount of the picrate ion is extracted into the organic phase. The key to the extraction is the presence of the crown ligand in the organic phase solubilizing the metal salt or hydroxide. The amount of the metal ion extracted by the organic phase is proportional to the stability of the crown-metal complex. Naturally, in order to maintain electrical neutrality, the complexed cation is extracted as a picrate, $ML^+ Pic^-$. Blank experiments have shown that in the absence of the crown, picrate is not extracted into the organic phase.

Picrate lends itself well to this type of study for two reasons:

(a) It has an absorbance band in the ultraviolet region and, therefore, its concentration can be determined by optical spectroscopy.

(b) The presence of a large anion, such as picrate, is necessary to measure the extent of cation extraction. Large anions, which possess low charge density and consequently low hydration energy, are more easily extracted into low dielectric constant solvents, hence favoring the solubilization of the cation into the organic phase. The stoichiometry of the ion pair complex formed in the organic phase is 1:1:1 in respect to crown, cation, and picrate anion; therefore, the determination of the picrate concentration in the organic phase, following extraction, is also the concentration of complex formed.

Although Pedersen's method was developed using picrate, other anions may be employed. Recalling the necessity of a large and highly polarizable anion, salts of such anions as fluoride or sulphate are inappropriate, while the iodide, thiocynate, permanganate, and fatty acid anions may be solubilized more easily (15).

In terms of the choice of the appropriate organic solvent, Pedersen (5) found that the overall efficiency of the extraction process decreased and the selectivity increased as the dielectric constant of the organic solvent decreased. However, high dielectric constant solvents are undesirable since the solvent must be immiscible with the aqueous phase.

The extraction technique proved to be helpful in investigating the crown complexating capabilities. Frensdorff (22) began studies to develop a more quantitative approach. He complimented Pedersen's procedure with his work by establishing the equilibria governing the processes, taking place between the phases, and analyzing them in terms of the underlying molecular processes. He analyzed the overall equilibrium in terms of three constituent equilibrium:

(a) Complex formation in the aqueous phase

(b) The partitioning of uncomplexed crown

(c) The partitioning of the complex itself

Frensdorff was also able to calculate a dissociation equilibrium constant of the complex cation-picrate ion pairs within the organic phase.

In his original work on the extraction technique, Pedersen (5) found that the counter ion of the principle salt had no effect on the extent of extraction observed, provided the salt was soluble in water. He performed a metal ion extraction, by DCH18C6 in methylene chloride, using NaOH as the sodium ion source in the aqueous phase. An identical system using NaF, rather than NaOH, was prepared and identical results, for the percentage of picrate extracted, were obtained. This will be true for any system as long as there are no cation-anion interactions in solution. However, the nature of the anion directly involved in the ion pair complex formation is very important.

Jawaid and Ingman (50) investigated the influence on extraction efficiency of different anions, such as dinitrophenols, picrates, and dipicrylamine, that can ion pair with the cation-crown complex. They used DCH18C6 and methylene chloride as the organic phase components and compared the extraction equilibria of the ion pairs formed with Na^+, K^+, and Ca^{2+}. As expected, the extraction increased in the order Ca<Na<K and reflected the increasing strength of the complexation between the ligand and metal. They found that the efficiency of extraction increased but the selectivity decreased with the hydrophobicity of the anion employed.

A variety of papers describing the use of the extraction technique in macrocyclic research have been published. In most cases either 18C6 or one of its substituted forms have been used in these studies. Some of the studies were analyzed by the equilibria proposed by Frensdorff; others made different assumptions in order to simplify the calculation of the extraction equilibrium constant.

Kopolow et al. (51, 52) synthesized 4'-vinyl derivatives of monobenzo-15C5 and monobenzo-18C6 and polymerized them quantitatively to high molecular weight polymers. Several different studies were performed to characterize their efficiency and selectivity in binding cations as compared to their monomeric analogues. Data were obtained by using a number of techniques. In salt distribution equilibria, studies in a water-methylene chloride system, they observed that for all cations the polymeric form of the crowns were found to extract more efficiently. The greater efficiency of the crown polymers was attributed partially to differences in the partitioning of the crowns between the two solvents.

The authors present extraction equilibrium constants for all systems studied; however, the calculations were based on the assumption that no ion pair dissociation occurs in the organic phase, which may be unrealistic. More correctly, as the authors themselves point out, their values should be considered as apparent equilibrium constants.

Sadakane and coworkers (53, 54) have employed the extraction technique using benzene as the organic phase. Their studies dealt with the extraction of alkali metal picrates with DB18C6 and 18C6. In both cases the extractability of complex cation-picrate ion pairs was found to decrease in the order K>Rb>Cs>Na. In their study of DB18C6 complexes, thermodynamic values of the enthalpy change, entropy change, and free energy change due to complexation are presented. The validity of these quantities is questionable since their value is dependent on the extraction constants, which in the mathematical treatment used, did not consider the dissociation of the complex ion pairs.

Mitchell and Shanks (55) studied the extraction of sodium into chloroform, by crown complexation, forming the ion pair complex $(Na\cdot DCH18C6)^{+}Ph_4B^{-}$. The accurate determination of quantities in the order of $\mu g\ Na^{+}/g$ sample was made possible by thermal neutron irradiation of standard and sample solutions, followed by comparison of the sodium isotope activity. Analysis of the interference effects of other alkali and alkaline earth metal ions, a few transition metals, and various anions were performed, producing little effect except in the case of K^+. Primary standard sodium oxalate solutions and silicon dioxide samples showed high precision in both separation and determination of sodium.

Jaber and coworkers (56) conducted studies designed to investigate the complexing abilities of nonylphenoxypoly (ethyleneoxy) ethanols (NP), a series of nonionic surfactants used in industry, with alkali and alkaline earth metal ions. The rigid cyclic arrangement of donor atoms, as the crowns possess, is not a necessity for complexation of a neutral molecule and metal cation. These workers examined the complexing tendency of the open chain structure of NPs in hopes of using these molecules as ion-selective electrode sensors. The extraction technique, between methylene chloride and water, was utilized to assess the extent of metal ion complexation by NP. The order of stability for the alkali metal ion-NP complexes was found to be Rb>K>Cs>Na>Li, while for the alkaline earth metal ions the stability decreased Be>>Ba>Sr>Ca>Mg.

A number of papers have been recently published dealing with the coextraction of water with alkali and alkaline earth metal hexanitrodiphenylaminates (HNPA) into nitrobenzene (57-59). Since the cations are strongly hydrated, the water molecules are transferred to the organic phase with the cation and with HNPA as water-separated ion pairs. The authors found that in the presence of a number of different crowns the cationic hydration number decreases, implying partial replacement of water molecules by the oxygen atoms of the crown. In several cases the number of released water molecules almost equaled the number of donor atoms of the crown.

Danesi and coworkers (60) performed several extractions using DB18C6 in various nitrobenzene-toluene mixtures, against aqueous solutions of the alkali metals. They found the same selectivity sequence, $K^+ > Rb^+ > Cs^+ > Na^+ > Li^+$, for all diluent compositions. Independent of the relative amounts of nitrobenzene and toluene in the organic phase, the same value for the selectivity constant (within error) of the reaction $Cs^+ + MLPic_{org} \rightleftharpoons CsLPic_{org} + M^+$ was observed for all the alkali metals, implying an apparent isostericity of the complexes. These results were attributed to the presence of water molecules shielding the cation, within the crown, from surrounding solvent medium. To substantiate this line of reason, Danesi et al. (61) conducted a study of Na^+ and K^+ complexes with DB18C6 in solvent mixtures that were carefully dried. In these studies they were able to detect differences in the selectivity constant due to the dissimilar interionic attractions in the ion pairs of Na^+ and K^+. These studies showed that the additional shielding the water molecules supplied the complexed cations was enough to considerably reduce any difference in the closest approach distance allowing for isosteric behavior of the complexes.

Danesi and coworkers (62) also prepared a substituted DB18C6 macrocycle in which four neutral alkyl t-butyl groups were placed on the benzene ring, in hopes of improving the solubility of DB18C6 in the organic phase. Studies in various nitrobenzene-toluene mixtures, with the cesium ion, indicated an enhancement in solubility; however, a slight decrease in cation complexation was also observed most probably due to steric effects.

In a more recent publication of the use of the extraction technique with polyethers by Marcus and Asher (63), comparative extractions of alkali metal halides are discussed. Studies were conducted in a variety of solvents and an attempt was made to correlate their findings with solvent properties. They report the order of extractibility among the halides as F>I>Br>Cl.

Sekine et al. (64) extended the use of the extraction procedure to include thallium cation (I and III) complexation in benzene and chloroform. The quantity of Tl^+ extracted into the organic phase by DB18C6 was determined by atomic absorption. The extraction equilibrium constant for the complex was calculated and compared to those of alkali metal ions in benzene. The equilibrium extraction constant they reported for thallium was log K = 4.49, as compared to sodium 2.20, potassium 4.65, rubidium 3.75, and cesium 3.07.

Sulfur-substituted polyethers have also been studied by the extraction technique. Pedersen (43) performed extractions of K^+, Na^+, and Ag^+ with several of these ligands in methylene chloride. The picrate extracted (the indicator of complex formation) was less than 6% for K^+ or Na^+ with the sulfur substituted crowns; however, excellent extraction efficiency was obtained with the silver ion.

Sevdic and Meider (65, 66) studied the complexing abilities of 1,4,8,11-tetrathiacyclotetradecane (TTP) and 1,4,8,11,15,18,22,25-octathiacyclooctacosane (OTO) for silver (I) and mercury (II), chloride and perchlorate, by extraction between water and nitrobenzene. They have shown the enhanced complex strength of the sulfur containing crown molecules with Ag^+ and Hg^{2+}. For example, they have reported extraction equilibrium constants $\log K_e = 11.11$ for $Hg(ClO_4)_2$ complexation with TTP and $\log K_e = 12.13$ for the ligand OTO.

Raman Studies of Solvation and Ion Association

The existence of a weak complex between 18C6 and the solvent acetonitrile (ACN) has served as an intermediate in the purification of the crown, as described by Gokel and coworkers (67). However, it has not been determined if the complex produces any observable change in the Raman spectrum, compared to the spectra obtained for pure 18C6 and pure ACN.

Both infrared and Raman spectroscopic methods are of great value since they provide information at the molecular level, allowing even weak local intermolecular forces to produce rather easily observable frequency changes in the intramolecular vibrations (68).

Several studies have been conducted in which IR or Raman, or both, techniques have been used to study solvation and ion association in nonaqueous solutions. These spectroscopic methods have also been used in studies of Li^+ (68), Mg^{2+} (68), and Na^+ (68, 69) perchlorates, of Na^+ and K^+ DB18C6 complexes (20), and of Li^+ and Na^+ cryptates (70) in several nonaqueous solvents. Even more specifically to the case to be presented here are studies performed using the solvent acetonitrile and observing its characteristic C≡N (2253 cm^{-1}) and C-C (919cm^{-1}) stretching frequencies change, as a function of electrolyte concentration. Balasubrahmanyam and Janz (71) studied the $AgNO_3$-CH_3CN system at various concentrations of $AgNO_3$. Analysis of the concentration dependence of the relative intensities and frequencies obtained of the C≡N and C-C bands in $AgNO_3$-CH_3CN

solutions helped in understanding the solute-solvent interactions occurring in the solution. These authors reported the appearance of bands at 928 cm^{-1} and 2272 cm^{-1} (in addition to the 2253 cm^{-1} and 919 cm^{-1} bands) which were attributed to the C-C symmetric stretch and C≡N symmetric stretch of the complex, respectively. Chang and Irish (72) extended the above studies by further characterizing the system, measuring the formation constant of the ion pair species $Ag^+NO_3^-$. They also provided evidence for multiple ion aggregates and the solvation of the Ag^+ and $Ag^+NO_3^-$ in solution.

Nuclear Magnetic Resonance

To a solution chemist, or in fact to any individual interested in studying a chemical reaction occurring in some solvent, a knowledge of what species are present and the influence of solvent properties is of utmost importance. However, this is only the beginning of the complex behavior of the different species which may be present. A variety of interactions, including solute-solute, solute-solvent, and solvent-solvent type, add tremendous complexity to any solution. The result of solute-solute interaction is the formation of ion pairs, which may be a single anion-cation attraction or be composed of several ions forming higher aggregates, depending on the nature of the ion. Two properties of the solvent come into play here:

(a) The dielectric constant of the solvent

(b) The solvent donor capabilities (solvating ability)

Solvent-solvent interactions of a given solvent may also change from solution to solution depending upon the nature of the ionic species introduced. In addition to the reaction under study, these solvent-solvent interactions may be important.

Many spectroscopic techniques have been used in hopes of understanding the variety of interactions occurring in a simple solution. One of the more recently utilized techniques is nuclear magnetic resonance (NMR), which has proved to be very sensitive to these solution interactions.

Alkali metal NMR has been studied extensively in this laboratory, not only in relation to the study of ionic association and solvation of alkali metal salts, but also in complex formation with a variety of ligands, particularly tetrazoles and macrocyclic crown ethers.

An older but very excellent review of NMR as an investigative tool for the study of ions in different solvents has been published by Hinton and Amis (73). A more recent review of specifically alkali metal NMR has been presented by Popov (19). Popov discussed the importance of this technique in studying the immediate chemical environment of alkali metal ions in solution. The NMR studies of solutions of alkali salts, alone and in the presence of a complexing ligand, were shown to be helpful in better understanding both solvation and complexation of these cations.

Cesium-133 NMR

A number of investigations of ionic association and solvation have been reported using nuclear magnetic resonance of ^{133}Cs. Those reported by DeWitte (74), Hsu (75), Mei (76), and Hourdakis (77) have characterized ion pair formation of the cesium salts and cesium complexation with crowns and cryptands, in several nonaqueous solvents, through chemical shift studies. The physical properties of the ^{133}Cs nucleus are shown in Table 1.

Different chemical shifts arise from the fact that the magnetic field experienced by the nucleus depends upon its environment and is not the same as the applied field. The screening of a nucleus, represented as the shielding constant (δ) incorporates several terms.

$$\delta = \delta_d + \delta_p + \delta_o$$

The diamagnetic shielding factor (δ_d) arises from the induced magnetic field due to the circulation of electrons around the nucleus. The paramagnetic term (δ_p) is a deshielding factor caused by the interaction of ground state with excited electronic states in the presence of the magnetic field. The shielding of the

Table 1. NMR Properties of the ^{133}Cs and ^{205}Tl Nuclei.

	^{133}Cs	^{205}Tl
Resonance frequency at 14.09 kgauss field (MHz)	7.8709	34.6113
Natural abundance (%)	100	70.48
Relative sensitivity for an equal number of ^{1}H at constant field	0.0474	0.192
Nuclear spin (in units of h/2π)	7/2	1/2
Nuclear magnetic moments (in units of nuclear magnetons, $^{eh}/4\pi Mc$, with diamagnetic correction)	2.579	1.627
Electric quadrapole moment (in multiples of barns, $10^{-24}cm^2$)	-0.003	
Relaxation time (T_1, in secs)	13	0.4

resonant nucleus by other atoms is represented by δ_o. The relative importance of the paramagnetic term increases as the number of electrons around the atom increases (78). For nuclei larger than ^{7}Li, δ_p is the dominant factor in determining the shielding constant (79).

DeWitte (74) studied the ^{133}Cs chemical shift of several cesium salts in different nonaqueous solvents and in water as a function of concentration. His results showed only a small concentration dependence of the chemical shifts for solutions of cesium perchlorate and tetraphenylborate but comparatively large dependence of similar solutions of cesium thiocynate, iodide, bromide, and chloride. The constancy of chemical shift with a changing concentration implies no ion pair formation whereas a concentration dependence is evidence of contact ion pair formation. From the data obtained, association constants (ion pair formation constants) were determined.

Hsu (73) reported several formation constants for complexes of different cryptands with cesium in a number of solvents. A temperature dependence study was also conducted for complexes in pyridine.

Mei's (76) work was concerned with the complexation of polyether crown and cryptand compounds with cesium salts. Complex formation constants were obtained for all systems studied and thermodynamic data (ΔG, ΔH, and ΔS values) was calculated from a temperature dependence study of cesium tetraphenylborate with 18C6 and C222.

Complexation studies of the dilactam of C222 by ^{133}Cs NMR were reported by Hourdakis (77).

The historical section of these theses amply cover the literature through 1977 and will not be presented again.

Thallium-205 NMR

The alkali metal ions have been shown to fulfill at least three functions in biological systems:

(a) Neutralization of ionic charges and maintainance of macromolecular conformations;

(b) Enzyme activation;

(c) Maintainance of a membrane potential for nerve and muscle function.

Several studies have shown that thallium (I) may substitute for alkali metal ions performing a number of these same functions (80). As a result of these findings, the study of the properties of thallium have proved interesting and seems to be a logical extension of alkali metal complexation studies.

Table 2 shows some physical properties of thallium (I) nucleus and of the alkali metal cations. The ionic radius of Tl^+ is quite similar to that of K^+ but the

Table 2. Physical Properties of Thallium (I) and the Alkali Metal Cations

M	Ionic Radii M^+ (A)	Polarizability M^+ (A^3)	Electronegativity M^+	Electron Affinity	Enthalpy of Hydration (kcal. $mole^{-1}$)
Li	0.86	0.03	0.98	0.60	-134
Na	1.12	0.41	0.93	0.35	-107
K	1.44	1.33	0.82	0.30	- 87
Rb	1.58	1.98	0.82	0.27	- 80
Cs	1.84	3.34	0.79	0.23	- 76
Tl	1.54	5.2	1.62	0.32 or 1.21	- 92

molecular polarizability of Tl^+ is considerably greater than that of any alkali ion. Therefore, the nature of bonding and, in general, solution behavior of Tl^+ should be quite different from those of the alkali ions. From the enthalpy of formation, shown in Table 2, one may see that Tl^+ is only weakly hydrated in solution.

Several workers have used ^{205}Tl NMR as a technique to study some problems of biological importance, using thallium as a probe of the role of alkali ions. For example, Reuben and Kayne (81, 82) have found ^{205}Tl NMR suitable for the investigation of the binding of thallium ions to biological macromolecules and have utilized it in a study of the complex between Tl^+ and rabbit muscle pyruvate kinase as well as of substrates of this enzyme. It had previously been shown that both a monovalent and divalent ion must be present for the pyruvate kinase enzymatic reaction to occur, but the role of the monovalent ion had not been understood. These workers determined the number of monovalent binding sites in the enzyme through substitution of Tl^+ for K^+.

Thallium-205 NMR has also become an important technique in examining solvation, solution structure, and complexation of thallium salts. The physical properties of the ^{205}Tl nucleus are shown in Table 1. The solvent dependent chemical shift for ^{205}Tl may be as great as 2600ppm, depending on the particular thallium salt and solvent under study, while ^{7}Li is 5ppm, ^{23}Na is 23ppm, ^{39}K is 35ppm, and ^{133}Cs is 120ppm. This greater range of chemical shifts should make ^{205}Tl a better probe of smaller changes in the environment of the nuclei (83). The spin-lattice relaxation time has also been shown to be strongly solvent dependent (84).

Freeman et al. (85, 86) have reported chemical shift data for different thallium salts in aqueous solutions. They found that at low concentrations the chemical shift varied nonlinearly with concentration of anion, which was attributed to ion pair formation. In solutions of higher concentration the variation of chemical shift with concentration was linear, which Freeman explained as being due to the effect of ions on the hydration atmosphere of the ion pair. The shift extrapolated to zero anion concentration is characteristic of the free solvated thallium (I) ion. In the second publication, these workers reported chemical shifts and line widths of solid thallium (I) and (III) compounds, as well as for aqueous solutions of thallium (III) salts. Line widths of the solid compounds were quite broad so that the precision with which the chemical shifts were measured was low. Line broadening in the solutions was explained by assuming varying contributions from spin-spin coupling between both the Tl^{+} ion and the anion and between unlike thallium isotopes.

Several studies concerning the solvent and anion dependence of chemical shifts have been performed by Dechter and Zink (e.g., 81 and 87). They reported chemical shifts extrapolated to infinite dilution in a number of nonaqueous solvents. The aim of the investigation was to determine whether or not the change in chemical shift was related to specific donor atoms or groups or corresponded to the Lewis basicity of the solvent. The results showed that there were two regions of shifts, one related to nitrogen coordinating and the other to oxygen coordinating solvents. An attempt to find a correlation between the chemical shifts and some bulk solvent property or some measure of solvent polarity was not possible. In contrast to Dechter and Zink's results, Hinton and Briggs (88) reported a reasonable correlation of the extrapolated infinite dilution resonance frequencies with solvent Gutmann donor number;[*] the resonance frequency increased with increasing donor number. They also found that the lower donor number solvent, DMSO, solvated the thallium ion better than did pyridine (py). This was also found by Popov and coworkers (89) in ^{23}Na NMR studies and explained in terms of solvent structure effects. Hinton

---

[*] Defined as the negative of the enthalpy of interaction of a base with $SbCl_5$ when the two are dissolved in equimolar amounts in an inert solvent, 1,2-dichloroethane.

and Briggs (90), in agreement with Popov's reasoning, explained that this phenomenon was due to a large solvent structural effect or to a steric effect related to the size of the py molecule which favors solvation of Tl^+ by DMSO.

Hinton and Briggs have done several preferential solvation studies of thallous ion occurring in binary systems of all combinations of water, formamide, N-methylformamide, and N-ethylformamide (91) as well as water, pyridine, and dimethyl sulfoxide (90). From their chemical shift data of ^{205}Tl and the solvent Gutmann donor numbers, they calculated needed donor numbers by a linear least squares analysis. They derived mathematical expressions for their binary systems to calculate the chemical shift due to donicity effects and assigned the difference, between this value and the observed chemical shift, to the shift caused by structural effects. They concluded from their findings that steric and structural effects are quite important in liquid ion-solvation processes, in fact, often more so than donicity effects.

Early studies of aqueous thallium-DB18C6 complexation were conducted using ultraviolet spectroscopy by Pedersen (1) and Shchori et al. (92). Koryta and Mittal (93) calculated stability constants of alkali metal ions and thallium ion for DCH18C6 by electrochemical reduction of the metal complexes at a dropping mercury electrode. Rodriguez and coworkers (94) reported a kinetic study of the complexation of Na^+, K^+, Rb^+, Tl^+, and Ag^+ cations with 15C5 in aqueous solutions by ultrasonic absorption using a laser acousto-optic technique.

The NMR technique has been employed recently for studies with both macrocyclic polyethers and cryptands. Srivanavit and coworkers (95) developed a method of measuring stability constants of several univalent cations relative to the thallium ion, with a number of polyethers, by ^{205}Tl chemical shifts. Measurements were obtained in methanol, dimethylformamide, and dimethyl sulfoxide. Concentration, anion, and solvent effects are discussed in conjunction with the method.

Complexation of thallium with cryptand C222 has been studied revealing the stability constant of Tl^+ in water to be greater, by an order of magnitude, than any of the alkali metals (96). The alkali metal ion complexes with C222 show a good correlation between the ionic radius and the stability constants; however, the stronger complexation with thallium implies that other effects must also be important here.

CHAPTER III

EXPERIMENTAL MATERIALS, INSTRUMENTS, AND PROCEDURES

Materials

Reagents

Hydrochloric acid (Mallinckrodt), picric acid (J. T. Baker), phosphorus pentoxide (Fisher), calcium chloride (anhydrous, J. T. Baker), sodium carbonate (anhydrous, Mallinckrodt) as well as all hydroxides of the metals, lithium ($LiOH \cdot H_2O$, Ventron-Alfa), sodium (Drake Brothers and Fisher), potassium (Fisher and Matheson, Coleman and Bell), and cesium (Ventron-Alfa, 99.9%), were used as received. Potassium hydrogen phthalate (Matheson, Coleman, and Bell), used in the standardization of the hydroxides, was dried at 110°C for at least two hours prior to use.

Potassium acetate (J. T. Baker) was dried in an oven at 110°C for 24 hours. While cesium perchlorate (Alfa Inorganics, 99%) necessitated drying at 110°C for a minimum 24 hours, the other cesium salts used required additional treatment. Cesium acetate (Alfa, technical) was recrystallized from methanol and vacuum dried over P_2O_5 for 48 hours. Cesium thiocynate (Rocky Mountain Research) was recrystallized from absolute ethanol and vacuum dried. Cesium tetraphenylborate* was precipitated from a metathetical reaction of sodium tetraphenylborate and cesium chloride in a mixed solvent system of tetrahydrofuran and water. The precipitate was filtered and washed with conductance water followed by drying under vacuum for 48 hours.

Both thallium nitrate (Ventron-Alfa) and thallium perchlorate (K and K) were dried at 110°C for 1.5 hours, while thallium acetate (Ventron-Alfa, ultrapure) was dried under vacuum for 48 hours. Thallium thiocynate was prepared by the addition of thallium acetate to sodium thiocynate solution (J. T. Baker) in methanol and dried under vacuum.

Ligands

The complexing ligands used in this work are macrocyclic crowns 18C6, DB18C6, and DT18C6. The 18C6 (Aldrich) was purified by forming a complex with acetonitrile (Matheson, Coleman, and Bell), according to the method developed by Gokel and coworkers (67). In addition, Shih (97) suggested that the procedure be

---

*Synthesis performed by Adamantia Hourdakis.

followed by dissolving the 18C6 in a minimal quantity of acetone (Drake Brothers) and vacuum filtering to remove any remaining impurities. The recrystallized 18C6 was dried under vacuum for 48 hours. Dibenzo-18C6 (Aldrich) was dried over P_2O_5 under vacuum for 48 hours. The melting point agreed well with the literature value of 164°C (1).

The sulfur-substituted DT18C6 was successfully synthesized following Bradshaw's procedure (44) to prepare 1-thia-9C3; DT18C6 is a solid by-product of this synthesis. An oligoethylene glycol dichloride was allowed to react with sodium sulfide as shown in the reaction

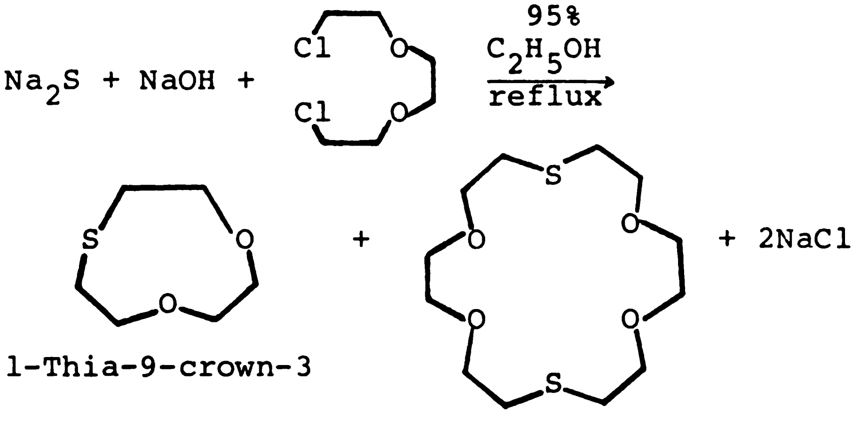

1-Thia-9-crown-3

1,10-Dithia-18-crown-6

A solution composed of 48g sodium sulfide nonahydrate (Mallinckrodt) and 0.96g sodium hydroxide (Drake Brothers), in 95% ethanol, was prepared and placed in a large three-necked round bottom flask. Also prepared was a solution containing 37g bis-(2-chloroethoxy)ethane (BCEE) (Eastman) in 300ml of 95% ethanol. This solution was added to the $Na_2S \cdot 9H_2O$/NaOH/EtOH solution in a dropwise fashion from a separatory funnel. The reaction flask was equipped with a mechanical stirrer as well as with a nitrogen gas inlet. In order to optimize the yield of the desired product, it was necessary to keep the reaction mixture at high dilution, vigorously and continuously stirring, under a nitrogen atmosphere. Once the two solutions were completely mixed, the resulting solution was refluxed for approximately 8 hours and finally allowed to cool to room temperature. The highly basic solution, initially made so to facilitate the reaction, was neutralized with hydrochloric acid. A solid precipitate, (NaCl) which had formed during refluxing, was filtered off from the solution and the ethanol was removed using the Rotovap-R (Büchi). The oil, which remained, was extracted four times with ether. Bradshaw reported that the DT18C6 formed in the ether extract and must be removed before any attempt to continue the 1-thia-9C3 recovery. However, no product was found in the ether fraction, rather, it was found crystallized among the precipitate filtered previously. The crystals were manually separated from the precipitate. A second synthesis performed reacted more typically. The product, DT18C6, was recrystallized several times using a 50-50 mixture of chloroform (Fisher) and hexane (J. T. Baker).

Following the purification of the DT18C6, by recrystallization, a melting point was measured on the Fisher-Johns Melting Point Apparatus and was found to be 89-90°C. Literature values are 90-91°C reported by Dann and coworkers and 89-90°C reported by Bradshaw. A proton NMR of the compound was also obtained using the Varian T-60 NMR (Figure 2). A 0.14M solution of DT18C6 in deuterated chloroform (Aldrich Diaprep, 99.9%) was used. Tetramethylsilane (Merck & Co.) was the internal standard. The chemical shifts obtained are shown in Table 3 and compared to those obtained by Bradshaw (44). The proton NMR is very characteristic for these compounds and this spectrum seemed to verify that the desired compound was prepared. A direct synthesis of DT18C6 was first attempted using the method proposed by Dann, Chiesa, and Gates (33). A solution of $Na_2S \cdot 9H_2O$ in a 50% ethanol water mixture was prepared and pure BCEE was added dropwise. The reaction mixture was refluxed for 88.5 hours, since the workers reported a greater yield with longer refluxing times. After the completion of refluxing a yellow oil formed, which should contain the product. It was separated from the solution, dissolved in hot ethyl acetate (Fisher), cooled to 7°C in a dry-ice-acetone

Varian T-60 NMR
Parameters

sweep width offset	0 Hz
spectrum amplitude	6.3 sample 2.0 TMS
integral amplitude	10 at 6.3 S.A.
spinning rate	40 RPS
sweep time	250 sec
sweep width	500 Hz
filter	1
R.F. power level	0.05

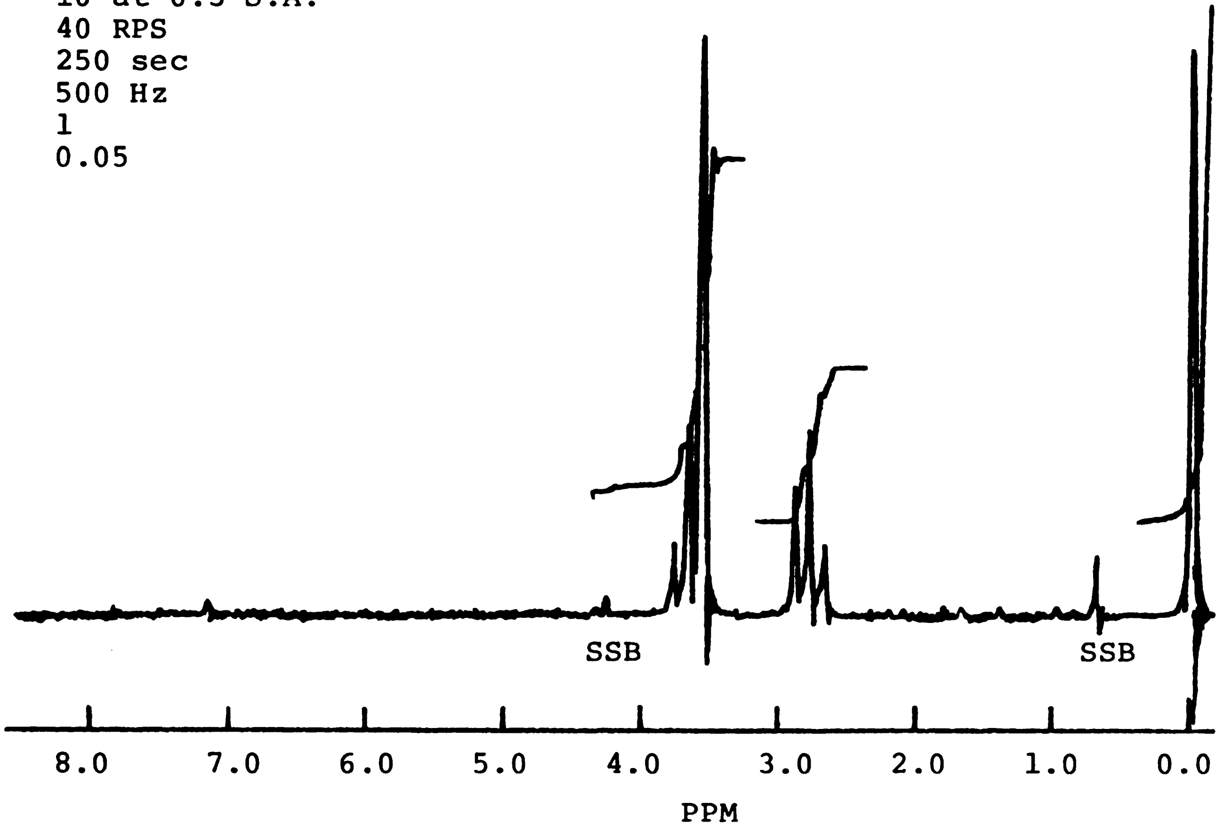

Fig. 2. Proton NMR of DT18C6 in deuterated chloroform with tetramethylsilane internal reference. (SSB = spinning side band)

bath, and the solution was quickly filtered to remove the white wax polymer which formed as a reaction by-product. The alcohol-ethyl acetate filtrate was evaporated to a small volume. At room temperature the product should form as a white solid, however, no crystals were obtained and the second by-product, an oil, was left. The polymer was formed in such a large amount that it was felt the reaction went predominantly in the direction of that product.

Table 3. The Chemical Shifts, Both Observed and Literature Values, Obtained for DT18C6/Deuterated Chloroform Proton NMR.

Protons Responsible	Splitting Pattern	Literature Chemical Shift	Observed Chemical Shift
SCH_2CH_2O	triplet	2.82	2.37
OCH_2CH_2O	singlet	3.63	3.55
OCH_2CH_2S	triplet	3.72	3.64

The method used by Bradshaw, although less direct, did produce the desired product and therefore was used for all subsequent synthesis of DT18C6 used in this work.

In one study the DT18C6 used was obtained from Parish Chemical Co. and required vacuum drying for 48 hours.

For the Raman studies of the 18C6-acetonitrile complex, the crown, 18C6, was purified prior to use and acetonitrile (ACN) was used as purchased. The 18C6·ACN complex was obtained by combining the crown and solvent, cooling in an ice-acetone bath and quickly vacuum filtering the precipitate.

Solvents

The nonaqueous solvent used in the extraction studies, methylene chloride (Drake Brothers and Mallinckrodt), was purified according to a method by Mathews (98). The process included first washing the methylene chloride with an equal volume of distilled water and then with an approximately 0.1M aqueous sodium carbonate solution. The washing procedure was carried out in a separatory funnel. The organic solvent was then separated, dried over anhydrous calcium chloride for 48 hours, and fractionally distilled. An additional precaution was taken, based on a known chemical reaction between the related solvent, chloroform. The reaction

$$CH_3Cl + O_2 \longrightarrow COCl_2 + HCl$$

is known to occur when chloroform is open to atmospheric oxygen. A simple chemical test for the detection of the decomposition involved an extraction of the solvent with distilled water; if the chloride ion was present (due to HCl formation), it would be transferred to the aqueous phase. Addition of a concentrated silver nitrate solution to the aqueous phase would result in the visible precipitation of silver chloride. However, no such precipitate was formed and decomposition was not a problem.

Toluene (Mallinckrodt), employed for a single extraction, was fractionally distilled before used.

Solvents used in the NMR studies included acetonitrile (Matheson, Coleman, and Bell), nitromethane (Aldrich), dimethylformamide (Mallinckrodt), pyridine (Fisher), and dimethyl sulfoxide (Fisher).

Acetonitrile was refluxed over calcium hydride and fractionally distilled. Nitromethane and dimethylformamide were fractionally distilled, under vacuum, over phosphorus pentoxide. Pyridine was refluxed over granulated barium hydroxide and fractionally distilled in a nitrogen atmosphere. All solvents were dried over molecular sieves for at least 2 days prior to use.*

Dimethyl sulfoxide was allowed to sit over freshly activated molecular sieves (8-12 mesh, Davison) for 24 hours, followed by vacuum distillation onto new sieves, which had been thoroughly washed prior to activation.

Molecular sieve activation entailed heating them at 500-700°C in a tube furnace (Lindberg) for 24 hours with a constant flow of nitrogen (bubbled through

---

*These solvents were prepared by members of the research group for community use.

sulfuric acid). The automatic Karl Fisher Titrator (Aquatest II, Photovolt) was used to test water content of the solvent, whenever possible, in order to assure the maintenance of water below 100ppm. Following the purification and drying steps, all solvents were placed in a dry box dry nitrogen atmosphere to prevent recontamination by water.

Instruments and Procedures

Extraction Studies

Direct preparation of a known concentration of an aqueous solution of picric acid was impossible due to the necessity of always keeping the solid slightly wet in order to avoid explosive decomposition. The concentration of the solution, therefore, was determined potentiometrically. The pH was measured at various increments of a standard NaOH solution with a Beckman Combination Electrode and a Heath Servo Digital pH/Volt Meter.

The basic procedure for the preparation of any of the systems for extraction measurements were identical. The crown compound studied was dissolved in the methylene chloride and a series of dilutions was made to obtain varying concentrations of the crown solution. The aqueous phase consisted of the particular cation of interest, picric acid, and a hydroxide. The extractions themselves were carried out by shaking equal volumes of the organic and aqueous solutions for a predetermined time, to ensure establishment of equilibrium. The solutions were shaken in the Wilkens-Anderson Shaker Bath. The systems were then allowed to set until a definite boundary between the two phases developed (approximately 1/2-1 hour).

Ultraviolet absorbance of the picrate component of the aqueous phase was measured both prior to and following the extraction procedure. The initial absorbance value provided the total picrate concentration before extraction. The absorbance after extraction was a measure of how much picrate was extracted into the organic phase with the metal cation. Measurements were obtained on systems containing a variety of component concentrations. Based upon calculations using an equation derived by Frensdorff (22), the dissociation constant (K_d) of the complex in the organic phase as well as an overall extraction equilibrium constant (K_e) were obtained. A more detailed look at the equilibria in solution and equilibrium constant calculations will be presented in Chapter IV.

All solutions were prepared using volumetric glassware and dilutions were made from a master solution delivered in various amounts from a buret. Flasks were wrapped with teflon tape and parafilm and the time of exposure to the atmosphere was minimized as much as possible to eliminate the difficulties arising from solvent evaporation.

All absorbance measurements were obtained on a Cary 17 UV-Vis Spectrophotometer at ambient room temperature, using rectangular one centimeter quartz cells. Any measurements made on organic phase components were made in cylindrical quartz cells with a ground glass stopper and wrapped with teflon tape. The Unicam SP.800 UV-Vis Spectrophotometer was used for some qualitative runs. An aqueous solution of K_2CrO_4 (dried at 110°C for 2.5 hours) in approximately 0.05$\underline{N}$ KOH was used as a standard to periodically check the spectrophotometer's performance (99).

Infrared Absorption and Laser Raman

Infrared spectra of the 18C6 ligand in acetonitrile solution, at room temperature, were obtained with a Perkin-Elmer 237B and 457 Grating Spectrophotometers. The samples were measured using sodium chloride discs (Barnes Engineering Company). Spectra were recorded of pure ACN, of pure nujol, and of 18C6 in nujol, so that the frequencies at which the bands were observed could be compared and assigned to a correct component.

The spectra collected for pure 18C6, ACN, and the 18C6·ACN complex were also obtained on the Spex Ramalog 4 Laser-Raman System which includes the Spex 1401

Double Spectrophotometer. The Spectra Physics-265-Excitor Argon Laser with the Ar-ion 5145Å line was utilized as the excitation source. In all cases the pulse counting mode was employed. Typical instrumental parameters are listed in Table 4.

Table 4. General Instrumental Parameters Used for the Collection of Raman Spectra.

Laser	5145Å Ar source
Laser power	1 Watt
Photomultiplier power	1940 Volts
Chart speed	5 cm/min
Pen period	0.5
Slit height	2 mm

The Raman spectra of the crown and the solvent-crown complex were obtained from a solid sample, whereas the ACN spectrum was obtained from a liquid sample. All samples were placed into 1.6-1.8 x 90 mm capillary tubes and sealed using tightly sealing parafilm. Once the complex had been formed and placed in the tube, it was necessary to store it in an ice bath because the complex noticeably broke down at room temperature. Since the laser beam did not heat the samples being measured, there was no concern of complex decomposition during spectrum collection.

NMR Specrometer

Measurements of ^{133}Cs and ^{205}Tl resonances were obtained with a Varian DA-60 spectrometer with a magnet operating at a field of 14.09kG. An external proton lock at 60MHz was used to maintain a stable field. The DA-60 is equipped with a wide-band probe (100), capable of accommodating different tunable inserts, allowing for multinuclear studies. Time averaging of spectra and Fourier transformation of data were made possible with an interfaced Nicolet Instrument Corporation 1083 computer. Wright and Rogers (101) have discussed the computer controlling, of necessary rf pulses and time delays for the particular nuclei under study, which the system possesses.

The glassware used in sample preparation was carefully cleaned and dried at 110°C overnight. All samples were prepared from stock metal solutions and various amounts of the complexing ligand under nitrogen atmosphere of the dry box. Upon complete dissolution of the ligand the solutions were transferred to 10mm OD NMR sample tubes (Wilmad), capped, and wrapped with teflon tape to prevent both contamination by atmospheric water and solvent evaporation.

Chemical shifts obtained for the different metal complexes were referenced to 0.5<u>M</u> aqueous solution of CsBr for ^{133}Cs and to 0.3<u>M</u> solution of $TlNO_3$ in water for ^{205}Tl measurements. Cesium-133 chemical shifts reported were finally referenced to infinite dilution, of the nuclei in water (a correction factor of -9.59ppm for 0.5$\underline{M}$ $CsBr_{aq}$ reference). All chemical shift data were obtained at ambient probe temperature. A positive value for a chemical shift is indicative of an upfield (diamagnetic) shift, while a negative value implies a downfield (paramagnetic) shift.

The chemical shifts are corrected for bulk susceptibility (102, 103) of the solvent in relationship to the water reference. Live and Chan (103) discussed the expression

$$\delta_{corr} = \delta_{obs} + 2/3(X_v^{ref} - X_v^{sam})$$

for nonsuperconducting spectrometers, which corrects for the difference between the reference and sample solvent. The variable δ_{obs} is the observed chemical shift; δ_{corr} is the chemical shift corrected for bulk susceptibility; and X_v^{ref} and X_v^{sam} refer to the volume magnetic susceptibilities of the reference and sample solutions, respectively. Table 5 contains the corrections applied as well as some of the important solvent properties to consider in discussion of solution behavior.

The collection of chemical shifts as a function of the relationship of crown to metal for a given solution, measured in terms of mole ratio of crown to

Table 5. Some Solvent Properties and Bulk Susceptibility Corrections Used in This Work.

Solvent	Dipole Moment (10^{-18} esu)	Dielectric Constant	Gutmann Donor Number	Volumetric Susceptibility ($\times 10^6$)	Chemical Shift Correction (ppm)
Acetonitrile	3.44	37.5	14.1	-0.534	-0.39
Dimethylformamide	3.86	36.71	26.6	-0.573	-0.31
Dimethyl Sulfoxide	3.9	46.68	29.8	-0.605	-0.24
Nitromethane	3.56*	35.9	2.7	-0.391	-0.69
Pyridine	2.37	12.40	33.1	-0.612	-0.23
Water	1.87	78.54	33.0	-0.720	0.00

*Dipole moments measured at 20°C; all others were obtained at 25°C.

metal, allowed for determination of complex formation constants. A nonlinear curve fitting program, KINFIT, written by Dye and Nicely (104) and the CDC 6500 Computer system were used for this purpose.

CHAPTER IV

SOLVENT EXTRACTION TECHNIQUE FOR THE DETERMINATION OF MACROCYCLIC LIGAND-METAL EQUILIBRIUM CONSTANTS

Introduction

Liquid-liquid extraction has proven to be an extremely valuable technique in chemical analysis. The movement of species across the interface, of the immiscible solvent pair, may be as uncharged molecules or as ion pairs. Solvent extraction with different complexing macrocyclic ligands involves transfer, into the organic phase, as ion pairs (M^+Pic^-). This method was one of the initial techniques employed to qualitatively compare the complexing abilities of these ligands.

If an aqueous solution of a metal cation, picrate anion, and an excess quantity of hydroxide ion (as compared to picrate) is shaken together and equilibrated with an immiscible organic solvent containing the macrocyclic ligand, the extent to which the picrate is extracted may be taken as a measure of metal-ligand complexation. Although the magnitude of extraction is not solely dependent upon the complexing equilibrium, it is useful in ranking the complex strengths of different ligands with a cation. Other system properties which may exert an effect upon the extraction include solubilities and partition coefficient of the various uncomplexed and complexed species.

Several different extraction systems will be presented here and with so many components to continuously note the following shorthand will be utilized for easy reference:

organic solvent	+	macrocyclic ligand	/	picric acid	+	metal salt or hydroxide	+	water

ORGANIC PHASE / AQUEOUS PHASE

Distribution Equilibria

Analysis of the extraction equilibrium constant for the metal-ligand complexation reaction involves a number of constituent equilibrium which must be considered.

Frensdorff (22) discussed the equilibria controlling the extraction processes and developed an expression for the calculation of the extraction equilibrium constant. The reaction which describes the total extraction process, for which the equilibrium constant is desired, is:

$$M^{+}_{aq} + Pic^{-}_{aq} + L_{org} \rightleftharpoons ML^{+}Pic^{-}_{org}$$

$$K_e = \frac{[ML^{+}Pic^{-}]org}{[M^{+}]_{aq}[Pic^{-}]_{aq}[L]_{org}} \qquad (1)$$

where $ML^{+}Pic^{-}$ is the ion pair, cation-ligand complex (ML^{+}) with the associated picrate (Pic^{-}) anion, formed in the organic phase. Since the organic solvents amendable to the extraction process are moderately polar and the concentrations of the components are quite low, the ion pairs in the organic phase are partially dissociated,

$$MLPic_{org} \rightleftharpoons ML^{+}_{org} + Pic^{-}_{org}$$

$$K_d = \frac{[ML^{+}]org[Pic^{-}]org}{[MLPic]_{org}} \qquad (2)$$

In addition one should consider the partition of the ligand between the two phases

$$L_{org} \rightleftharpoons L_{aq} \qquad P_e = \frac{[L]aq}{[L]_{org}} \qquad (3)$$

as well as the formation of the complexes in the aqueous phase

$$M^{+}_{aq} + L_{aq} \rightleftharpoons ML^{+}_{aq} \qquad K_s = \frac{[ML^{+}]aq}{[M^{+}]_{aq}[L]_{aq}} \qquad (4)$$

Frensdorff determined that the concentrations of hydroxide ion, uncomplexed metal cation, and picrate in the organic phase can be neglected in equilibrium calculations. He took into consideration the activity coefficient of the aqueous metal ion; however, all other activity corrections were neglected, since the other components were either neutral species or ions at very low concentrations. It is implicit in the mathematical treatment of the data that equal volumes of each phase be used in the extraction procedure, although the concentrations of the phase components may vary widely. It is also assumed that the ion pair complex involved is in a 1:1:1 stoichiometry. Considering the various equilibrium reactions occurring within the extraction system, the following equation may be used to determine the value of extraction equilibrium constant (K_e):

$$K_e = \frac{[2E + K_d - (K_d^2 + 4K_dE)^{\frac{1}{2}}]\ [1 + P_e + P_eK_sf(C_M - E)]}{2\ f(C_M - E)\ (C_{Pic} - E)(C_L - E)} \tag{5}$$

where C_M, C_{Pic}, and C_L are the total concentrations of the metal ion, the picrate, and the ligand, respectively; f is the single ion activity coefficient of the aqueous cation, and E is the concentration of the picrate ion extracted into the organic phase. The derivation of this expression may be found in Appendix A.

Before any attempt to determine the overall extraction equilibrium constant may be made, due to the complexity of component behavior within the extraction system, the complex stability constant in water (K_s) as well as the partition coefficient (P_e) must be known. The values of C_M, C_{Pic}, and C_L are of course known, that of f is obtained from the Debeye-Huckel equation, and that of E from absorbance measurements.

Characterization of Picric Acid Ultraviolet Absorption

The picric acid (2,4,6-trinitrophenol) anion was utilized in these extraction studies as a monitor of metal-ligand complexation. Extraction efficiency is high since the anion is large and easily polarized. Because the aqueous absorbance change of picrate, before and after extraction, was the basis of this technique, a clear view of picrate absorption characteristics was necessary.

Figure 3 is a Beer's law plot for aqueous solutions of picric acid of maximum absorbance at 356 nm. The calculated molar absorptivity is $(1.44 \pm 0.01) \times 10^4$ $\underline{M}^{-1}cm^{-1}$. Several spectra were run after different time periods to check the stability of picric acid solutions. At a given concentration neither the spectral shape nor the absorbance changed.

The extractions had to be performed in a basic system, consequently it was of interest to explore spectral changes of aqueous picric acid solutions upon addition of a strong acid or a base. Since picric acid has a pK value of 0.29, at 25°C, it should be largely

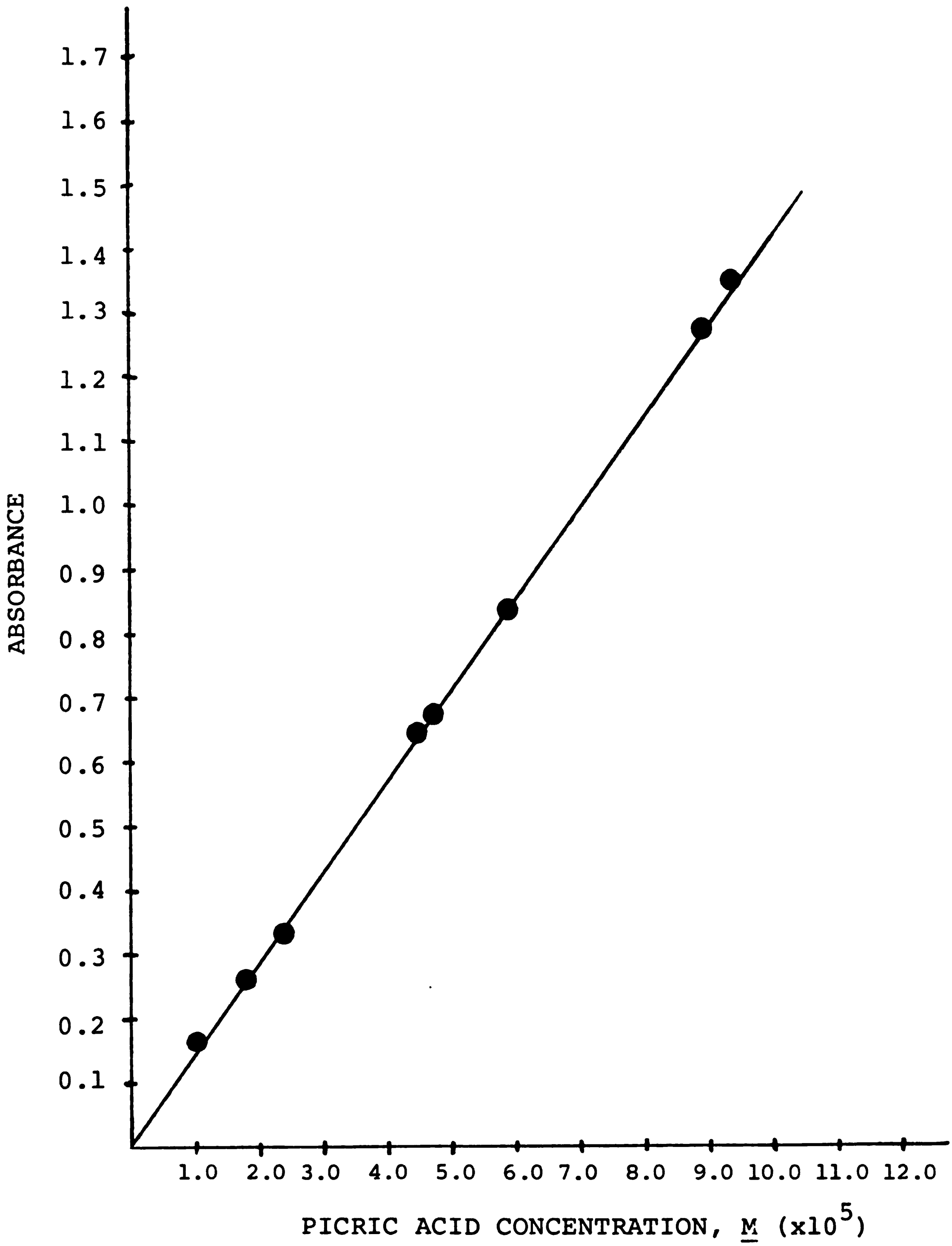

Fig. 3. Beers law plot for picric acid in water, λ = 356 nm.

dissociated in aqueous solutions. In fact the spectra showed only a peak at 356 nm. It would be expected that the addition of a strong acid to an aqueous solution of picric acid would shift the equilibrium towards the formation of undissociated acid. A solution, 1.6M in hydrochloric acid, produced a spectrum in which the peak was shifted from 356 nm to 341 nm. This peak corresponds to undissociated picric acid (105). Several spectra were taken of solutions with addition of strong base in which there appeared to be no change in the spectra. Later studies, at higher metal hydroxide concentrations, did cause a shift of the wavelength maxima, as great as 35 nm, to higher values, with a corresponding increase in peak absorbance for a given picric acid concentration. This phenomenon was reported by Abe (106). He also found the absorbancy of the picrate peak slightly increased at low concentrations of sodium hydroxide up to approximately 0.4N and then decreased at higher concentrations. Identical results were obtained in this study. Abe attributed the new band to the formation of a complex between the picrate anion and hydroxide ion.

Possible Sources of Error in Extraction Procedures

The problems in obtaining accurate extraction data arise from various sources including:

(a) Extraction of picrate anion into the organic phase due to factors other than ion pair formation;

(b) The removal of metal ions (Na^+, K^+) by the ligand from the surface of the glassware;

(c) Dissolution of some of the organic solvent in the aqueous phase;

(d) Measurements obtained before the system has reached equilibrium.

Several experiments were initially performed to determine the magnitude of these difficulties and to develop the technique to alleviate them. It was shown by measurement of an extraction system with all components except the ligand that no picrate, and hence no metal ion, was transferred to the organic phase and; therefore, interaction with the ligand was responsible for the extraction. The possibility of ligand complexation with metal ions originating on container surfaces was negated by a comparative study of two extraction systems:

(a) CH_2Cl_2 / Bu_4NOH + PicH + H_2O

(b) CH_2Cl_2 + DB18C6 / Bu_4NOH + PicH + H_2O

Tetrabutylammonium hydroxide was used as the hydroxide ion contributor because it is a reagent for ion pair extractions (107). Some extraction was desirable to enhance detection of differences between the two systems. The first system was used as a blank, while the second system would show an enhanced extraction if any metal ion-ligand complexation occurred; however, no change in absorbance was observed. Pure water was used as a reference in absorbance measurements; however, the aqueous phase after extraction could contain traces of the organic solvent. A UV spectrum of pure water extracted with methylene chloride, referenced to distilled water, was identical to a pure water versus pure water spectrum. Identical samples of the extraction system

$$CH_2Cl_2 + 18C6 \ / \ KOH + PicH + H_2O$$

were prepared and measured as a function of time, that the two phases were together, to demonstrate the establishment of equilibrium.

Figure 4 contains the results of the study. The plot of picrate concentration in the organic phase versus time shows that no trends occurred as a function of time implying that the differences are due to experimental error and that equilibrium has been established by two minutes.

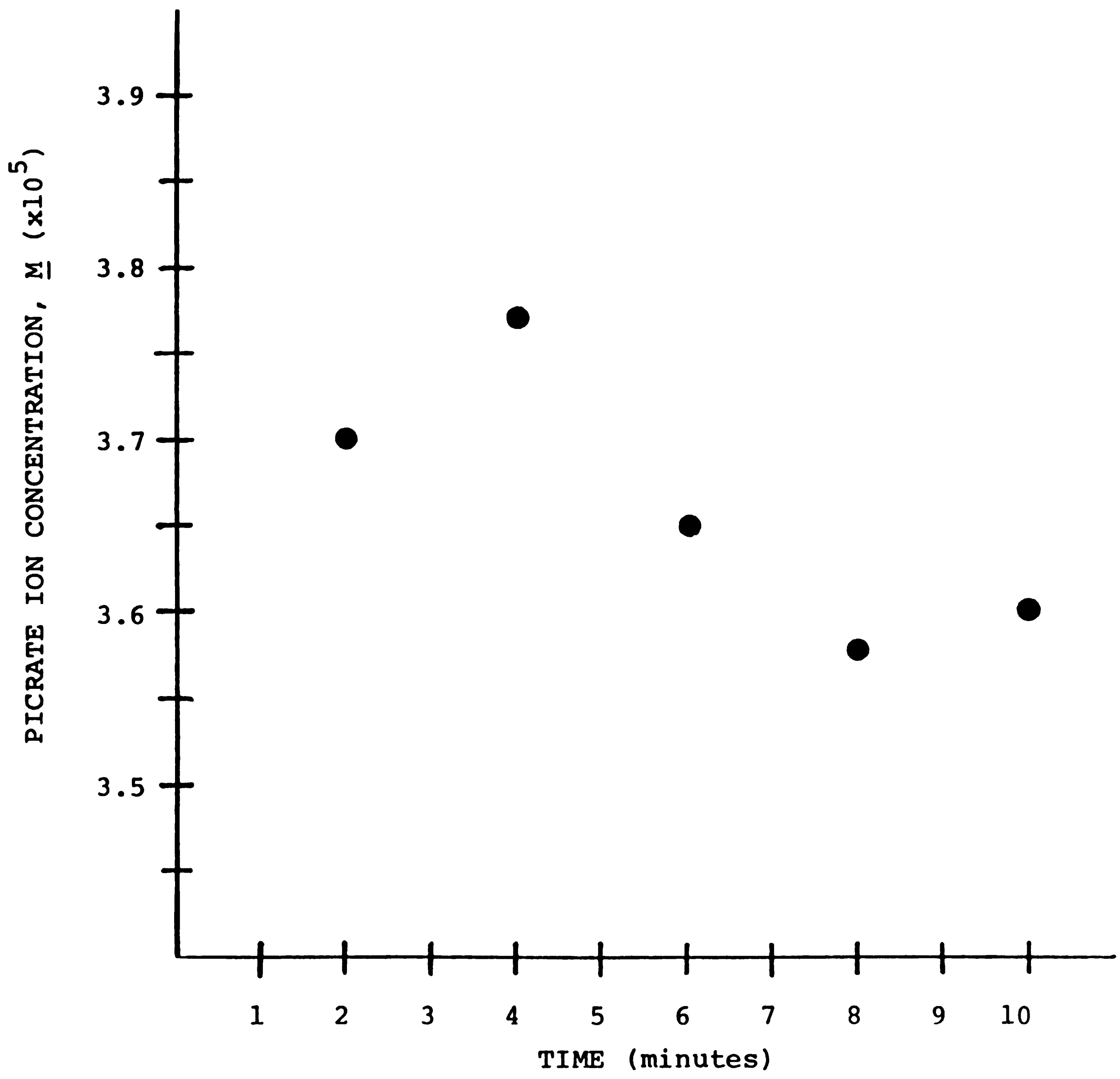

Fig. 4. Extraction equilibrium determination of the concentration of picrate ion extracted into methylene chloride as a function of time.

Ligand Partition Coefficient Studies

Dibenzo-18C6: Spectrophotometric Determination

The studies of partitioning of DB18C6 between equal volumes of methylene chloride and water were performed using ultraviolet spectroscopy. Dibenzo-18C6, in methylene chloride, absorbs at 277 nm. The DB18C6 solutions' absorbances were measured both before and following extraction with distilled water. The mean partition coefficient was found to be 0.09 ± 0.07. In this particular solvent system the value of the partition coefficient is not very significant in the extraction equilibrium constant calculation, therefore, the large standard deviation was tolerable.

18C6 and 1,10-Dithia-18C6: Gravimetric Determination

Since both 18C6 and DT18C6 cannot be studied spectrophotometrically, a gravimetric determination of each was performed. Several solutions of varying concentration, in methylene chloride, were prepared and a given volume, prior to and after the extraction process, were delivered into pre-weighed vials. Following evaporation to dryness under vacuum, the difference between each blank and the corresponding organic phase after extraction was taken as the weight of ligand which was transferred into the water. The partition coefficient obtained for 18C6 was 0.23 ± 0.04. In the case of DT18C6, no partitioning was detected, which indicates that the upper limit of P_e is 0.01. As shown later, the calculations of K_e are relatively insensitive to the exact values of P_e.

The literature values for the complex stability constants are presented in Table 6.

Table 6. Stability Constants (K_s) in Water for the Metal-Ligand Complexes.

Macrocycic Ligand	Metal Ion	Log K_s	Reference
18C6	K	2.03	12
	Cs	0.99	12
	Tl	2.27	12
DB18C6	K	1.67	92
DT18C6	Tl	0.93	23

Extraction Systems

The picrate extraction data needed to calculate K_e for the systems studied is derived from absorbance measurements of both the total picrate and that remaining in the aqueous phase after extraction. The concentration of picrate extracted into the organic phase (E) was found by difference between the initial picrate concentration (C_{Pic}) and the unextracted concentration ($[Pic]^{aq}$).

Extraction Studies Utilizing the DB18C6 Ligand

The complexing ability of DB18C6 macrocyclic ligand with the potassium ion was studied for the system

$$CH_2Cl_2 + DB18C6 \; / \; KOH + PicH + H_2O$$

To enable the calculation of an accurate extraction equilibrium constant, it is mandatory that absorbance data be collected at varying concentrations of all components within the system. Table 7 contains the results of these studies. Figure 5 contains the composite graph of each set of data points. The results are presented as percent picrate extracted, $(E \times 100)/C_{Pic}$, as a function of the ligand to picrate (C_{Pic}) mole ratio. For a particular set (each curve represents one set) the metal and picrate concentrations are constant. Aliquots are extracted with the organic phase containing different ligand concentrations. Since the picrate is extracted in a 1:1 relationship with the amount of metal complexation, the graphs actually relate the concentration of the complex formed to the concentration of ligand introduced in the organic phase prior to extraction. The curves prove helpful in allowing visual comparison of the effect of increasing potassium and DB18C6 concentrations and that the amount of picrate extracted into the organic phase, relative to the initial picrate

Table 7. Equilibrium Extraction Study of the System CH_2Cl_2 + DB18C6 / KOH + PicH + H_2O.

Mole Ratio (C_L^{org}/C_{Pic}^{aq})	Aqueous Picrate Absorbance After Extraction	$[Pic]^{aq}$ $\underline{M}$ (x10^5)	$[Pic]^{org}$ $\underline{M}$ (x10^5)	Percent Picrate Extracted
	$C_{K^+}^{aq} = 0.005\underline{M}$	$C_{Pic}^{aq} = 5.61 \times 10^{-5}\underline{M}$		
0.28	0.783	5.44	0.17	3.1
0.55	0.773	5.37	0.24	4.3
1.11	0.758	5.26	0.35	6.2
1.94	0.740	5.14	0.47	8.4
2.49	0.728	5.06	0.56	9.9
2.77	0.721	5.01	0.60	10.8
	$C_{K^+}^{aq} = 0.010\underline{M}$	$C_{Pic}^{aq} = 1.121 \times 10^{-4}\underline{M}$		
0.15	1.563	10.85	0.36	3.2
0.31	1.535	10.65	0.56	4.9
0.61	1.488	10.33	0.88	7.8
1.07	1.430	9.93	1.13	11.4
1.38	1.391	9.65	1.16	13.8
1.53	1.369	9.51	1.70	15.2
	$C_{K^+}^{aq} = 0.043\underline{M}$	$C_{Pic}^{aq} = 9.22 \times 10^{-5}\underline{M}$		
0.95	1.006	6.99	2.23	24.2
1.93	0.853	5.92	3.29	35.7
3.75	0.683	4.74	4.47	48.5
4.66	0.609	4.23	4.99	54.1
5.68	0.572	3.97	5.24	56.9

Table 7. Continued.

Mole Ratio (C_L^{org}/C_{Pic}^{aq})	Aqueous Picrate Absorbance After Extraction	$[Pic]^{aq}$ $\underline{M}$ $(x10^5)$	$[Pic]^{org}$ $\underline{M}$ $(x10^5)$	Percent Picrate Extracted
	$C_{K^+}^{aq} = 0.086\underline{M}$	$C_{Pic}^{aq} = 1.110 \times 10^{-4}\underline{M}$		
0.52	1.309	9.09	2.01	18.1
1.03	1.099	7.63	3.47	31.3
2.06	0.826	5.74	5.36	48.3
3.61	0.588	4.08	7.02	63.2
4.64	0.485	3.37	7.74	69.7
	$C_{K^+}^{aq} = 0.090\underline{M}$	$C_{Pic}^{aq} = 8.62 \times 10^{-5}\underline{M}$		
1.29	0.844	5.86	2.76	32.0
1.94	0.711	4.94	3.68	42.7
2.58	0.633	4.40	4.22	49.0
3.23	0.555	3.85	4.76	55.3
6.46	0.349	2.42	6.19	71.9
	$C_{K^+}^{aq} = 0.849\underline{M}$	$C_{Pic}^{aq} = 1.118 \times 10^{-4}\underline{M}$		
0.15	1.400	9.72	1.46	13.0
0.61	0.875	6.08	5.10	45.6
0.92	0.630	4.38	6.80	60.9
1.22	0.471	3.27	7.91	70.7
1.53	0.367	2.55	8.63	77.2

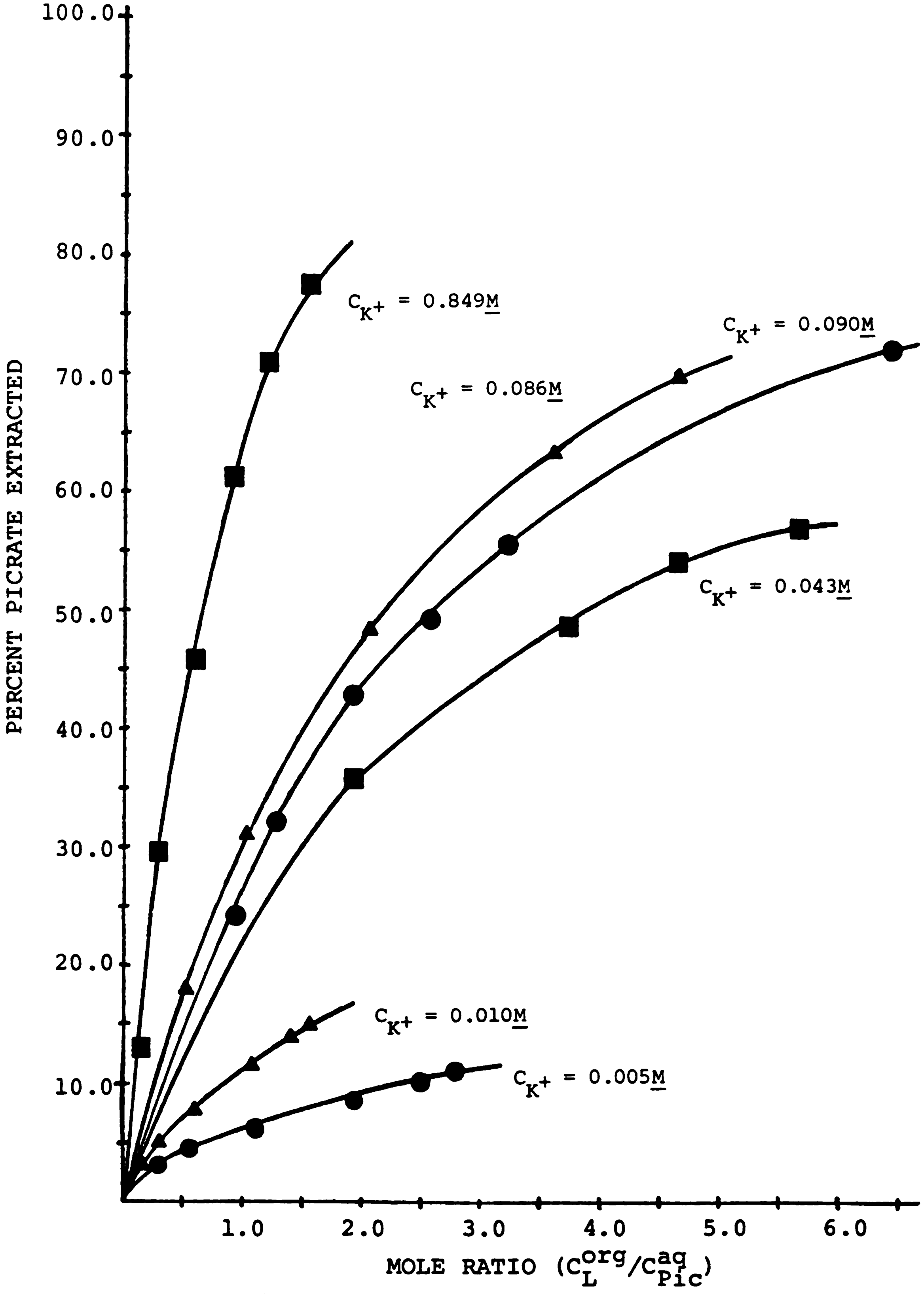

Fig. 5. Extraction of potassium picrate into methylene chloride by DB18C6 at various cation and ligand concentrations.

concentration, increased at a faster rate as the K^+ concentration was raised.

Extraction Studies Utilizing the 18C6 Ligand

A number of studies using 18C6 as the complexing macrocycle were performed with potassium, cesium, and thallium cations. Although the stability of these metal-crown complexes have been well characterized, it was of interest to find the extraction equilibrium constants in methylene chloride, as well as provide a basis of comparison for the later studies using a sulfur-substituted macrocycle.

The system components used for the potassium and cesium extractions were,

$$CH_2Cl_2 + 18C6 \ / \ MOH + PicH + H_2O$$

however, the thallium studies were conducted using a thallium salt, either acetate or thiocynate, and lithium hydroxide, rather than TlOH.

A few systems were measured in which the hydroxide source was LiOH, rather than from that of the metal of interest. Using LiOH presents the danger of the lithium ion and the thallium ion competing for complex formation with the ligand. However, the extensive work gone into the property of cation selectivity demonstrated by the crown ligands has shown that 18C6 does not accommodate the lithium because of its small size and high degree of solvation by the solvent (for example 24). In this work, it was found that if the lithium concentration was maintained below approximately 0.004M in the aqueous phase, no extraction could be attributed to lithium ion-ligand complexation.

The picrate absorbance data and calculated results of the extent of complex formation are shown in Tables 8-10. Figures 6-8 show the corresponding curves of percent picrate extracted versus mole ratio of ligand to initial picrate. The same relationship described for the DB18C6$\cdot$K$^+$ data are observed with these as well; that is, greater extraction is observed as the ligand and/or metal concentration is increased. In all systems the curves level off at high mole ratios, as maximum complexation is approached for a given metal concentration.

A comparison of the 18C6$\cdot$K$^+$ extraction curves with those of DB18C6$\cdot$K$^+$ demonstrates the higher efficiency of the 18C6 ligand in extracting the metal cation and, hence, implying a stronger complex formed in this system.

Extraction studies have been conducted in a number of organic solvents. Low dielectric constant solvents are used since uncomplexed alkali metal picrates are scarcely extracted into the solvents and their non-ionizing property prohibits the complex ion pair from dissociating to any great extent. Pedersen noted that

Table 8. Equilibrium Extraction Study of the System CH_2Cl_2 + 18C6 / KOH + PicH + H_2O.

Mole Ratio (C_L^{org}/C_{Pic}^{aq})	Aqueous Picrate Absorbance After Extraction	$[Pic]^{aq}$ $\underline{M}$ $(x10^5)$	$[Pic]^{org}$ $\underline{M}$ $(x10^5)$	Percent Picrate Extracted
	$C_{K^+}^{aq} = 0.005\underline{M}$	$C_{Pic}^{aq} = 8.90 \times 10^{-5}\underline{M}$		
0.25	1.098	7.63	1.27	14.4
1.26	0.654	4.54	4.36	49.0
2.53	0.410	2.85	6.05	68.0
3.23	0.337	2.34	6.56	73.7
3.80	0.290	2.01	6.89	77.4
4.43	0.255	1.77	7.13	80.1
5.06	0.225	1.56	7.34	82.5
6.33	0.188	1.31	7.59	85.3
	$C_{K^+}^{aq} = 0.008\underline{M}$	$C_{Pic}^{aq} = 9.06 \times 10^{-5}\underline{M}$		
0.28	1.040	7.22	1.84	20.3
0.62	0.808	5.61	3.45	38.1
0.86	0.688	4.78	4.36	48.1
1.70	0.407	2.83	6.23	68.8
2.55	0.275	1.91	7.15	78.9
3.45	0.204	1.42	7.64	84.3
5.10	0.139	0.97	8.09	89.3
6.90	0.104	0.72	8.34	92.0

Table 8. Continued.

Mole Ratio $(C_L^{org}/C_{Pic}^{aq}$	Aqueous Picrate Absorbance After Extraction	$[Pic]^{aq}$ $\underline{M}$ $(x10^5)$	$[Pic]^{org}$ $\underline{M}$ $(x10^5)$	Percent Picrate Extracted
	$C_{K^+}^{aq} = 0.018\underline{M}$	$C_{Pic}^{aq} = 8.78 \times 10^{-5}\underline{M}$		
0.26	1.025	7.12	1.66	18.9
1.28	0.478	3.32	5.46	62.2
2.56	0.240	1.67	7.11	81.0
3.27	0.183	1.27	7.51	85.5
3.88	0.151	1.05	7.73	88.0
4.49	0.130	0.90	7.88	89.8
5.13	0.113	0.78	8.00	91.1
6.42	0.090	0.63	8.15	92.8
	$C_{K^+}^{aq} = 0.020\underline{M}$	$C_{Pic}^{aq} = 9.10 \times 10^{-5}\underline{M}$		
0.28	1.015	7.05	2.05	22.5
0.62	9.739	5.13	3.97	43.6
0.85	0.594	4.13	4.97	54.6
1.69	0.300	2.08	7.02	77.1
2.54	0.180	1.25	7.85	86.3
3.43	0.128	0.89	8.21	90.2
5.08	0.090	0.63	8.47	93.1

Table 8. Continued.

Mole Ratio (C_L^{org}/C_{Pic}^{aq})	Aqueous Picrate Absorbance After Extraction	$[Pic]^{aq}$ $\underline{M}$ ($\times 10^5$)	$[Pic]^{org}$ $\underline{M}$ ($\times 10^5$)	Percent Picrate Extracted
	$C_{K^+}^{aq} = 0.052\underline{M}$	$C_{Pic}^{aq} = 9.62 \times 10^{-5}\underline{M}$		
0.26	1.045	7.26	2.42	25.2
0.58	0.727	5.05	4.57	47.5
0.81	0.552	3.83	5.79	60.2
1.60	0.236	1.64	7.98	83.0
2.40	0.142	0.99	8.63	89.7

Table 9. Equilibrium Extraction Study of the System CH_2Cl_2 + 18C6 / CsOH + PicH + H_2O.

Mole Ratio (C_L^{org}/C_{Pic}^{aq})	Aqueous Picrate Absorbance After Extraction	$[Pic]^{aq}$ $\underline{M}$ ($x10^5$)	$[Pic]^{org}$ $\underline{M}$ ($x10^5$)	Percent Picrate Extracted
	$C_{Cs^+}^{aq} = 0.005\underline{M}$	$C_{Pic}^{aq} = 8.91 \times 10^{-5}\underline{M}$		
0.39	1.193	8.28	0.63	7.1
0.90	1.143	7.93	0.98	11.0
1.19	1.097	7.61	1.30	14.6
2.40	0.991	6.88	2.03	22.8
3.59	0.912	6.33	2.58	29.0
4.87	0.839	5.82	3.09	34.7
7.21	0.724	5.02	3.89	43.7
9.75	0.637	4.42	4.49	50.4
	$C_{Cs^+}^{aq} = 0.009\underline{M}$	$C_{Pic}^{aq} = 8.95 \times 10^{-5}\underline{M}$		
0.39	1.167	8.10	0.85	9.5
0.89	1.083	7.52	1.43	15.0
1.18	1.047	7.27	1.68	18.8
2.39	0.905	6.28	2.67	29.8
3.57	0.813	5.64	3.31	36.9
4.85	0.720	5.00	3.95	44.2
7.18	0.602	4.18	4.77	53.3
9.70	0.509	3.53	5.42	60.5

Table 9. Continued.

Mole Ratio (C_L^{org}/C_{Pic}^{aq})	Aqueous Picrate Absorbance After Extraction	$[Pic]^{aq}$ $\underline{M}$ ($x10^5$)	$[Pic]^{org}$ $\underline{M}$ ($x10^5$)	Percent Picrate Extracted
	$C_{Cs^+}^{aq} = 0.020\underline{M}$	$C_{Pic}^{aq} = 9.52 \times 10^{-5}\underline{M}$		
0.36	1.196	8.30	1.22	12.8
0.84	1.071	7.43	2.09	22.0
1.11	1.013	6.94	2.58	27.1
2.24	0.809	5.60	3.92	41.2
3.36	0.689	4.77	4.75	49.9
4.56	0.581	4.03	5.49	57.7
6.75	0.452	3.13	6.39	67.1
9.12	0.364	2.52	7.00	73.5

Table 10. Equilibirum Extraction Study of the System CH_2Cl_2 + 18C6 / $TlC_2H_3O_2$ + LiOH + PicH + H_2O.

Mole Ratio (C_L^{org}/C_{Pic}^{aq})	Aqueous Picrate Absorbance After Extraction	$[Pic]^{aq}$ $\underline{M}$ $(x10^5)$	$[Pic]^{org}$ $\underline{M}$ $(x10^5)$	Percent Picrate Extracted
	$C_{Tl^+}^{aq} = 0.008\underline{M}$	$C_{Pic}^{aq} = 9.23 \times 10^{-5}\underline{M}$	$C_{Li^+}^{aq} = 0.004\underline{M}$	
0.35	0.905	6.28	2.97	32.1
0.81	0.549	3.81	5.44	58.8
1.08	0.414	2.88	6.38	68.9
2.17	0.175	1.22	8.04	86.9
3.25	0.104	0.72	8.54	92.2
4.41	0.063	0.44	8.82	95.3
6.53	0.047	0.33	8.93	96.5
8.83	0.038	0.26	8.99	97.2
	$C_{Tl^+}^{aq} = 0.016\underline{M}$	$C_{Pic}^{aq} = 9.56 \times 10^{-5}\underline{M}$	$C_{Li^+}^{aq} = 0.004\underline{M}$	
0.34	0.889	6.17	3.40	35.5
0.79	0.519	3.60	5.97	62.3
1.04	0.386	2.68	6.89	72.0
2.10	0.156	1.08	8.49	88.7
3.14	0.090	0.62	8.94	93.5
4.27	0.072	0.50	9.07	94.8
6.32	0.047	0.33	9.24	96.6
8.54	0.037	0.26	9.31	97.3

Table 10. Continued.

Mole Ratio (C_L^{org}/C_{Pic}^{aq}	Aqueous Picrate Absorbance After Extraction	$[Pic]^{aq}$ $\underline{M}$ (x10^5)	$[Pic]^{org}$ $\underline{M}$ (x10^5)	Percent Picrate Extracted
	$C_{Tl^+}^{aq} = 0.048\underline{M}$	$C_{Pic}^{aq} = 1.084 \times 10^{-4}\underline{M}$	$C_{Li^+}^{aq} = 0.004\underline{M}$	
0.30	0.871	6.05	4.80	44.2
0.69	0.485	3.37	7.48	69.0
0.92	0.347	2.41	8.44	77.8
1.85	0.153	1.06	9.79	90.7
2.77	0.086	0.60	10.25	94.5
3.77	0.078	0.54	10.31	95.0
5.57	0.060	0.42	10.43	96.1
7.53	0.053	0.37	10.48	96.6

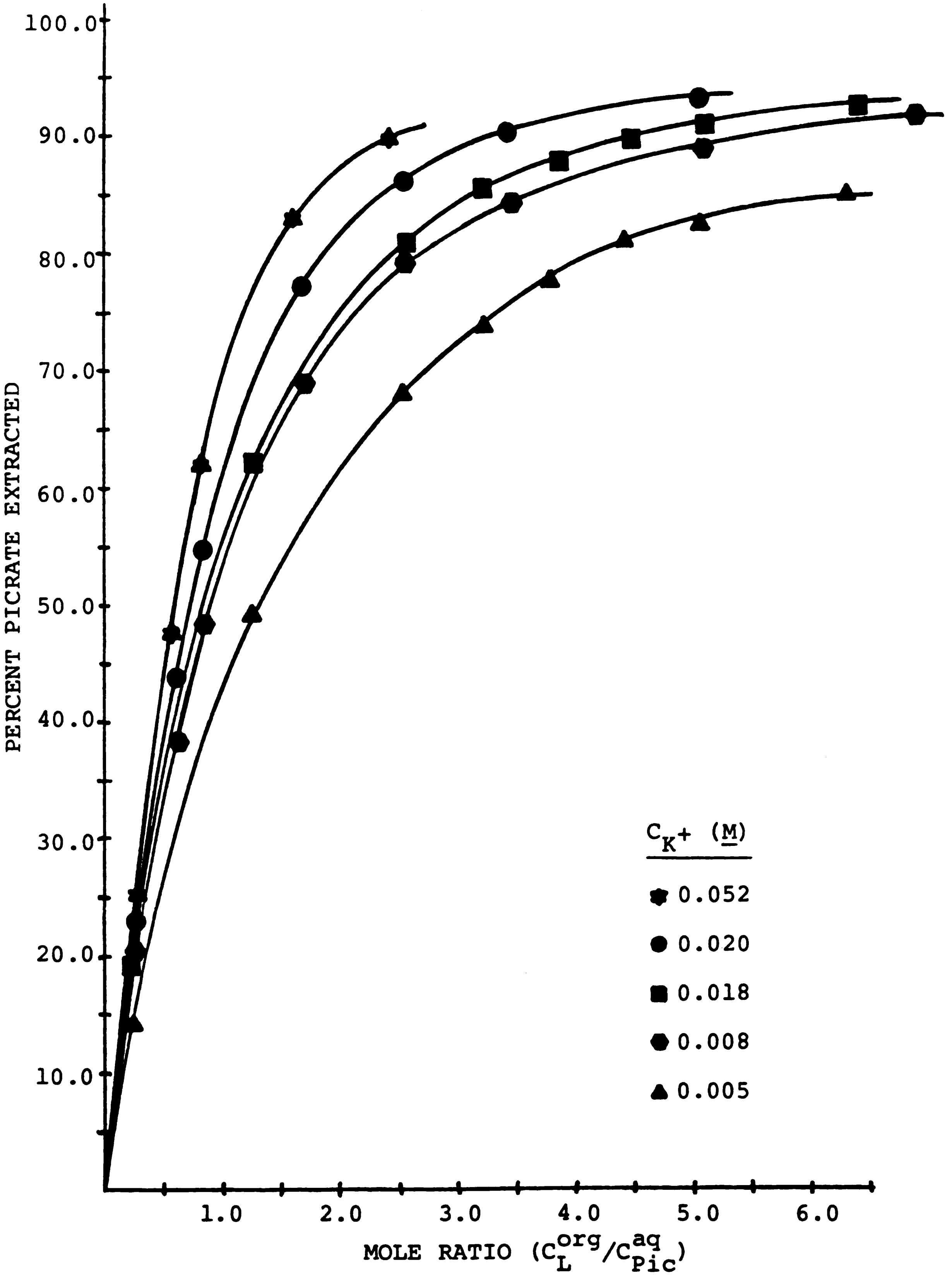

Fig. 6. Extraction of potassium picrate into methylene chloride by 18C6 at various cation and ligand concentrations.

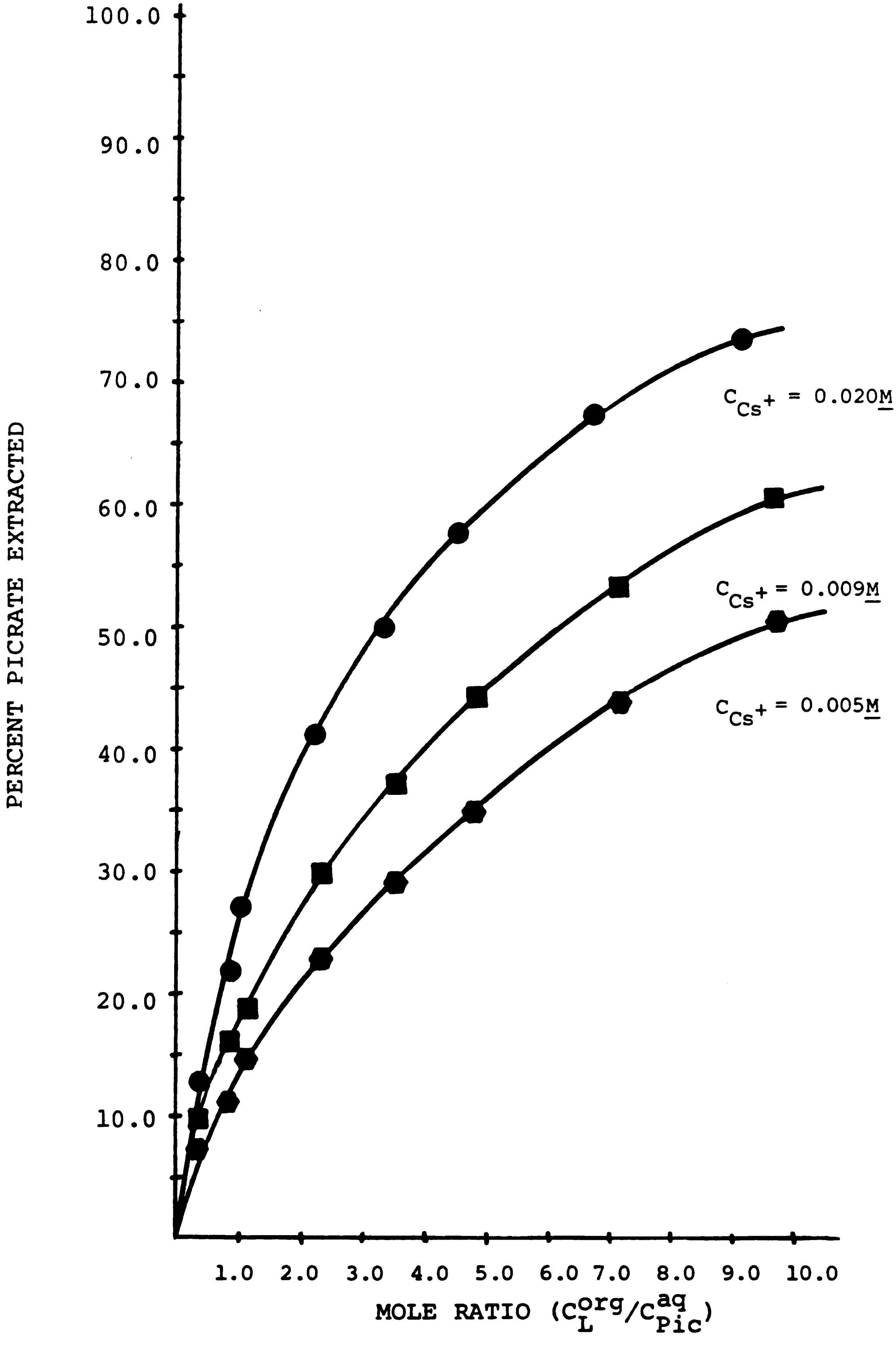

Fig. 7. Extraction of cesium picrate into methylene chloride by 18C6 at various cation and ligand concentrations.

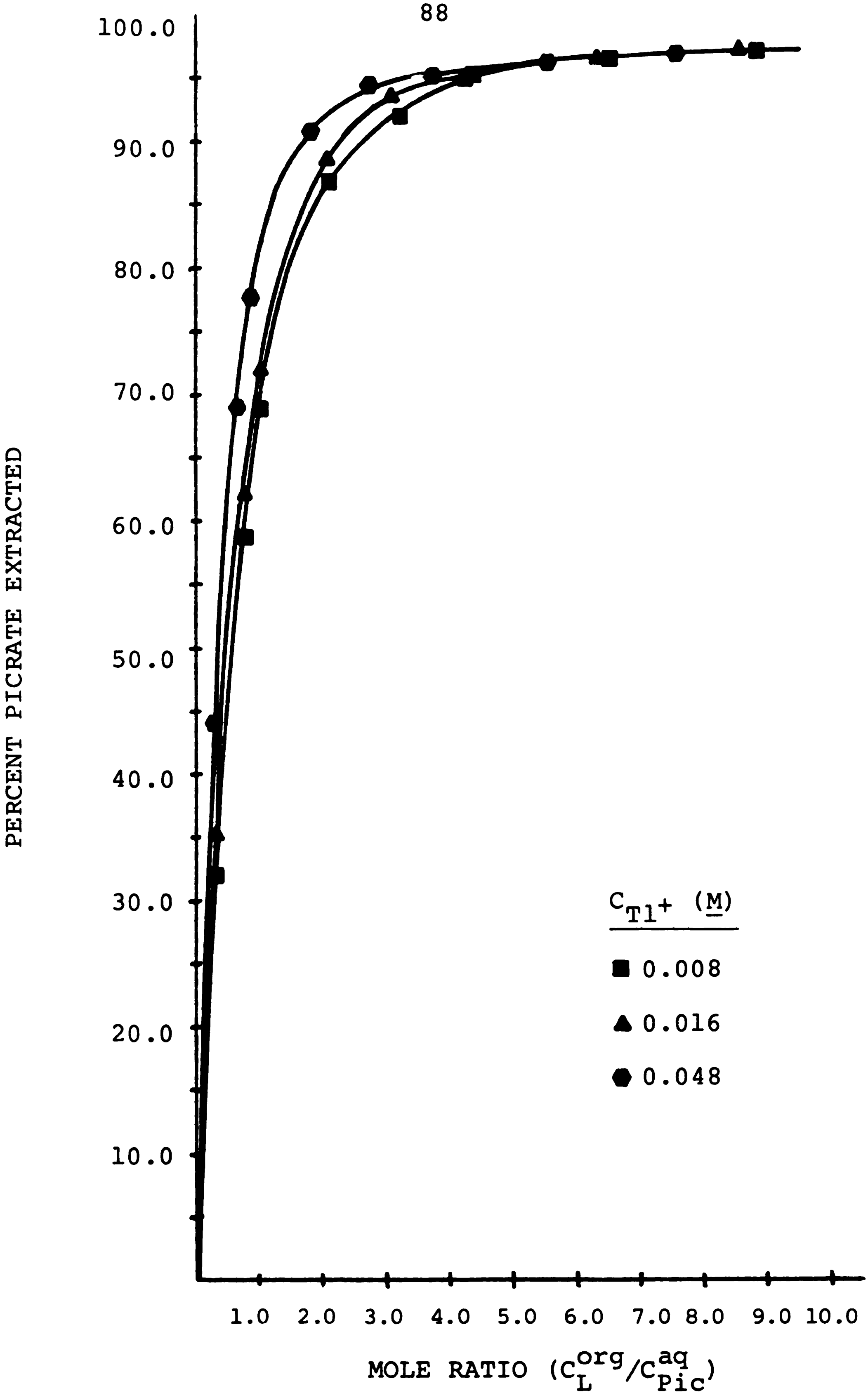

Fig. 8. Extraction of thallium picrate into methylene chloride by 18C6 at various cation and ligand concentrations.

as the dielectric constant of the organic solvent is lowered the extraction efficiency drops, and the selectivity of the ligand increases. The lower efficiency of extraction when toluene (dielectric constant, $\varepsilon = 2.38$) comprised the organic phase, in relation to methylene chloride ($\varepsilon = 8.93$) was shown here. Figure 9 shows the extraction curves for $18C6 \cdot K^+$ systems in which toluene (curve A) and methylene chloride (curve B) were used. At the potassium concentrations shown, one can see the tremendous reduction in the extent of picrate extraction.

A comparative study was conducted for the systems

$$CH_2Cl_2 + 18C6 \;/\; TlSCN + LiOH + PicH + H_2O$$

and

$$CH_2Cl_2 + 18C6 \;/\; TlC_2H_3O_2 + LiOH + PicH + H_2O$$

in order to determine the effect of changing the thallium (I) cation's counterion. The studies were performed using the same series of ligand solutions and the concentration of thallium ion in the two aqueous phases were similar. The results, in Figure 10, show that, at least, in the case of TlSCN and $TlC_2H_3O_2$, a change in the anion does not affect extraction data.

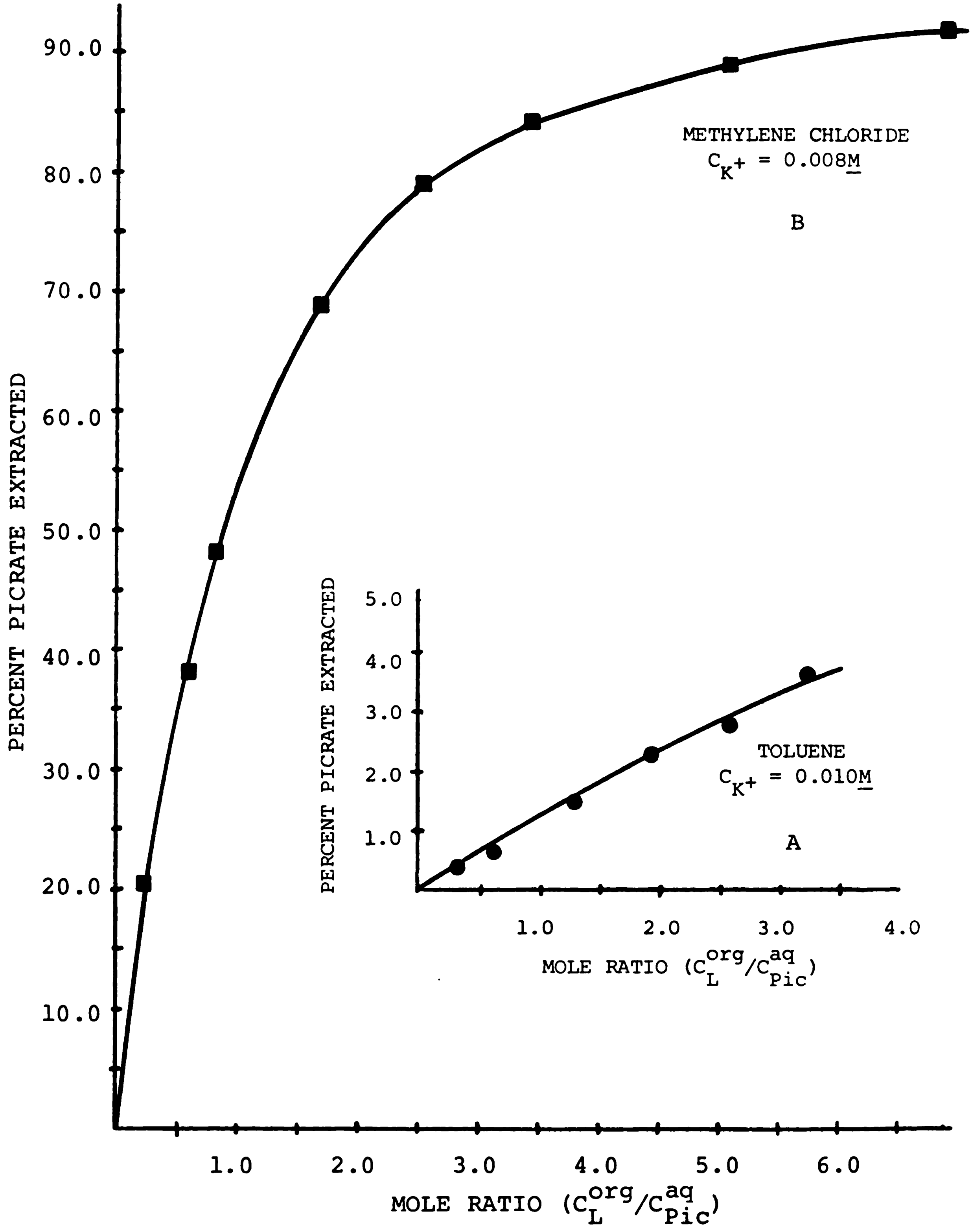

Fig. 9. Comparative potassium picrate extraction efficiency into methylene chloride and toluene.

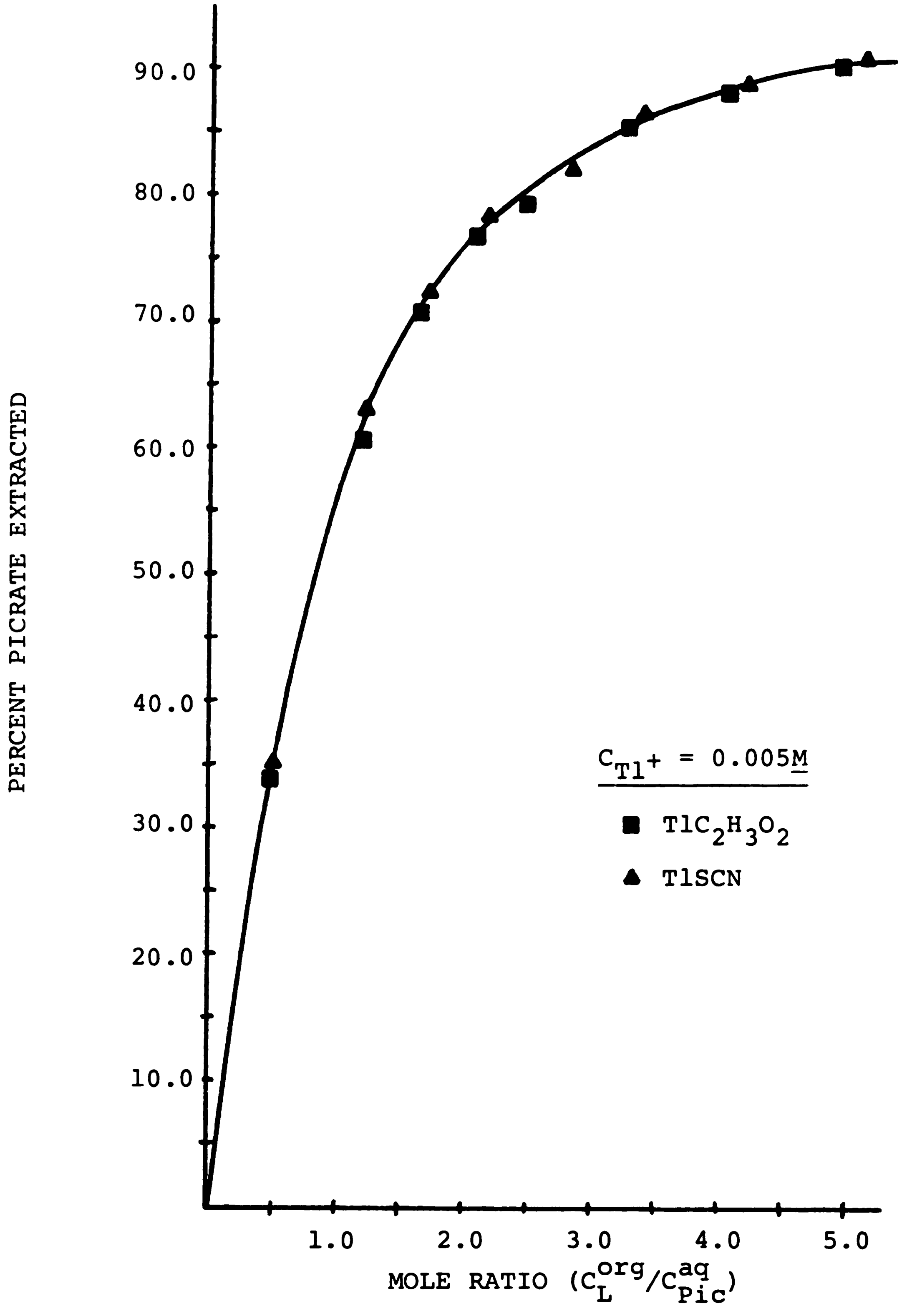

Fig. 10. Comparative extraction of thallium picrate using two different counterions.

Extraction Studies Utilizing the 1,10-Dithia-18C6 Ligand

Picrate extraction studies were conducted with the metal cations potassium, cesium, and thallium. Tables 11-13 contain the data collected for these systems with the corresponding percent picrate extracted versus ligand to picrate mole ratio graphs in Figures 11-14. The magnitude of the extraction, and, hence, metal-ligand complexation, was drastically reduced for potassium and cesium as compared to those studies with 18C6. Much higher concentrations were necessary in order to measure any extraction. Much larger extractions were obtained when thallium (I) was used as the metal cation. At metal and ligand concentrations required for cesium and potassium systems to extract less than 20% of the total picrate concentration, the thallium system was extracting up to 95%, however, not with the same efficiency as in the Tl^+-18C6 systems.

Extraction Equilibrium Constant Determination

Once the extraction data have been collected, calculation of the equilibrium constant for the complex formation becomes the primary goal. A Fortran computer program was written which used the picrate absorbance measured, complex stability constant in water (K_s), and the ligand partition coefficient (P_e), to determine the overall extraction equilibrium constant (K_e), according

Table 11. Equilibrium Extraction Study of the System CH_2Cl_2 + DT18C6 / $KC_2H_3O_2$ + PicH + LiOH + H_2O.

Mole Ratio (C_L^{org}/C_{Pic}^{aq})	Aqueous Picrate Absorbance After Extraction	$[Pic]^{aq}$ $\underline{M}$ (x10^5)	$[Pic]^{org}$ $\underline{M}$ (x10^5)	Percent Picrate Extracted
	$C_{K^+}^{aq}$ = 0.096$\underline{M}$	C_{Pic}^{aq} = 9.18 x $10^{-5}\underline{M}$	$C_{Li^+}^{aq}$ = 6.45 x $10^{-4}\underline{M}$	
27.23	1.283	8.90	0.28	3.0
51.20	1.268	8.80	0.38	4.1
75.16	1.258	8.73	0.45	4.9
99.13	1.243	8.63	0.55	6.0
123.09	1.232	8.55	0.63	6.9
147.06	1.219	8.46	0.72	7.8
171.02	1.209	8.39	0.79	8.6
	$C_{K^+}^{aq}$ = 0.209$\underline{M}$	C_{Pic}^{aq} = 9.21 x $10^{-5}\underline{M}$	$C_{Li^+}^{aq}$ = 6.45 x $10^{-4}\underline{M}$	
27.23	1.274	8.84	0.37	4.0
51.20	1.251	8.68	0.53	5.8
75.16	1.229	8.53	0.68	7.4
99.13	1.209	8.39	0.82	8.9
123.09	1.192	8.27	0.94	10.2
147.06	1.170	8.12	1.09	11.8
171.02	1.153	8.00	1.21	13.1

Table 11. Continued.

Mole Ratio (C_L^{org}/C_{Pic}^{aq})	Aqueous Picrate Absorbance After Extraction	$[Pic]^{aq}$ $\underline{M}$ ($x10^5$)	$[Pic]^{org}$ $\underline{M}$ ($x10^5$)	Percent Picrate Extracted
	CH_2Cl_2 + DT18C6 / KOH + PicH + H_2O			
	$C_{K^+}^{aq}$ = 0.151$\underline{M}$	C_{Pic}^{aq} = 9.90 x $10^{-5}$$\underline{M}$		
42.02	1.360	9.44	0.46	4.6
84.04	1.335	9.27	0.63	6.4
105.05	1.329	9.22	0.68	6.9
126.06	1.309	9.09	0.81	8.2
147.07	1.291	8.96	0.94	9.5
168.08	1.274	8.83	1.07	10.8
189.09	1.260	8.75	1.15	11.6
210.10	1.257	8.72	1.18	11.9
	$C_{K^+}^{aq}$ = 0.228$\underline{M}$	C_{Pic}^{aq} = 1.145 x $10^{-4}$$\underline{M}$		
36.33	1.543	10.71	0.74	6.5
72.66	1.512	10.50	0.95	8.3
90.83	1.492	10.36	1.09	9.5
109.00	1.474	10.23	1.22	10.6
127.16	1.457	10.11	1.34	11.7
145.33	1.426	9.90	1.55	13.5
163.49	1.398	9.70	1.7	15.3
181.66	1.401	9.72	1.73	15.1

Table 11. Continued.

Mole Ratio (C_L^{org}/C_{Pic}^{aq})	Aqueous Picrate Absorbance After Extraction	$[Pic]^{aq}$ $\underline{M}$ ($x10^5$)	$[Pic]^{org}$ $\underline{M}$ ($x10^5$)	Percent Picrate Extracted
	$C_{K^+}^{aq} = 0.451\underline{M}$	$C_{Pic}^{aq} = 8.87 \times 10^{-5}\underline{M}$		
67.64	1.102	7.65	1.22	13.8
99.21	1.072	7.44	1.43	16.1
162.34	1.013	7.03	1.84	20.7
193.91	0.997	6.92	1.95	22.0
225.48	0.974	6.76	2.11	23.8

Table 12. Equilibrium Extraction Study of the System CH_2Cl_2 + DT18C6 / $CsC_2H_3O_2$ + PicH + LiOH + H_2O.

Mole Ratio (C_L^{org}/C_{Pic}^{aq})	Aqueous Picrate Absorbance After Extraction	$[Pic]^{aq}$ $\underline{M}$ ($\times 10^5$)	$[Pic]^{org}$ $\underline{M}$ ($\times 10^6$)	Percent Picrate Extracted
	$C_{Cs^+}^{aq} = 0.034\underline{M}$	$C_{Pic}^{aq} = 9.21 \times 10^{-5}\underline{M}$	$C_{Li^+}^{aq} = 6.45 \times 10^{-4}$	
27.14	1.288	8.94	2.7	2.9
51.03	1.279	8.88	3.3	3.6
74.92	1.278	8.87	3.4	3.7
98.81	1.271	8.82	3.9	4.2
122.69	1.267	8.79	4.2	4.6
146.58	1.262	8.76	4.5	4.9
170.47	1.258	8.73	4.8	5.2
	$C_{Cs^+}^{aq} = 0.072\underline{M}$	$C_{Pic}^{aq} = 9.40 \times 10^{-5}\underline{M}$	$C_{Li^+}^{aq} = 6.45 \times 10^{-4}$	
26.60	1.310	9.09	3.1	3.3
50.00	1.301	9.03	3.7	3.9
73.40	1.299	9.02	3.8	4.0
96.81	1.290	8.95	4.5	4.8
120.21	1.283	8.90	5.0	5.3
143.62	1.277	8.06	5.4	5.7
167.02	1.269	8.81	5.9	6.3

Table 13. Equilibrium Extraction Study of the System CH_2Cl_2 + DT18C6 / $TlC_2H_3O_2$ + PicH + LiOH + H_2O.

Mole Ratio (C_L^{org}/C_{Pic}^{aq})	Aqueous Picrate Absorbance After Extraction	$[Pic]^{aq}$ M ($\times 10^5$)	$[Pic]^{org}$ M ($\times 10^5$)	Percent Picrate Extracted
	$C_{Tl^+}^{aq} = 0.024\underline{M}$	$C_{Pic}^{aq} = 1.120 \times 10^{-4}\underline{M}$	$C_{Li^+}^{aq} = 2.15 \times 10^{-4}\underline{M}$	
1.71	1.382	9.59	1.61	14.4
3.42	1.280	8.88	2.32	20.7
4.71	1.221	8.47	2.73	24.4
6.42	1.153	8.00	3.20	28.5
7.71	1.110	7.70	3.50	31.2
9.42	1.056	7.33	3.87	34.6
10.71	1.012	7.02	4.18	37.2
	$C_{Tl^+}^{aq} = 0.079\underline{M}$	$C_{Pic}^{aq} = 9.59 \times 10^{-5}\underline{M}$	$C_{Li^+}^{aq} = 2.15 \times 10^{-4}\underline{M}$	
2.00	1.031	7.15	2.44	25.4
4.00	0.893	6.20	3.39	35.3
5.50	0.814	5.65	3.94	41.1
7.50	0.732	5.08	4.51	47.0
9.00	0.679	4.71	4.88	50.9
11.00	0.611	4.24	5.35	55.8
12.50	0.578	4.01	5.58	58.2

Table 13. Continued.

Mole Ratio (C_L^{org}/C_{Pic}^{aq})	Aqueous Picrate Absorbance After Extraction	$[Pic]^{aq}$ $\underline{M}$ ($x10^5$)	$[Pic]^{org}$ $\underline{M}$ ($x10^5$)	Percent Picrate Extracted
	$C_{Tl+}^{aq} = 0.171\underline{M}$	$C_{Pic}^{aq} = 9.50 \times 10^{-5}$	$C_{Li+}^{aq} = 6.45 \times 10^{-4}\underline{M}$	
24.21	0.275	1.90	7.60	80.0
45.26	0.169	1.17	8.33	87.7
66.32	0.124	0.80	8.64	91.0
87.37	0.097	0.67	8.83	93.0
108.42	0.082	0.56	8.94	94.1
129.47	0.072	0.50	9.00	94.7
150.53	0.062	0.43	9.07	95.5
	$C_{Tl+}^{aq} = 0.201\underline{M}$	$C_{Pic}^{aq} = 9.77 \times 10^{-5}\underline{M}$	$C_{Li+}^{aq} = 6.45 \times 10^{-4}\underline{M}$	
23.54	0.256	1.77	8.00	81.9
44.01	0.155	1.07	8.70	89.0
64.48	0.111	0.77	9.00	92.1
84.95	0.087	0.60	9.17	93.9
105.43	0.073	0.50	9.27	94.9
125.90	0.065	0.45	9.32	95.4
146.37	0.059	0.40	9.37	95.9

Table 13. Continued.

Mole Ratio (C_L^{org}/C_{Pic}^{aq})	Aqueous Picrate Absorbance After Extraction	$[Pic]^{aq}$ M ($x10^5$)	$[Pic]^{org}$ M ($x10^5$)	Percent Picrate Extracted
	$C_{Tl^+}^{aq} = 0.248M$	$C_{Pic}^{aq} = 9.46 \times 10^{-5}M$	$C_{Li^+}^{aq} = 6.47 \times 10^{-4}$	
33.83	0.190	1.31	8.14	86.1
63.42	0.108	0.75	8.71	92.1
93.02	0.079	0.54	8.92	94.3
122.62	0.064	0.44	9.02	95.4
152.22	0.053	0.36	9.10	96.2
181.82	0.042	0.29	9.17	96.9
211.42	0.035	0.24	9.22	97.5
	CH_2Cl_2 + DT18C6 / $TlNO_3$ + LiOH + PicH + H_2O			
	$C_{Tl^+}^{aq} = 0.142M$	$C_{Pic}^{aq} = 1.268 \times 10^{-4}M$	$C_{Li^+}^{aq} = 1.08 \times 10^{-3}M$	
25.24	0.378	2.62	10.06	79.3
47.32	0.236	1.63	11.05	87.1
69.40	0.188	1.30	11.38	89.8
98.41	0.136	0.94	11.74	92.6
113.57	0.117	0.81	11.87	93.6
135.65	0.101	0.70	11.98	94.5
157.73	0.087	0.60	12.08	95.3

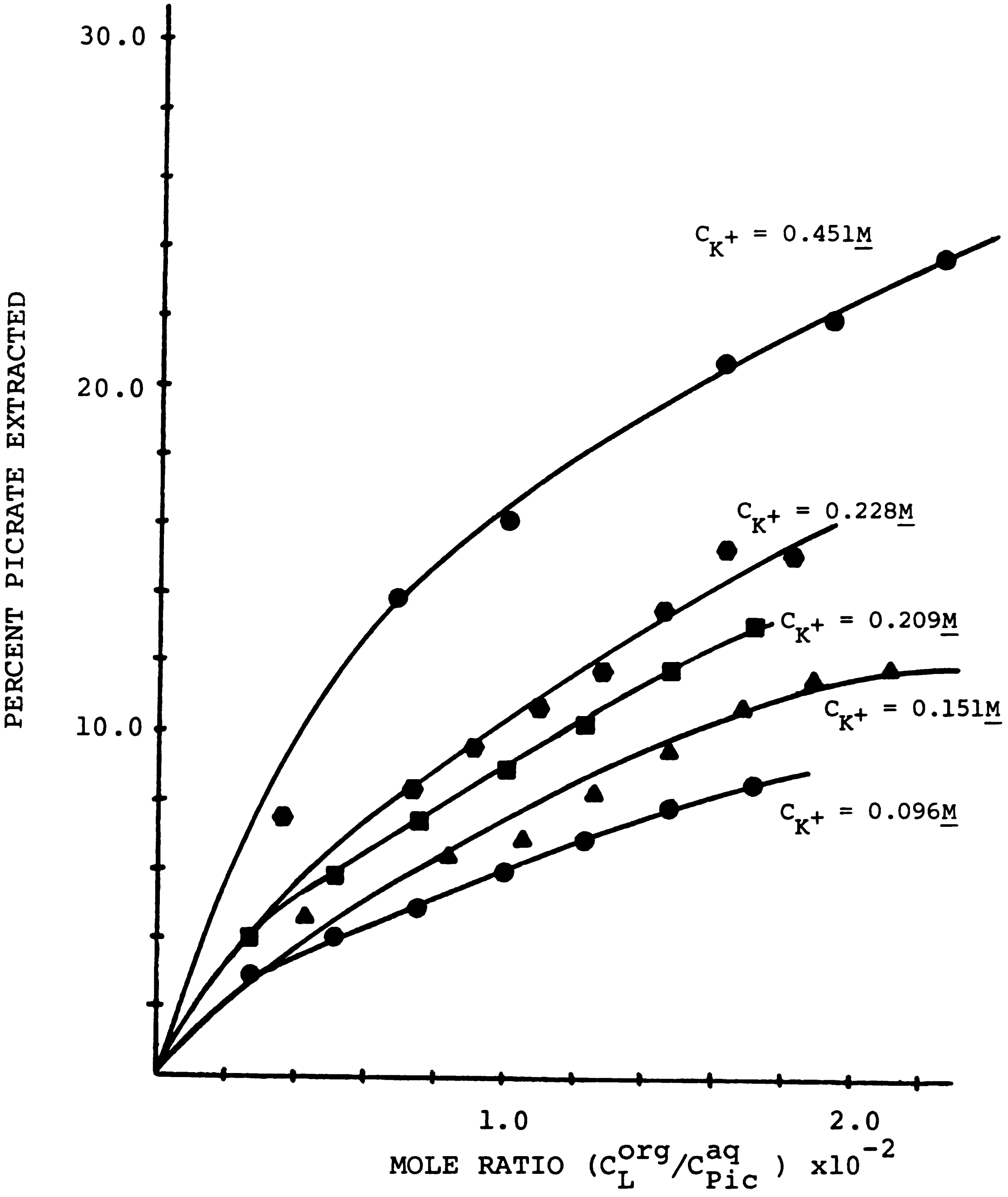

Fig. 11. Extraction of potassium picrate into methylene chloride by DT18C6 at various cation and ligand concentrations.

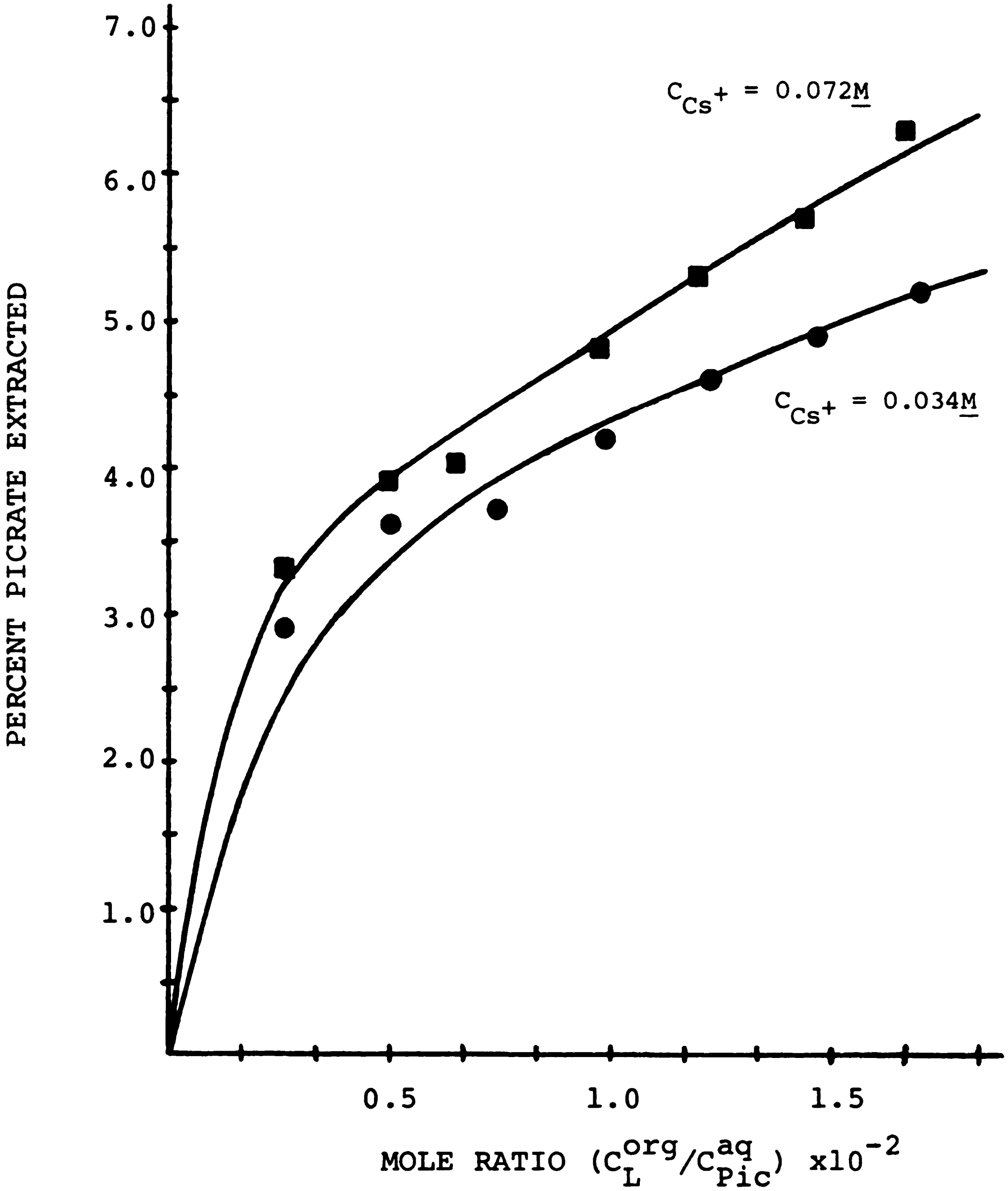

Fig. 12. Extraction of cesium picrate into methylene chloride by DT18C6 at various cation and ligand concentrations.

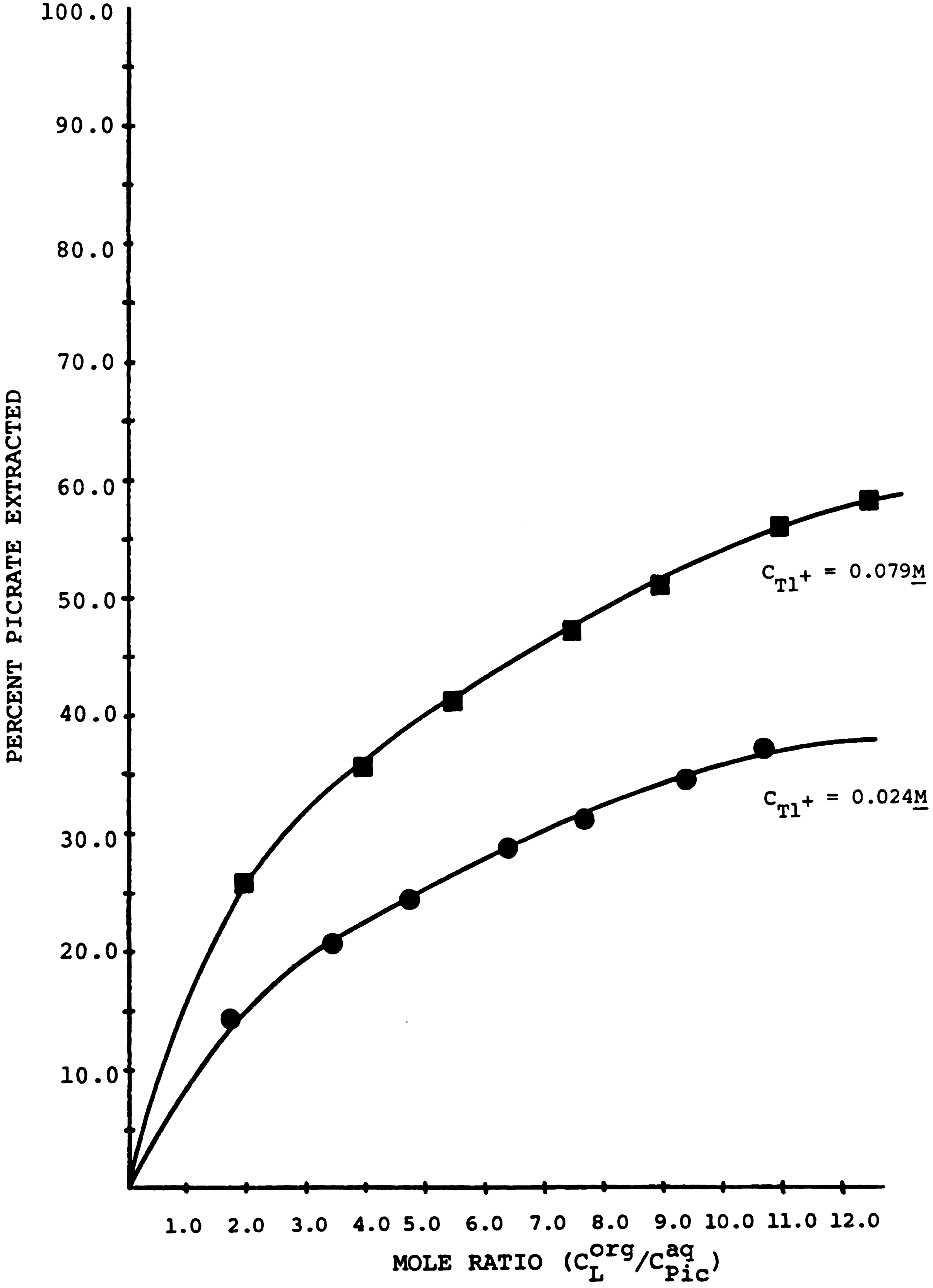

Fig. 13. Extraction of thallium picrate into methylene chloride by DT18C6 at cation concentrations of $0.024\underline{M}$ and $0.079\underline{M}$ with various ligand concentrations.

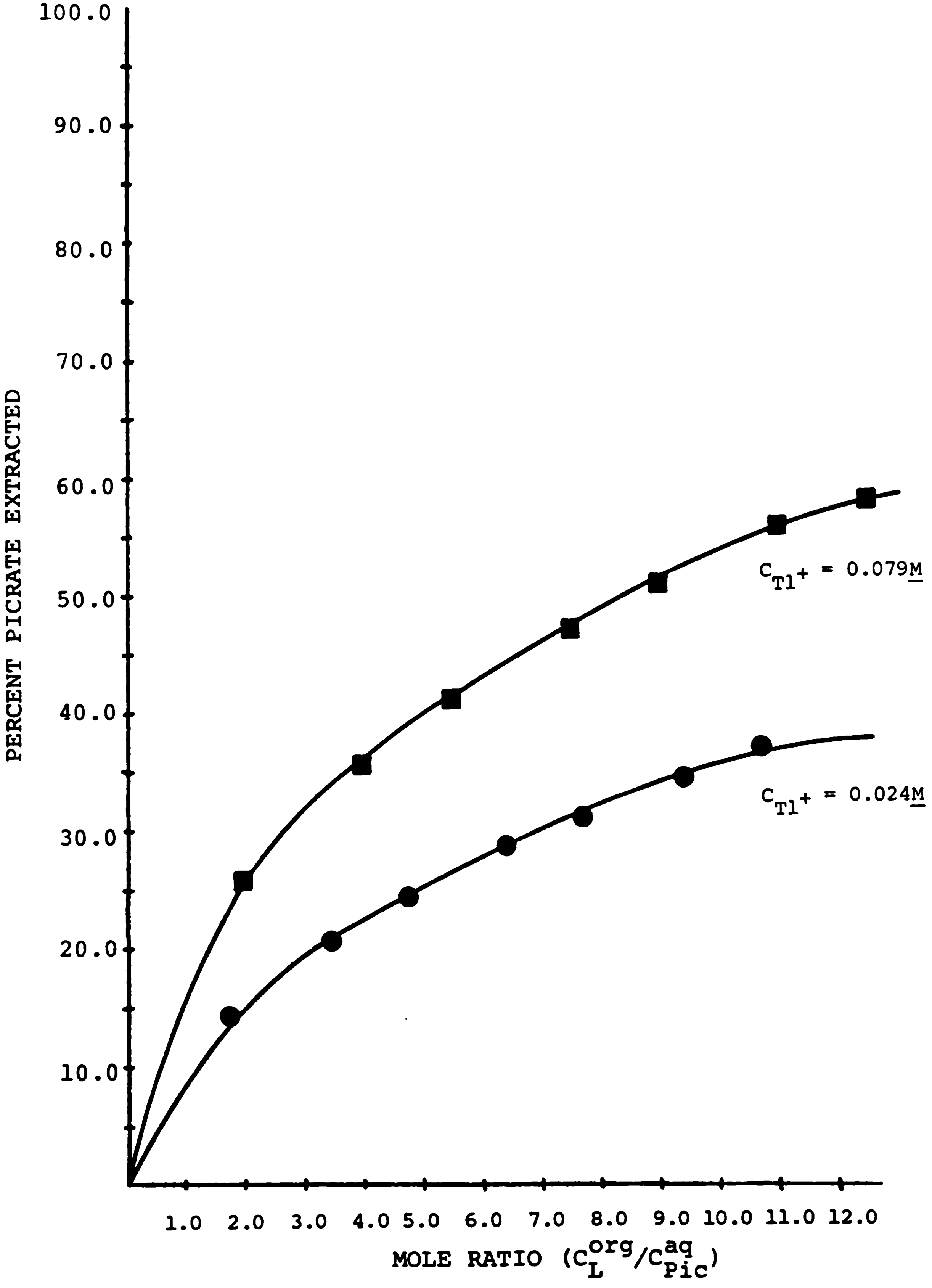

Fig. 13. Extraction of thallium picrate into methylene chloride by DT18C6 at cation concentrations of 0.024$\underline{M}$ and 0.079$\underline{M}$ with various ligand concentrations.

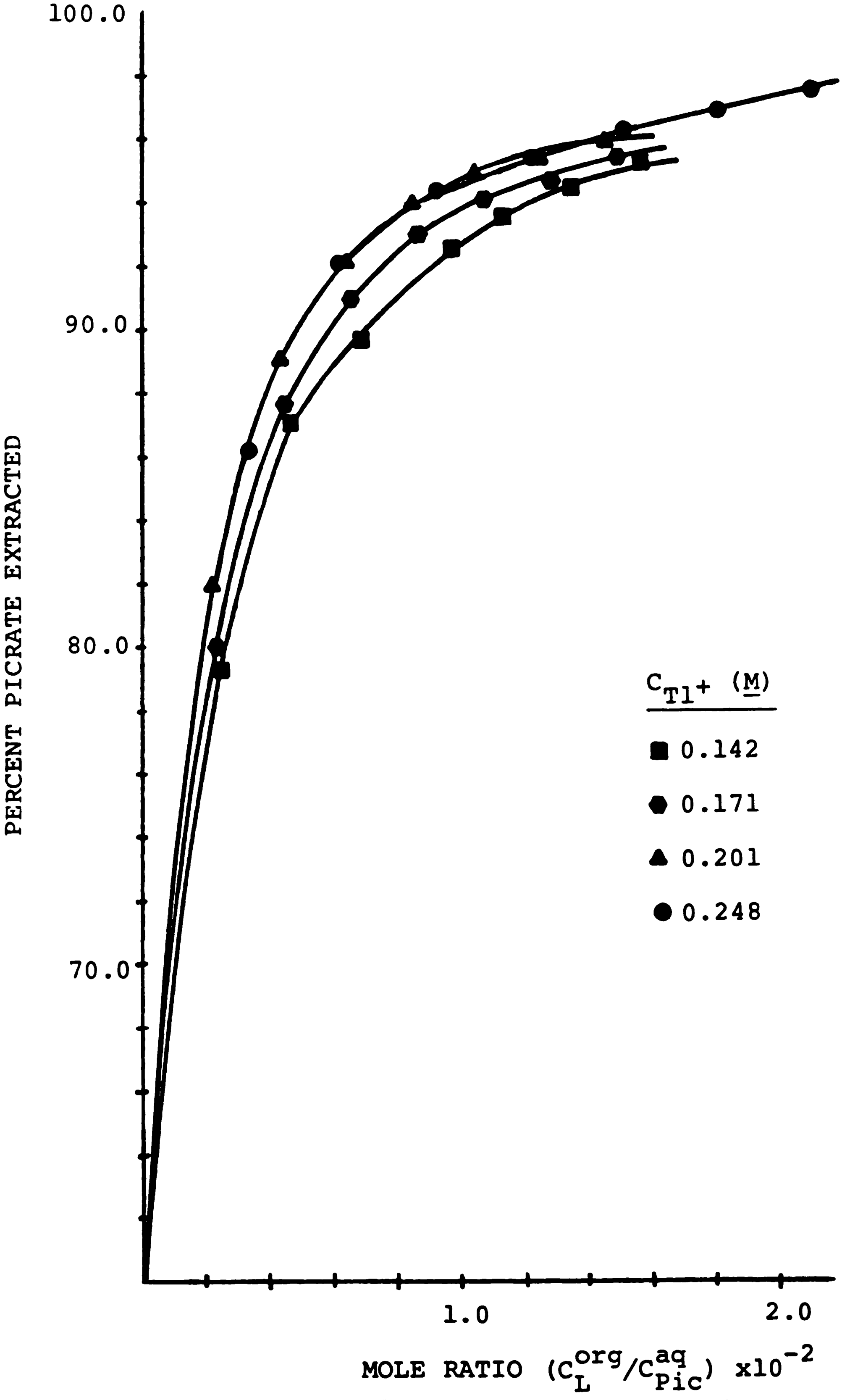

Fig. 14. High efficiency extractions of thallium picrate into methylene chloride by DT18C6 at various cation and ligand concentrations.

to equation 5. The program used is included in Appendix B. The user supplies a numerical range for K_d, as well as the number of K_d values to be employed within that range. Each K_d value yields an average equilibrium constant for a complete data set at a single metal ion concentration. A plotting subroutine plots the deviation in the calculated average extraction equilibrium constant versus each K_d. The K_d for the system is found at the minimum value in the standard deviation plot. The average K_e calculated using this K_d is the extraction equilibrium constant for the complex.

Extraction constants were calculated for all systems studied except for the complexes of K^+ and Cs^+ with DT18C6, because of the low picrate extractions observed. In order to calculate a reliable constant, data should be available in the range of 10-90% extracted. Table 14 contains the results of these calculations as well as the corresponding K_d values for ion pair dissociation. The complexing strength of 18C6 for the metal cations decreases in the order $K^+ > Tl^+ > Cs^+$ while DT18C6 decreases $Tl^+ > K^+ > Cs^+$. Although the actual extraction equilibrium constants for $(DT18C6 \cdot K)^+$ and $(DT18C6 \cdot Cs)^+$ complexes were not calculated, the percent picrate extracted imply this order.

The lower the partition coefficient, the more is the hydrophobic character of the ligand. Since K^+-ligand complexation for all three macrocycles were studied, an

Table 14. Extraction Equilibrium and Complex Dissociation Constants.

Complex	log K_d	log K_e
$K^+ \cdot$DB18C6	-4.61 ± 0.13	4.79 ± 0.22
$K^+ \cdot$18C6	-4.85 ± 0.31	6.38 ± 0.06
$Cs^+ \cdot$18C6	-4.67 ± 0.32	5.56 ± 0.41
$Tl^+ \cdot$18C6[a]	-2.89	5.81 ± 0.05
$Tl^+ \cdot$DT18C6[b]	-4.08 ± 0.00	3.80 ± 0.01

[a] The standard deviation could not be obtained for K_d since it was calculated from only a single curve.

[b] The standard deviation shown for K_d reflects the precision obtained for all curves (Figure 13); however, the author acknowledges that an error value exists below 0.01.

interesting comparison may be made. The partition coefficients for 18C6, DB18C6, and DT18C6 reported values were 0.23, 0.09, and $<10^{-2}$, respectively, implying that ligand hydrophobicity falls in the order DT18C6>DB18C6>18C6. The magnitude of the ligand hydrophobic character should have no effect on the stability of the complex, but it will have a slight effect on the value of K_e. It is apparent from this work, as well as of other investigators, that less hydrophobic ligands facilitate the extraction of the alkali metal ions into the organic phase.

Since the overall extraction equilibrium is much too complex to deduce the specific molecular processes, the equilibrium may be studied more effectively by analysis of three constituent equilibria (22):

$$M^{+}_{aq} + L_{aq} \rightleftharpoons ML^{+}_{aq} \qquad K_s \qquad (7)$$

$$L_{org} \rightleftharpoons L_{aq} \qquad P_e \qquad (8)$$

$$ML^{+}_{aq} + Pic^{-}_{aq} \rightleftharpoons MLPic_{org} \qquad P_c \qquad (9)$$

Since these three equilibria may be summed to give the original equilibrium expression, the overall extraction equilibrium constant is given by

$$K_e = K_sP_eP_c \qquad (10)$$

where P_c is the partition coefficient of the complex from separate ions in the aqueous to ion pairs in the organic phase, and K_e, P_e, and K_s retain their usual meaning.

Table 15 contains the equilibrium constants of the component equilibria from the extraction systems presented in this work. The partition coefficient, P_c, was calculated from equation 10. The data presented shows that the log P_c values, for the 18C6 complexes of K^+ and Cs^+ are similar enough not to be the important factor in determining K_e. The tremendous difference in the stability constant, K_s, appears to be the determining factor. Thallium and potassium possess comparable extraction equilibria constants, however, for the complex $(18C6 \cdot Tl)^+$ the K_s value is substantially greater than that of $(18C6 \cdot K)^+$. The less efficient extraction of Tl^+ may be attributed to the smaller value of P_c.

The order of stability of metal complexes has been an important area of study. One theory proposed to explain the preference in binding is based on Pearson's concept of hard-soft acid-base interactions (108). "Hard" species are small and only slightly polarizable, while "soft" species are larger and more polarizable. Pearson suggested that the stability of "acid-base" complexes is determined by the rule that hard acids prefer to bind to hard bases and vice versa. The hard alkali and

Table 15. Equilibrium Constants for the Extraction of Picrates.

Ligand	Cation	K_e	K_d	K_s	P_e^*	P_c	log P_c
DB18C6	K	6.18×10^4	2.61×10^{-6}	46.77	0.09	1.47×10^4	4.17
18C6	K	2.40×10^6	1.41×10^{-5}	107.2	0.23	9.73×10^4	4.99
	Cs	1.45×10^5	9.84×10^{-6}	9.77	0.23	6.45×10^4	4.81
	Tl	6.47×10^5	1.28×10^{-3}	186.2	0.23	1.51×10^4	4.18
DT18C6	Tl	6.42×10^3	8.21×10^{-5}	8.51	0.01	7.46×10^4	4.87
		6.34×10^3			0.001	7.46×10^5	5.87
		6.34×10^3			0.0001	7.46×10^6	6.87
		6.34×10^3			0.00001	7.46×10^7	7.87

*Partition coefficients used in calculation are assumed values.

alkaline earth and early transition metal ions preferentially bind in the order O>N>S while the softer species (greater number of d electrons), favor ligands S>N>O. This theory considers hard-hard interactions as primarily electrostatic in nature, while the soft-soft interactions are due more to covalent character in the bond. The polarizability of d electrons is important for the soft-soft interactions, with metals containing d^{10} configuration being very soft acids. By substitution of sulfur donor atoms for some, or all, of the oxygen atoms in the macrocyclic ring, the ligand's binding sites are becoming softer, therefore, DT18C6 would be a softer base than 18C6. The potassium ion is considered a hard acid while the thallium ion, with an electron configuration of $[Xe]4f^{14}5d^{10}6s^{2}$, is classified as a soft acid. Based upon this theory, one would expect K^{+} to complex better with hard base 18C6 than with soft base DT18C6 and Tl^{+} to complex more strongly with DT18C6 than with 18C6. The results reported in this thesis support the theory in the case of K^{+} but not Tl^{+}. The extraction equilibrium constant of $(DT18C6 \cdot Tl)^{+}$ is less than $(18C6 \cdot Tl)^{+}$ by a factor of 100, although complexation between DT18C6 and Tl^{+} is substantially greater than with the alkali metals ions.

CHAPTER V

INFRARED AND RAMAN STUDIES OF 18C6·ACETONITRILE COMPLEX

Introduction

The infrared (IR) and Raman studies of 18C6 in acetonitrile (ACN) were conducted to investigate the weak binding interaction between the crown and the solvent. Solid 18C6 is soluble in ACN up to approximately 0.20M, however, beyond this concentration a precipitate forms which has been shown to be the 18C6·ACN complex. Gokel and coworkers (67) reported that depending on experimental conditions the complex may be of variable stoichiometry. Two possible factors the authors proposed would favor formation of the "host-guest adduct":

(a) The substantial size and lack of rigidity of the 18-membered ring might prefer the formation of the solid complex, stabilized by the ACN molecule within the crystal lattice;

(b) The presence of so many electronegative atoms in the ring would make it capable of interacting with and further ordering the ACN in the lattice.

Infrared and Raman spectroscopic methods were chosen to study this interaction since both are sensitive to small changes in intermolecular forces and because ACN molecules produce distinctive bands (C-C and C≡N symmetric stretches, 928 cm^{-1} and 2253 cm^{-1}, respectively) affected by molecular interactions (71). One would expect either a shift in the pure solvent bands and/or formation of new bands due to vibrations within the complex.

Infrared and Raman Spectral Data

Infrared and Raman spectra were obtained for pure samples of ACN and of 18C6 so that the various bands arising in the complex spectrum could be identified as belonging to either the crown or the solvent. Since the complex is known to be weak, one would expect the spectrum to be predominantly the sum of the spectra of the two components.

The interaction of 18C6 and ACN could be either through the carbon or nitrogen atom of the solvent, therefore, the solvent's C-C and C≡N symmetric stretch regions were particularly investigated.

Table 16 contains the IR and Raman band frequencies of pure 18C6, of pure ACN, and of the crown-solvent complex. The Raman spectrum was obtained from the solid complex. The infrared spectrum of the solid, however, could not be obtained because the physical stress applied when preparing a sample in nujol or as a KBr pellet

Table 16. Infrared and Raman Band Frequencies of 18C6 and ACN Samples (Regions: IR 600-4000 cm^{-1} and Raman 840-3010 cm^{-1}).

ACN		18C6		18C6·ACN Complex	
IR	Raman	IR	Raman	IR	Raman
750				749	
					832
		860	867	841	860
	902		894		
912	921				921
		944	938	959	945
		985	988		
1039	1032	1043	1047	1042	
			1064		1068
			1092		1081
			1112	1117	1106
		1130	1134		1125
			1138	1138	
			1159		
			1238	1242	
		1252	1260	1254	
			1278	1287	1274
			1298		1292
			1337		
		1351	1357		1367
1374	1376		1375		1375
	1419		1391		
	1429		1415		1409
	1449		1447		1455
			1475		1477
			1479		
			1495		
					2195
2250	2254			2252	2243
2294	2294			2290	2291
2414				2411	2414
2622				2626	
					2682
	2735				2727
					2769
					2783
	2844				
	2884				
2939	2943			2942	
2996	3003			2993	3005
3154				3168	

caused the complex to decompose. The spectrum of 18C6 in ACN solution was, therefore, recorded. Considering small variations in the instrument's frequency calibration for the different spectra, the bands of the complex (in both solution and as the solid) do appear to be a combination of the frequencies of the individual components.

Raman spectra of ACN, of 18C6, and of 18C6·ACN complex in the C-C and C≡N symmetric stretch regions of the ACN molecule were separately studied under identical instrumental settings, at a low scan rate (10 $cm^{-1}min^{-1}$) in order to help optimize the electronic response time. The solvent's C-C stretch band appeared at 921 cm^{-1} in pure ACN and in the complex, at 920 cm^{-1}. In this region pure 18C6 possessed a very weak band at 938 cm^{-1} and a moderate sized band at 989 cm^{-1}, however, the complex only showed a band at 943 cm^{-1}, of intensity comparable to the 989 cm^{-1} band.

In the region of higher frequency three bands appeared in pure ACN, 2294 cm^{-1}, 2254 cm^{-1} (C≡N symmetric stretch) and 2205 cm^{-1}. The Raman spectrum of 18C6 showed no bands in this region, however, the solid 18C6·ACN complex produced bands at 2290 cm^{-1} and 2244 cm^{-1}. The disappearance of the band at 2205 cm^{-1} could be attributed to a lower concentration of the ACN in the complex. It is difficult to determine the significance of these small shifts, but they were repeatedly observed.

These studies do show the sensitivity of IR and Raman spectroscopy in detecting the existence of the crown-solvent interaction and indicate that a more thorough study, using these spectroscopic techniques, could provide for better characterization of the nature of the binding and possibly lead to identification of the binding site.

CHAPTER VI

DETERMINATION OF CESIUM- AND THALLIUM-DT18C6 COMPLEX STABILITY CONSTANTS IN NONAQUEOUS SOLVENTS BY NMR

Introduction

A second technique employed to help characterize the complexing abilities of DT18C6 was nuclear magnetic resonance. Specifically, studies of the DT18C6 complexing with cesium and thallium ions were performed using ^{133}Cs and ^{205}Tl NMR. A shift of the resonant frequency from that of free metal ions is caused by the disturbance of its electrons. Since the ^{133}Cs and ^{205}Tl chemical shifts are dominated by the paramagnetic term, if the electron density around the nuclei is increased by an interaction with an anion, a ligand, or solvent molecules, a downfield (paramagnetic) chemical shift will occur. However, if the electron density is decreased then the shift is upfield (diamagnetic). Polarization of the cesium and thallium ions are such that chemical shifts may be quite large (especially for the thallium ion) 130 ppm and 2600 ppm, respectively. The wide range of chemical shifts provides for high sensitivity to the variations in the immediate environment of the nuclei, whether they be due to ionic interactions, complexation, or both, and, therefore, metal NMR should be a very useful technique for the study of DT18C6 complexes.

Concentration Formation Constants from NMR Chemical Shift Measurements

A sample prepared for studying a metal ion-ligand complex in a particular solvent will consist of two forms of metal ions (assuming that the ion is not totally complexed), the free metal ion and the complexed metal ion, which will give rise to resonance at two different frequencies. If the exchange between the free solvated metal ion and the complex is fast on the NMR time scale a single resonance is observed (population-average resonance) and the observed chemical shift (ppm) is given by the expression (109).

$$\delta_{obs} = X_f\delta_f + X_c\delta_c \tag{1}$$

where X_f and X_c are the mole fractions of the free cation and complexed cation and δ_f and δ_c are the chemical shifts of the free and complexed cations, respectively. Given that

$$X_f = \frac{C_f^M}{C_{total}^M} \tag{2}$$

C_f^M and C_{total}^M are the concentrations of free and total metal ion, the following expression may be written

$$\delta_{obs} = \frac{C_f^M}{C_{total}^M}(\delta_f - \delta_c) + \delta_c \qquad (3)$$

Since the ultimate goal is to obtain the formation constant, assuming 1:1 stoichiometry

$$M^+ + L \rightleftarrows ML^+ \qquad (4)$$

the concentration equilibrium constant is expressed as

$$K_f = \frac{(ML^+)}{(M^+)(L)} = \frac{C^C}{C_f^M\, C_f^L} \qquad (5)$$

where C^C is the concentration of the complex and C_f^M and C_f^L are the concentration of the free metal and the free ligand. The expression can be rewritten in the form

$$K_f = \frac{C_{total}^M - C_f^M}{C_f^M(C_{total}^L - C_{total}^M + C_f^M)} \qquad (6)$$

The final expression

$$\delta_{obs} = [(K_f C_{total}^M - K_f C_{total}^L - 1) \pm (K_f^2 C_{total}^{L^2} + K_f^2 C_{total}^{M^2} - 2K_f^2 C_{total}^L C_{total}^M + 2K_f C_{total}^L + 2K_f C_{total}^M + 1)^{\frac{1}{2}}]\left[\frac{\delta_f - \delta_c}{2K_f C_{total}^M}\right] + \delta_c \qquad (7)$$

can be derived by combining equations 3, 5, and 6. Measurements of δ_{obs} were obtained for a series of solutions, possessing a constant metal concentration but a varying concentration of the ligand. Since δ_f may be measured, using the metal salt solution with no ligand, equation 7 contains two unknown quantities, δ_c and K_f.

A nonlinear least-squares program KINFIT was used to solve the expression by supplying the experimental parameters δ_{obs}, δ_f, C^L_{total}, and C^M_{total} and adjusting K_f and δ_c until the allowed error in curve-fitting was obtained.

The expressions above are valid when there is no ion pairing in solution, or if the ion pair formation constant is very small compared to K_f. It is possible that both the ligand and anion compete for the metal ion in solution, and the change in the observed chemical shift is the summation of anionic association and complexation by the ligand. In this situation the expression for the observed chemical shift must include a term accounting for the ion pairing interaction

$$\delta_{obs} = X_f\delta_f + X_c\delta_c + X_{ip}\delta_{ip} \qquad (8)$$

where X_f, X_c, and X_{ip} are the mole fractions and δ_f, δ_c, and δ_{ip} are the chemical shifts for the free, complexed, and ion paired metal ion, respectively. Derivation of the final expression used to fit the experimental chemical shifts yields

$$\delta_{obs} = \frac{[M]}{C^L}\delta_f + \frac{K_f C^L[M]}{C^M(K_f[M]+1)}\delta_c + \frac{K_{ip}C^M[M]\delta_{ip}}{C^M(K_{ip}[M]+1)} \qquad (9)$$

with K_{ip} representing the ion pair formation constant. The values of K_{ip}, C^M, δ_{ip}, and δ_f must be supplied for analysis by KINFIT while K_f and δ_c are adjusted until the statistical error has been minimized to the allowed limit.

In both situations the data supplied was weighted such that the more accurate measurements would be relied on more heavily in determining the formation constant and limiting chemical shift of the complex.

Cesium-133 NMR Study

Although ^{133}Cs NMR appears highly suitable for the study of cesium complexation reactions, it is not without difficulties, particularly the limited solubility of the metal salts in nonaqueous solvents. The range of a cesium salt solubility is typically 0.01M, therefore, a greater number of scans must be performed to obtain a reasonable NMR signal (a respectable signal-to-noise ratio). However, the sensitivity provided by the narrow NMR lines helps in resolving the signal from background noise.

Another difficulty encountered was the ligand solubility. In propylene carbonate and acetone, it was found that DT18C6 was insoluble, or at most, soluble to a very small extent, impractical for NMR measurements.

Cesium-133 chemical shifts were determined as a function of DT18C6 to cesium ion mole ratio for the formation of the $(Cs\cdot DT18C6)^+$ complex in nitromethane (NM), pyridine (py), dimethylformamide (DMF), and acetonitrile (ACN). The cesium salt used, for a particular solvent, was chosen for maximum solubility in the solvent of interest, and minimal ion pairing in solution, therefore, different anions were utilized.

The chemical shift results, shown in Table 17, possess an estimated error in the measurements of ±0.10 ppm. The plot of chemical shift versus ligand-to-metal mole ratio (Figure 15) shows that $(Cs\cdot DT18C6)^+$ complexation in all four solvents yielded shifts, paramagnetic in nature, resulting from an increase in the electron density about the cesium ion. In all cases, the plots show little curvature, implying very weak metal-ligand interaction.

Before any attempt could be made to numerically access the strength of the $(Cs\cdot DT18C6)^+$ complex, it was of utmost importance to characterize the solute-solute and solute-solvent interactions in solution. These interactions will be dependent upon the solvation number of the ions, the solvating ability of the solvent, the solvent's dielectric constant, and the ion pairing

Table 17. Cesium-133 Chemical Shifts of $(Cs\cdot DT18C6)^+$ Complexes in Various Solvents (ambient probe temperature 32-33°C).

Nitromethane[a]		Dimethylformamide[b]	
C_L/C_{Cs^+}	δ (ppm)	C_L/C_{Cs^+}	δ (ppm)
0.00	60.27	0.00	0.96
0.88	56.25	0.54	0.72
0.99	56.02	0.87	0.57
1.26	54.70	1.06	0.49
1.71	54.32	1.46	0.34
2.47	49.82	2.69	0.18
2.59	49.90	3.79	-0.28
2.66	49.12		
2.89	49.04		

Acetonitrile[c]		Pyridine[d]	
C_L/C_{Cs^+}	δ (ppm)	C_L/C_{Cs^+}	δ (ppm)
0.00	-35.29	0.00	41.36
0.34	-35.84	0.34	39.00
0.79	-36.41	0.93	35.96
1.08	-36.84	1.56	32.18
1.46	-37.40	1.63	31.93
1.72	-37.52	1.93	30.26
2.39	-38.27	2.27	28.52
2.82	-38.70	2.43	27.96
3.70	-39.26	2.86	26.28
4.02	-39.63	3.51	22.81
4.60	-38.83	3.62	22.87
		4.50	19.96

[a] $[CsClO_4] = 0.0044\underline{M}$

[b] $[CsClO_4] = 0.0494\underline{M}$

[c] $[CsSCN] = 0.0345\underline{M}$

[d] $[CsBPh_4] = 0.0148\underline{N}$

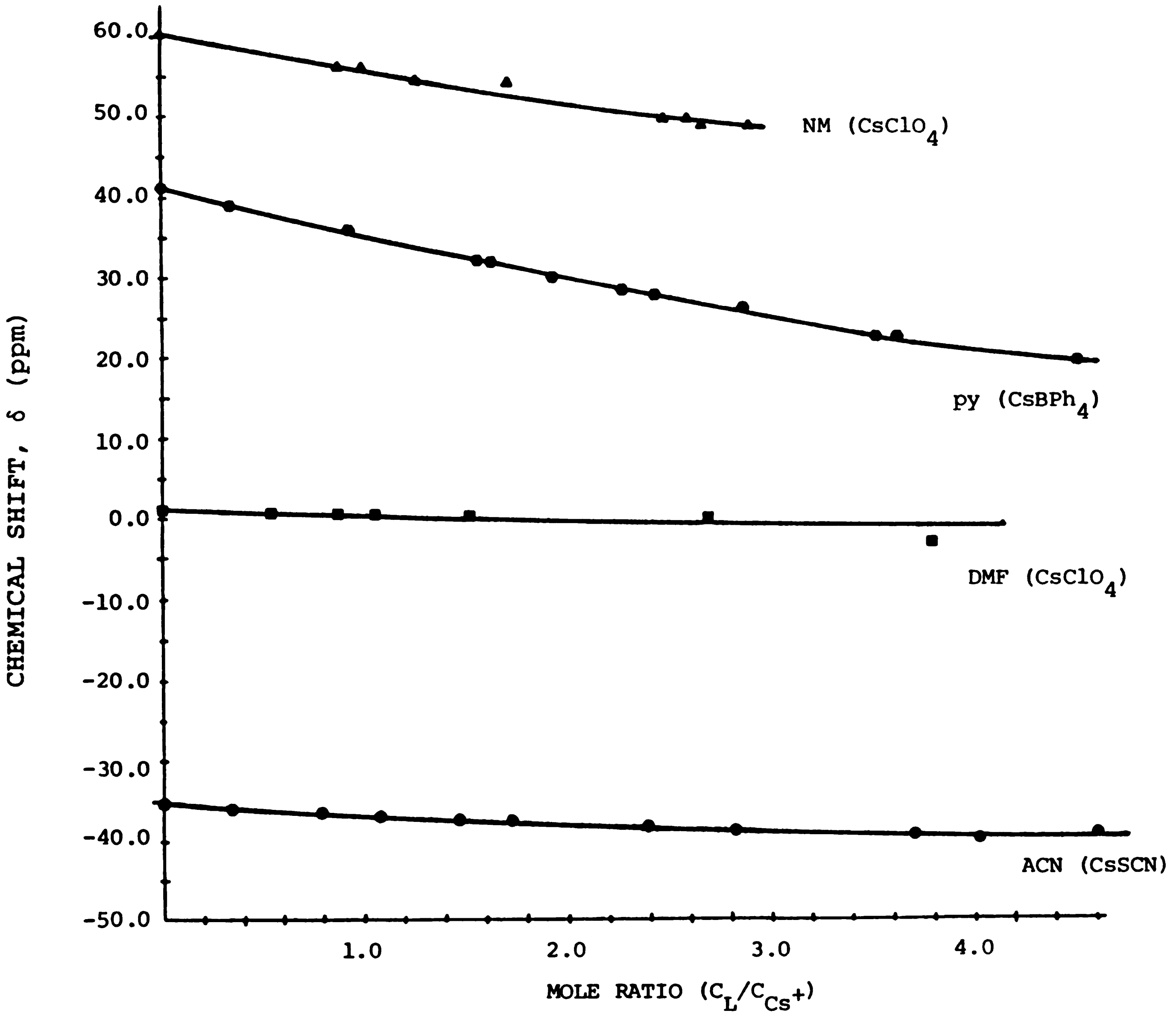

Fig. 15. Cesium-133 chemical shifts versus ligand to metal mole ratio for $(Cs \cdot DT18C6)^+$ complex formation.

capabilities of the cation and anion. In solvents of intermediate to low values of dielectric constant and of donor ability, the association of the cation and anion would be strong, producing a concentration dependence of the chemical shift, implying contact-ion pair formation. Alternatively, in solvents of high dielectric constant and donor ability contact-ion pair formation is not expected. However, of the alkali metal ions, cesium is the most poorly solvated, owing to its large size and low charge density; hence, it is possible that it may undergo contact-ion pair formation, even in polar-solvating solvents (110).

The concentration dependence of ^{133}Cs chemical shifts as a function of salt concentration have previously been established by DeWitte et al. (110). Ion pairing was shown to be significant in cesium tetraphenylborate-pyridine solutions. The ion pair formation constant was reported to be 370 ± 20 with the ion pair limiting chemical shift (δ_{ip}) of 40.0 ppm. Cesium thiocyanate-acetonitrile solutions were also shown to be concentration dependent, however, to a much lesser extent. Hsu (75) found the ion pair formation constant to be 13.2 ± 3.8 and a value of -36.7 ppm as the limiting chemical shift of the ion pair. Cesium perchlorate solutions of both dimethylformamide and nitromethane were shown to exhibit no ion pairing, by DeWitte (74) and Hsu (75), respectively.

The formation constants for the complex reaction in the different solvents are listed in Table 18. The curves (Figure 15) showed no observable break at any mole ratio so the constants were calculated based on a complex stoichiometry of 1:1. It should be noted that the equilibrium constant is expressed in concentration units and, therefore, it cannot be considered a thermodynamic constant. The calculated formation constants, for cesium complexation with DT18C6, in each solvent, were of comparable magnitude. The influence of solvent properties on metal-ligand complexation has been established. Generally one would expect that in solvents of high donicity the complex stability should decrease due to the competition between the ligand and the solvent molecules for the metal ion. The results obtained in this work do not strictly fit this generality. A more valid comparison of the effects of solvent properties on complex formation would be in studies in which the same counterion was used. The complex $(Cs \cdot DT18C6)^+ClO_4^-$ was more stable in NM, a poor donor solvent, than in DMF, a solvent of comparable dielectric constant but larger Gutmann donor number. Complexation was greatest in ACN, which possesses a medium donor number and a high dielectric constant; however, the formation constant of the complex in py was surprisingly high. Pyridine possesses a high donor number, yet it does not solvate the cesium

Table 18. Complex Formation Constants for Cesium Complexes with DT18C6 in Four Nonaqueous Solvents.

Solvent	Counterion	log K_f	Limiting Chemical Shift
NM	ClO_4^-	0.65 ± 1.09	-155.8 ± 4.77
DMF	ClO_4^-	0.56 ± 0.29	-2.10 ± 1.27
ACN	SCN^-	0.90 ± 0.27	-44.10 ± 3.03
py	BPh_4^-	0.84 ± 0.15	-127.8 ± 49.8

ion as well as expected, leading to a stronger cesium-DT18C6 complex. An explanation, based on the hard-soft acid-base theory, contends that since py is a nitrogen donor and, therefore, a soft base, it does not strongly solvate the alkali metal ion, a hard acid (111, 112). In the case of $CsClO_4$ in NM and DMF the formation constant values should be considered only as estimates of the true concentration constant because of the large error involved in the curve fitting; however, they do provide insight into the complexing abilities of DT18C6 toward the alkali ion, Cs^+.

Sulfur-substituted crowns have been shown to possess complexation strengths much lower than their polyether analogue. Complexation studies of cesium with 18C6 were performed by Mei (113) in the solvents pyridine, acetone, propylene carbonate, acetonitrile, dimethylformamide, and dimethyl sulfoxide. Regardless of the solvent used, 1:1 and 2:1 (ligand:metal) complexes were observed. The weakest complex was found in DMSO and possessed formation constants, $K_1 = 1100 \pm 100$ and $K_2 = 1.0 \pm 0.4$.

Thallium-205 NMR Study

Chemical shift measurements of the ^{205}Tl resonance frequency of solutions containing thallium perchlorate and DT18C6 were obtained in DMSO and py.

The chemical shift was measured as a function of ligand-to-metal mole ratio. Table 19 contains the results

Table 19. Thallium-205 Chemical Shifts for $(Tl \cdot DT18C6)^+$ Complexes in Two Nonaqueous Solvents.

Pyridine[a]		Dimethyl Sulfoxide[b]	
C_L/C_{Tl^+}	δ (ppm)	C_L/C_{Tl^+}	δ (ppm)
0.00	-596.72	0.00	-317.92
0.43	-540.87	0.84	-316.07
0.80	-493.22	2.01	-314.49
1.06	-467.98	2.82	-312.72
1.34	-434.70	3.18	-315.19
1.81	-385.10	3.80	-314.31
1.98	-369.23	4.67	-316.16
2.27	-339.47	6.94	-312.37
2.52	-322.50	7.87	-313.25
2.79	-299.35	9.03	-312.81
3.30	-257.69		
3.63	-231.46		

[a] $[TlClO_4] = 0.0574\underline{M}$ (probe temperature = 34°C)

[b] $[TlClO_4] = 0.0098\underline{M}$ (probe temperature = 29°C)

of the two complexation studies, which are graphically presented in Figure 16.

In DMSO, a solvent of high donicity and relatively high dielectric constant, no evidence of complexation was observed, implying that the solvent strongly solvates the Tl (I) ion blocking any ion-ligand interaction. Srivanavit and coworkers (95) have studied the complexation of $TlClO_4$ and 18C6 in DMSO, and obtained information indicative of a strong complex. The chemical shift versus mole ratio plot possessed an extrapolated break at 1:1 stoichiometry (as found in several solvents) and obtained the limiting chemical shift of the complex at a mole ratio of four. The complex formation constant was found to be greater than 10^3, implying that 18C6 could successfully compete with the solvent, therefore, ligand complexation rather than metal ion solvation resulted, in contrast to the results of DT18C6.

Figure 16 also contains the plot of the results for $TlClO_4$ and DT18C6 in py. The chemical shift is upfield (diamagnetic) and extremely large, spanning from -600 ppm for the free solvated Tl (I) ion to -230 ppm at a mole ratio 3.6. A very slight curvature in this plot implies formation of a weak $(Tl \cdot DT18C6)^+$ complex. Just as noted with the cesium complexation in py, it is evident that the solvent does not solvate the Tl (I) ion as effectively as DMSO even though it possesses greater

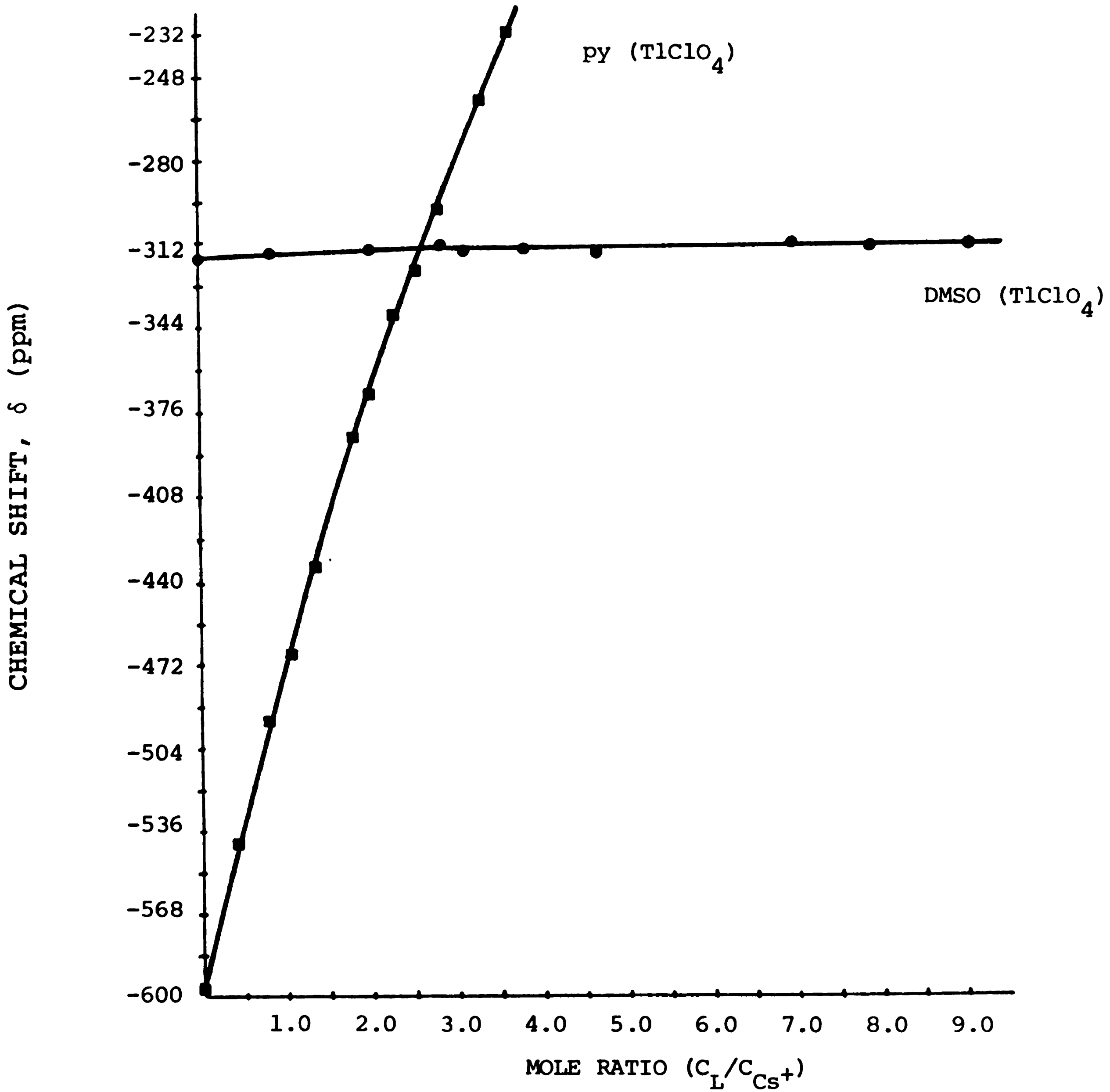

Fig. 16. Thallium-205 chemical shifts versus ligand to metal mole ratio for $(Tl\cdot DT18C6)^+$ complex formation.

donor ability. However, in the case of the Tl (I) ion, which is classified as a soft acid, the previous explanation based upon the hard-soft acid-base theory does not seem appropriate.

Computer analysis of the chemical shift data determined the formation constant of the complex, in py, to be log K = 0.34 ± 0.02 with a limiting chemical shift of 632.4 ± 44.3 ppm. The constant was calculated based on a 1:1 complex stoichiometry with no ion pair considerations. However, Briggs and Hinton's (90) NMR studies, of thallium salts, have shown that ion pairing is significant in py. The authors referenced their chemical shifts to infinite dilution aqueous $Tl^{+}NO_3^{-}$. For the system $TlClO_4$ in py they reported the chemical shift of the free solvated Tl (I) ion and the limiting chemical shift of the ion pair, as -781 ppm and -660 ppm, respectively. These workers did not report any ion pair formation constant (K_{ip}), however, from their data, our KINFIT program was utilized to calculate K_{ip}. An attempt to take into consideration activity effects did not result in an acceptable fitting of the data, however, the concentration ion pair formation constant fitting was very good. For $TlClO_4$ in py, K_{ip} = 715 ± 69 indicative of a significant amount of cation-anion interaction. Both ligand and anion compete for the thallium ion in solution and the change in the observed chemical shift (Table 19), for this system, is partly due to changes in the degree of anionic association with the thallium ion upon complexation with DT18C6. Re-evaluation of the complex formation constant, taking into consideration the extent of ion pairing, resulted in a more realistic value, K_f = 20.28 ± 9.10 with the limiting chemical shift of the complex of 1125 ± 444 ppm.

CHAPTER VII

COMMENTARY

The studies presented in this thesis demonstrate the weak complexing strength of DT18C6 for the alkali metal ions, potassium and cesium. The substitution of sulfur atoms for the oxygen atoms in the 18C6 macrocyclic ligand is responsible for the reduction in binding compared to the polyether. Although DT18C6 prefers binding with the thallium (I) ion, rather than the alkali metal ions studied, a decrease in the complex strength is still observed when the sulfur-substituted ligand is used, instead of 18C6.

The two techniques employed to determine the binding preference of DT18C6, distribution equilibria studies and metal NMR measurements, led to the same order of complex strengths $(\mathrm{Tl \cdot DT18C6})^+ > (\mathrm{K \cdot DT18C6})^+ > (\mathrm{Cs \cdot DT18C6})^+$ regardless of the solvent the complexation reaction took place in.

It would be interesting to determine, by these techniques, the complexing capabilities of nitrogen substituted 18C6 ligands for these same metals.

Preliminary ^{205}Tl NMR studies, in our laboratories, indicate that 1,10-diaza-18C6-metal ion complexes are much stronger than those using the DT18C6 ligand. A more thorough investigation of these ligands as well as the monosubstituted sulfur and nitrogen 18C6 molecules are necessary in order to explain the binding preferences. Pearson's (108) hard-soft acid-base theory does not appear to fully explain the complex strengths observed. In accord with the theory, the hard acid, alkali metal ion, prefers to bind to the ligand possessing donor atoms in the order O>N>S, which is the order of hard to soft donor atoms, but the soft acid, thallium metal ion, shows the same preference, O>N>S, contrary to the theory. However, the hard-soft acid-base theory does apply in one sense, for example K^+ is complexed more strongly by 18C6 than is Tl^+, but less strongly by DT18C6.

APPENDICES

APPENDIX A

EXTRACTION EQUILIBRIUM CONSTANT DETERMINATION FROM DISTRIBUTION EQUILIBRIA STUDIES

APPENDIX A

EXTRACTION EQUILIBRIUM CONSTANT DETERMINATION FROM DISTRIBUTION EQUILIBRIA STUDIES

The determination of the overall extraction equilibrium constant (K_e) for the complexation of a metal ion and macrocyclic ligand in the organic phase was discussed in Chapter IV. The derivation of the final expression used to calculate K_e follows.

If C_M, C_{Pic}, and C_L are the total concentrations of the metal ion, picrate ion, and the ligand, respectively, then for a univalent metal ion the following relations may be defined:

$$[M^+] = f(C_M - E) \quad (1)$$

$$[Pic] = C_{Pic} - E \quad (2)$$

$$C_L = [L]_{org} + P_e[L]_{org} + P_eK_sf(C_M - E) + E \quad (3)$$

where the brackets ([]) represent equilibrium concentrations of the particular species, f is the single ion activity coefficient of the aqueous cation, and E is the concentration of the picrate ion extracted into the organic phase. The equilibrium constants, P_e and K_s, represent the ligand partitioning between the phases and the complex stability constant in water, respectively. In equation 3 the first and fourth terms represent the free and complexed ligand in the organic phase. The second and third terms account for the uncomplexed ligand and the complexed ligand in the aqueous phase.

The equilibrium concentration of the complex ion pair is

$$[\mathrm{MLPic}]_{org} = [2E + K_d - (K_d^2 + 4K_dE)^{\frac{1}{2}}]/\ 2 \tag{4}$$

where K_d is the dissociation of the ion pair in the organic phase. Equation 4 is obtained by considering the equilibrium expression for K_d, the stoichiometry relation

$$E = [\mathrm{MLPic}]_{org} + [\mathrm{Pic}]_{org} \tag{5}$$

and the neutrality condition

$$[\mathrm{Pic}]_{org} = [\mathrm{ML}^+]_{org} \tag{6}$$

Substitution of equations 1-4 into the equilibrium expression for the overall extraction process

$$K_e = \frac{[\mathrm{MLPic}]_{org}}{[\mathrm{M}^+]_{aq}[\mathrm{Pic}]_{aq}[\mathrm{L}]_{org}} \tag{7}$$

gives a single expression

$$K_e = \frac{[2E + K_d - (K_d^2 + 4K_dE)^{\frac{1}{2}}]\ [1 + P_e + P_eK_sf(C_M - E)]}{2f(C_M - E)(C_{Pic} - E)(C_L - E)}$$

containing two unknowns, K_e and K_d.

APPENDIX B

COMPUTER PROGRAM EXTRACT

APPENDIX B

COMPUTER PROGRAM EXTRACT

The Fortran computer program written to determine the extraction equilibrium constant for the metal-ligand complexation studies is presented below.

```
PROGRAM EXTRACT

      PROGRAM EXTRACT (INPUT, OUTPUT, TAPE60 = INPUT, TAPE61 = OUTPUT)
      COMMON D(20,100), SD(20,100), NSTEP, RECORD (7), TAPE60, TAPE61,
     *KSET
      DIMENSION DK(50), EK(20,50), SDDEV(50), AVKE(50), CRTOT(20), ABS
     *(20), PICTOT(20), RSD(50)
      REAL KS, MTOT(20), KDMIN, KDMAX
      INTEGER TAPE60, TAPE61
      TAPE60 = 60
      TAPE61 = 61
      KSET=1
C     READ CONSTANTS, PE IS CROWN PARTITION COEFFICIENT, KS IS METAL
C     CROWN FORMATION CONSTANT IN THE AQUEOUS PHASE.
C     EPS IS THE MOLAR ABSORPTIVITY OF PICRATE ION, KDMIN IS THE LOWER
C     LIMIT FOR ESTIMATES OF KD, KDMAX THE UPPER LIMIT
C     NSTEP IS THE NUMBER OF STEPS TO BE TAKEN BETWEEN KDMIN AND
C     KDMAX (49 MAXIMUM), LSET IS THE NUMBER OF DATA SETS
C     (USING THESE VALUES OF PE, KS, ETC) TO BE RUN.
      READ (TAPE60,10) PE, KS, EPS, KDMIN, KDMAX, NSTEP, LSET
      NSTEP = NSTEP + 1
   20 READ (TAPE60,30) RECORD, NPT
C     RECORD IS THE TITLE (UP TO 70 CHARACTERS) OF THIS DATA
C     SET, NPT IS THE NUMBER OF DATA POINTS.
C     PICTOT (I), MTOT (I), CRTOT (I), AND ABS (I) ARE THE TOTAL
C     PICRATE, METAL, AND CROWN CONCENTRATIONS AND MEASURED ABSORBANCE
C     FOR EACH DATA POINT, 20 DATA POINTS MAXIMUM AS CURRENTLY
C     DIMENSIONED
      READ (TAPE60,40) (PICTOT (I), MTOT (I), CRTOT (I), ABS (I),
     *I = 1,NPT)
C     START INCREMENTAL ESTIMATES OF KD
      DO 500 J = 1,NSTEP
      DK (J) = KDMIN + (J - 1)*(KDMAX -KDMIN)/NSTEP
      SUMK = 0.0
      SUMSQK = 0.0
C     CALCULATE KE FOR EACH DATA POINT
      DO 100 K = 1, NPT
      GAMMA = 10.**(-0.51*SQRT(MTOT(K))/(1.+SQRT(MTOT(K))))
      PIC = PICTOT (K) - ABS (K)/EPS
      A=2.*PIC+DK(J)-SQRT(DK(J)**2+4.*DK(J)*PIC)
      B = GAMMA*(MTOT(K) - PIC)*(PICTOT(K) - PIC)
      C = (CRTOT(K) - PIC)/(1. + PE + PE*KS*GAMMA*(MTOT(K) - PIC))
      EK(J,K) = (A/2.)/(B*C)
      SUMK = EK(J,K) + SUMK
      SUMSQK = EK(J,K)**2 + SUMSQK
  100 CONTINUE
C     CALCULATE AVERAGE AND ST. DEVIATION FOR KE AT THIS VALUE OF KD.
      SDDEV (J) = SQRT((SUMSQK - SUMK**2/NPT)/(NPT - 1))
      AVKE (J) = SUMK/NPT
  500 RSD(J)=SDDEV(J)/AVKE(J)*100.
      WRITE (TAPE61,600) (DK(J),AVKE(J), SDDEV(J), RSD(J), J= 1,NSTEP)
      DO 550 L = 1, NSTEP
      D (1,L) = DK (L)
  550 SD(1,L)=RSD(L)
      CALL PLOT
      LSET = LSET - 1
      IF (LSET) 700,700,20
  700 CONTINUE
      STOP
   10 FORMAT (5E10.0, 2I5)
   30 FORMAT(7A10,I5)
   40 FORMAT(4E10.0)
  600 FORMAT(1H,*KD = *,E14.8, 10X, *KE = *, F14.8, *   +/-*, F14.8,
     *10X,*RDS =*, E14.8, 10/0*)
      END
```

SUBROUTINE PLOT

```
      SUBROUTINE PLOT
      DIMENSION XC(101),YC(51),ICHAR(120),SYMBA(21)
      COMMON X(20,100),Y(20,100),NPT        ,RECORD(7),TAPE60,TAPE61,NSET
      REAL ICHAR
      INTEGER TAPE61
      DATA SYMBB/1H /,SYMBX/1HX/
      DATA SYMBA/1HA,1HB,1HC,1HE,1HG,1HH,1HI,1HJ,1HK,1HL,1HM,1HN,1HO,1HP
     1,1HR,1HS,1HT,1HU,1HW,1HX,1H=/
C     FIND MAXIMUM AND MINIMUM X AND Y VALUES
      XMAX=X(1,1)
      XMIN=X(1,1)
      YMAX=Y(1,1)
      YMIN=Y(1,1)
      DO 24 II=1,NSET
      DO 24 I=1,NPT
      IF(X(II,I)-XMIN)10,12,12
   10 XMIN=X(II,I)
   12 IF(X(II,I)-XMAX)15,15,14
   14 XMAX=X(II,I)
   15 IF(Y(II,I)-YMIN)16,18,18
   16 YMIN=Y(II,I)
   18 IF(Y(II,I)-YMAX)20,20,19
   19 YMAX=Y(II,I)
   20 CONTINUE
   24 CONTINUE
C     CALCULATE RANGES OF X AND Y
      RANGEX=XMAX-XMIN
      RANGEY=YMAX-YMIN
C     MAKE PLOT LIMITS 10 0/0 LARGER THAN RANGES
      XMAX=XMAX+0.05*RANGEX
      XMIN=XMIN-0.05*RANGEX
      YMAX=YMAX+0.05*RANGEY
      YMIN=YMIN-0.05*RANGEY
C     SET 100 X AND 50 Y INCREMENTS
      XSTEP=(XMAX-XMIN)/100.
      YSTEP=(YMAX-YMIN)/50.
C     ESTABLISH X,Y ARRAY
      DO 30 J=1,101
   30 XC(J)=XMIN+(J-1)*XSTEP
      DO 35 K=1,51
   35 YC(K)=YMAX-(K-1)*YSTEP
C     BLANK ARRAY
      DO 74 KK=1,100
   74 ICHAR(KK)=SYMBB
C     BEGIN PLOT CONSTRUCTION
      WRITE(TAPE61,40)RECORD
   40 FORMAT(1H1,/////,15X,7A10,///)
      WRITE(TAPE61,41)YMAX
   41 FORMAT(1H ,5X,E10.3,1H-,1HI,20(5H----I),1HI)
C     PLACE DATA IN ARRAY
      DO 60 L=1,50
      DO 8 II=1,NSET
      DO 55 LL=1,NPT
      IF((Y(IL,LL).LE.YC(L)).AND.(Y(IL,LL).GT.YC(L+1)))GO TO 72
      GO TO 55
   72 DO 58 LLL=1,100
      LPT=LLL
      IF((X(IL,LL).GE.XC(LLL)).AND.(X(IL,LL).LT.XC(LLL+1))) GO TO 75
   58 CONTINUE
      GO TO 55
   75 IF(ICHAR(LPT).NE.SYMBB) GO TO 78
      ICHAR(LPT)=SYMBA(IL)
      GO TO 55
   78 ICHAR(LPT)=SYMBA(21)
   55 CONTINUE
    8 CONTINUE
C     PRINT CHARACTER LINE
      IF(MOD(L,10))63,65,63
   63 WRITE(TAPE61,80)(ICHAR(M),M=1,100)
   80 FORMAT(1H ,16X,1HI,100A1,1HI)
      GO TO 69
   65 WRITE(TAPE61,67)YC(L),(ICHAR(M),M=1,100)
   67 FORMAT(1H ,5X,E10.3,1H-,1HI,100A1,1HI)
C     BLANK OUT ARRAY
   69 CONTINUE
      DO 81 MM=1,100
   81 ICHAR(MM)=SYMBB
   60 CONTINUE
C     COMPLETE THE PLOT
      WRITE(TAPE61,85)
   85 FORMAT(1H ,16X,1HI,20(5H----I),1HI)
      WRITE(TAPE61,89)
   89 FORMAT(1H ,16X,1H+,19X,5(1H+,19X))
      WRITE(TAPE61,90)XMIN,XC(20),XC(40),XC(60),XC(80),XC(100)
   90 FORMAT(1H ,6(10X,E10.3),///)
      WRITE(TAPE61,88)XMIN,XMAX,YMIN,YMAX
   88 FORMAT(1H ,*MINIMUM X IS *,E14.7,5X,*MAXIMUM X IS *,E14.7,//,* MIN
     *IMUM Y IS *,E14.7,5X,*MAXIMUM Y IS *,E14.7,///)
      RETURN
      END
```

LIST OF REFERENCES

LIST OF REFERENCES

1. C. J. Pederson, *J. Amer. Chem. Soc.*, **89**, 7017 (1967).
2. B. Dietrich, J. M. Lehn, and J. P. Sauvage, *Tetrahedron Lett*. 2885 (1969).
3. B. Dietrich, J. M. Lehn, J. P. Sauvauge, and J. Blanzat, *Tetrahedron*, **29**, 1629 (1973).
4. H. K. Frensdorff, *J. Amer. Chem. Soc.*, **93**, 600 (1971).
5. C. J. Pedersen, *Fed. Proc.*, **27**, 1305 (1968).
6. W. H. Delphin and E. P. Horwitz, *Anal. Chem.*, **50**, 843 (1978).
7. E. Blasius and P. G. Maurer, *J. Chromatog.*, **125**, 511 (1976).
8. B. E. Jepson and R. A. Schwind, First Symposium on Macrocyclic Compounds, Provo, Utah Aug. 15-17 (1977).
9. A. Knochel and R. D. Wilken, *J. Radioanal. Chem.*, **32**, 345 (1976).
10. B. C. Pressman, E. J. Harris, W. S. Jagger, and J. H. Johnson, *Proc. Nat. Acad. Sci. U.S.*, **89**, 1949 (1967).
11. H. K. Wipf, L. A. R. Pioda, Z. Stefanac, and W. Simon, *Helv. Chim. Acta*, **51**, 377 (1968).
12. R. M. Izatt, R. E. Terry, B. L. Haymore, L. D. Hansen, N. K. Dalley, A. G. Avondett, and J. J. Christensen, *J. Amer. Chem. Soc.*, **98**, 7620 (1976).
13. R. M. Izatt, R. E. Terry, D. P. Nelson, Y. Chan, D. J. Eatough, J. S. Bradshaw, L. D. Hansen, and J. J. Christensen, *J. Amer. Chem. Soc.*, **98**, 7626 (1976).
14. J. M. Lehn, *Acc. Chem. Res.*, **11**, 49 (1978).

15. C. J. Pedersen and H. K. Frensdorff, *Angew. Chem., Int. Ed.*, **11**, 16 (1972).

16. N. Matsuura, K. Umemoto, Y. Takeda, and A. Sasaki, *Bull. Chem. Soc. Jap.*, **49**, 1246 (1976).

17. J. Smid, *Angew. Chem., Int. Ed.*, **11**, 112 (1972).

18. M. Bourgoin, K. H. Wong, J. Y. Hui, and J. Smid, *J. Amer. Chem. Soc.*, **97**, 3462 (1975).

19. A. I. Popov, *Solute-Solvent Interactions*, New York: Marcel Dekker, Inc., J. F. Coetzee and C. D. Ritchie, eds., 1976, pp. 271-230.

20. D. N. Reinhoudt, R. T. Gray, F. DeJong, and C. J. Smit, *Tetrahedron*, **33**, 563 (1977).

21. A. T. Tsatsas, R. W. Stearns, and W. M. Risen, *J. Amer. Chem. Soc.*, **94**, 5247 (1972).

22. H. K. Frensdorff, *J. Amer. Chem. Soc.*, **93**, 4684 (1971).

23. J. D. Lamb, R. M. Izatt, J. J. Christensen, and D. J. Eatough, *Thermodynamics and Kinetics of Cation-Macrocycle Interaction*, in press.

24. J. J. Christensen, J. O. Hill, and R. M. Izatt, *Science*, **174**, 459 (1971).

25. J. M. Lehn, *Pure Appl. Chem.*, **49**, 857 (1977).

26. J. M. Lehn and F. Montavon, *Helv. Chim. Acta*, **61**, 67 (1978).

27. C. J. Pedersen, *J. Amer. Chem. Soc.*, **92**, 386 (1970).

28. D. Bright and M. R. Truter, *Nature*, **225**, 177 (1970).

29. M. A. Bush and M. R. Truter, *Chem. Comm.*, 1439 (1970).

30. C. J. Pedersen, *J. Amer. Chem. Soc.*, **92**, 391 (1970).

31. D. J. Cram, R. C. Helgeson, L. R. Sousa, J. M. Timko, M. Newcomb, P. Moreau, F. DeJong, P. W. Gokel, D. H. Hoffman, L. A. Domeier, S. C. Peacock, K. Madan, and L. Kaplan, *Pure Appl. Chem.*, **43**, 327 (1975).

32. E. M. Arnett and T. C. Moriarity, *J. Amer. Chem. Soc.*, **93**, 4908 (1971).

33. J. R. Dann, P. P. Chiesa, and J. W. Gates, *J. Org. Chem.*, **26**, 1991 (1961).

34. L. A. Ochrymowyca, C. P. Mak, and J. D. Michna, *J. Org. Chem.*, **39**, 2079 (1974).

35. F. Vogtle and E. Weber, *Angew. Chem.*, **89**, 126 (1974).

36. D. St. C. Black and I. A. McLean, *Tetrahedron Lett.*, 3961 (1971).

37. W. Rosen and D. H. Busch, *Inorg. Chem.*, **9**, 262 (1970).

38. W. Rosen and D. H. Busch, *J. Amer. Chem. Soc.*, **91**, 4694 (1969).

39. M. D. Glick, D. P. Gavel, L. L. Diaddario, and D. B. Rorabacher, *Inorg. Chem.*, **15**, 1190 (1976).

40. J. J. Christensen, D. J. Eatough, and R. M. Izatt, *Chem. Rev.*, **74**, 351 (1974).

41. N. B. Tucker and E. E. Reid, *J. Amer. Chem. Soc.*, **55**, 775 (1933).

42. J. R. Meadow and E. E. Reid, *J. Amer. Chem. Soc.*, **56**, 2177 (1934).

43. C. J. Pedersen, *J. Org. Chem.*, **36**, 254 (1971).

44. J. S. Bradshaw, J. Y. K. Hui, B. L. Haymore, J. J. Christensen, and R. M. Izatt, *J. Hetero. Chem.*, **10**, 1 (1973).

45. J. S. Bradshaw, J. Y. K. Hui, Y. Chan, B. L. Haymore, R. M. Izatt, and J. J. Christensen, *J. Hetero. Chem.*, **11**, 45 (1974).

46. J. S. Bradshaw and J. Y. K. Hui, *J. Hetero. Chem.*, **11**, 649 (1974).

47. J. S. Bradshaw, R. A. Reeder, M. D. Thompson, E. D. Flanders, R. L. Carruth, R. M. Izatt, and J. J. Christensen, *J. Org. Chem.*, **41**, 134 (1976).

48. N. K. Dalley, J. S. Smith, S. B. Larson, K. L. Matheson, J. J. Christensen, and R. M. Izatt, Chem. Comm., **84** (1975).

49. B. Metz, D. Moras, and R. Weiss, J. Inorg. Nucl. Chem., **36**, 785 (1974).

50. M. Jawaid and F. Ingman, *Talanta*, **25**, 91 (1978).

51. S. Kopolow, Z. Machacek, U. Takaki, and J. Smid, *J. Macromol. Sci.-Chem.*, **A7(5)**, 1015 (1973).

52. S. Kopolow, T. E. Hogen Esch, and J. Smid, *Macromolecules*, **6**, 133 (973).

53. A. Sadakane, T. Iwachido, and K. Toei, *Bull. Chem. Soc. Jap.*, **48**, 60 (1975).

54. T. Iwaichido, A. Sadakane, and K. Toei, *Bull. Chem. Soc. Jap.*, **51**, 629 (1978).

55. J. W. Mitchell and D. L. Shanks, *Anal. Chem.*, **47**, 642 (1975).

56. A. M. Y. Jaber, G. J. Moody, and J. D. R. Thomas, *Inorg. Nucl. Chem.*, **39**, 1689 (1977).

57. M. Kawasaki, K. Toei, and T. Iwachido, *Chem. Lett.*, 417 (1972).

58. T. Iwachido, M. Kimura, and K. Toei, *Chem. Lett.*, 1101 (1976).

59. T. Iwachido, M. Minami, A. Sadakane, and K. Toei, *Chem. Lett.*, 1511 (1977).

60. P. R. Danesi, H. Meider-Gorican, R. Chiarizia, adn G. Scibona, *J. Inorg. Nucl. Chem.*, **37**, 1479 (1975).

61. P. R. Danesi, R. Chiarizia, C. Fabiani, and C. Domenichini, *J. Inorg. Nucl. Chem.*, **38**, 1226 (1976).

62. Lj. Tusek, P. R. Danesi, and R. Chiarizia, *J. Inorg. Nucl. Chem.*, **37**, 1538 (1975).

63. Y. Marcus and L. E. Asher, *J. Phys. Chem.*, **82**, 1246 (1978).

64. T. Sekine, H. Wakabayashi, and Y. Hasegawa, *Bull. Chem. Soc. Jap.*, **51**, 645 (1978).

65. D. Sevdic and H. Meider, *J. Inorg. Nucl. Chem.*, **39**, 1403 (1977).

66. D. Sevdic and H. Meider, *J. Inorg. Nucl. Chem.*, **39**, 1409 (1977).

67. G. W. Gokel, D. J. Cram, C. L. Liotta, H. P. Harris, and F. L. Cook, *J. Org. Chem.*, **39**, 2445 (1974).

68. I. S. Perelygin and M. A. Klimchuk, *Russ. J. Phys. Chem.*, **47**, 1138 (1973).

69. M. S. Greenberg and A. I. Popov, *J. Soln. Chem.*, **5**, 653 (1976).

70. Y. M. Cahen and A. I. Popov, *J. Soln. Chem.*, **4**, 599 (1975).

71. K. Balasubrahmanyam and G. J. Janz, *J. Amer. Chem. Soc.*, **92**, 4189 (1970).

72. T. G. Chang and D. E. Irish, *J. Soln. Chem.*, **3**, 161 (1974).

73. J. F. Hinton and E. S. Amis, *Chem. Rev.*, **67**, 367 (1967).

74. W. J. DeWitte, Ph.D. Thesis, Michigan State University, East Lansing, Mich. (1976).

75. L. L. Hsu, Masters Thesis, Michigan State University, East Lansing, Mich. (1976).

76. E. H. Mei, Ph.D. Thesis, Michigan State University, East Lansing, Mich. (1977).

77. A. R. Hourdakis, Ph.D. Thesis, Michigan State University, East Lansing, Mich. (1978).

78. N. F. Ramsey, *Phys. Rev.*, **78**, 699 (1950).

79. W. G. Schneider and A. D. Buckingham, *Discuss. Faraday Soc.*, **34**, 147 (1962).

80. A. G. Lee, *Coord. Chem. Rev.*, **8**, 289 (1972).

81. F. J. Kayne and J. Reuben, *J. Amer. Chem. Soc.*, **92**, 220 (1970).

82. J. Reuben and F. J. Kayne, *J. Biol. Chem.*, **246**, 6227 (1971).

83. J. J. Dechter and J. I. Zink, *J. Amer. Chem. Soc.*, **97**, 2937 (1975).

84. J. F. Hinton and R. W. Briggs, *J. Mag. Res.*, **25**, 379 (1977).

85. R. Freeman, R. P. H. Gasser, R. E. Richards, and D. H. Wheeler, *Molecular Phys.*, **2**, 75 (1959).

86. R. Freeman, R. P. H. Gasser, and R. E. Richards, *Molecular Phys*., **2**, 301 (1959).

87. J. J. Dechter and J. I. Zink, *Chem. Comm*., 96 (1974).

88. J. F. Hinton and R. W. Briggs, *J. Mag. Res*., **19**, 393 (1975).

89. R. H. Erlich, M. S. Greenberg, and A. I. Popov, *J. Amer. Chem. Soc*., **92**, 4989 (1970).

90. R. W. Briggs and J. F. Hinton, *J. Soln. Chem*., **7**, 1 (1978).

91. R. W. Briggs and J. F. Hinton, *J. Soln. Chem*., **6**, 827 (1977).

92. E. Shchori, N. Nae, and J. Jagur-Grodzinski, *J. C. S. Dalton*, 2381 (1975).

93. J. Koryta and M. L. Mittal, *J. Electroanal. Chem*., 36, App. 14 (1972).

94. L. J. Rodriguez, G. W. Liesegang, R. D. White, M. M. Farrow, N. Purdie, and E. M. Eyring, *J. Phys. Chem*., **81**, 2118 (1977).

95. C. Srivanavit, J. I. Zink, and J. J. Dechter, *J. Amer. Chem. Soc*., **99**, 5876 (1977).

96. J. M. Lehn and J. P. Sauvage, *Chem. Comm*., 440 (1971).

97. J. S. Shih, private communication.

98. J. H. Mathews, *J. Amer. Chem. Soc*., **48**, 562 (1926).

99. M. G. Mellon, *Analytical Absorption Spectroscopy*, New York: John Wiley & Sons, Inc., 1950, p. 261.

100. D. D. Traficante, J. A. Simms, and M. Mulcay, *J. Mag. Res*., **15**, 484 (1974).

101. D. A. Wright and M. T. Rogers, *Rev. Sci. Instr*., **44**, 1189 (1973).

102. J. R. Zimmerman and M. R. Foster, *J. Phys. Chem*., **61**, 282 (1957).

103. D. H. Live and S. I. Chan, *Anal. Chem*., **42**, 791 (1970).

104. J. L. Dye and V. A. Nicely, *J. Chem. Ed.*, **48**, 443 (1971).

105. C. M. French and I. G. Roe, *Trans. Faraday Soc.*, **49**, 791 (1953).

106. T. Abe, *Nature*, **187**, 234 (1960).

107. A. Brandstrom, P. Berntsson, S. Carlsson, A. Djurhuus, K. Gustavii, U. Junggren, B. Lamm, and B. Samuelsson, *Acta. Chem. Scand.*, **23**, 2202 (1969).

108. R. G. Pearson, *J. Amer. Chem. Soc.*, **85**, 3533 (1963).

109. E. T. Roach, P. R. Handy, and A. I. Popov, *Inorg. Nucl. Chem. Lett.*, **9**, 359 (1973).

110. W. L. DeWitte, L. Liu Hau, E. Mei, J. L. Dye, and A. I. Popov, *J. Soln. Chem.*, **6**, 337 (1977).

111. A. Hourdakis and A. I. Popov, *J. Soln. Chem.*, **6**, 299 (1977).

112. E. Mei, L. Liu Hsu, J. L. Dye, and A. I. Popov, *J. Soln. Chem.*, **6**, 771 (1977).

113. E. Mei, A. I. Popov, and J. L. Dye, *J. Phys. Chem.*, **81**, 1677 (1977).